Techniques for Efficient Spectrum Usage for Next Generation Mobile Communication Networks. An LTE and LTE-A Case Study

Kumar, Sanjay

Publication date:
2009

Document Version
Publisher's PDF, also known as Version of record

Techniques for Efficient Spectrum Usage for Next Generation Mobile Communication Networks

An LTE and LTE-A Case Study

PhD Thesis
by

Sanjay Kumar

A Dissertation submitted to
the Faculty of Engineering, Science and Medicine of Aalborg University
in partial fulfillment for the degree of
Doctor of Philosophy.
Aalborg, Denmark
June 2009

Supervisors:
Ramjee Prasad, PhD,
Professor, Director, CTIF, Aalborg University, Denmark.
Preben Elgaard Mogensen, PhD,
Professor, Aalborg University, Denmark.

Assessment Committee:
Uma S. Jha, PhD,
Director, Product Management, Qualcomm Inc., USA.
Markku Juntti, PhD,
Professor, University of Oulu, Finland.
Troels B. Sorensen, PhD,
Associate Professor, Aalborg University, Denmark.

Moderator:
Flemming B Frederiksen,
Associate Professor, Aalborg University, Denmark.

ISBN 978-87-92328-29-8

To
My Parents,
My wife Babita,
My daughter Shraddha, son Nitin,
and
to the respectful memories of
My Grandparents.

Abstract

This PhD study aims to investigate techniques for efficient usage of spectrum for next generation mobile communication networks. The Long Term Evolution (LTE) and LTE-Advanced (LTE-A) systems are taken as case studies. The LTE is under development within 3rd Generation Partnership Project (3GPP) and heading towards its final phase of standardization. The LTE aims for reduced latency, higher user data rates, improved system capacity and coverage, and reduced cost for the operators. Currently the International Telecommunications Union (ITU) is working on specifying the system requirements towards next generation mobile communication systems called International Mobile Telecommunications-Advanced (IMT-A). The 3GPP aims to further evolve LTE towards LTE-A in order to meet or exceed the IMT-A requirements as well as its own requirements for advancing LTE for long term competitiveness.

The first half of the PhD study is mainly concerned with LTE, with the main focus on higher order sectorization and inter-cell interference avoidance to improve system capacity and coverage. Typically three antennas are considered rendering 3 sector site deployments for LTE. A migration to 6 sector site deployment has been investigated. A mixed network topology composed of a combination of 3 and 6 sectors site deployment is also proposed. The mixed network topology is found to provide significantly high performance gains in terms of cell throughput and user outage throughput performance, and therefore recommended as a potential solution to meet high traffic demands in localized areas such as hot spots.

LTE uses Orthogonal Frequency Division Multiple Access (OFDMA) in the downlink with universal frequency reuse. Due to the characteristics of OFDMA, the intra-cell interference is ideally avoided , but the environment still remains interference limited due to the presence of inter-cell interference. Our focus in this study is on development of schemes for inter-cell interference avoidance under fractional load conditions. The fractional load conditions arise when all the resources are not required to be used due to lack of traffic in the cell. We propose several autonomous inter-cell interference avoidance schemes, which do not require inter-cell signaling and provide significant improvements in cell throughput and user outage throughput performance.

The second half of the study is concerned with LTE-A, which aims to provide peak data rates in the order of 1 Gbps in downlink and 500 Mbps in uplink for the nomadic local area/indoor deployment scenarios. Such high data rates may require high spectral efficiency and a wide bandwidth spectrum allocation in the order of 100 MHz. Such high bandwidth allocation may require sharing of spectrum among operators in a flexible manner. Currently, Home e-nodeB (HeNB) is emerging as a potential solution to provide high data rate high quality indoor coverage.

Potentially large scale uncoordinated deployment of HeNBs, sharing over the same

radio spectrum is expected, giving rise to severe radio interference problems. A new mechanism is required to ensure coexistence of HeNBs in the given area. The concept of Flexible Spectrum Usage (FSU) is considered a key enabler, which allows spectrum allocation from a common pool and ensures coexistence. The Spectrum Load Balancing (SLB) and Resource Chunk Selection (RCS) algorithms are proposed for FSU among HeNBs, which ensure coexistence by partially or completely preventing mutual interference on the shared spectrum and also provide self configurable solutions towards uncoordinated HeNBs deployment. The framework of the FSU study is further extended to autonomous component carrier selection schemes that also allow uncoordinated HeNB deployment without prior radio network planning.

Further, a policy assisted light cognitive radio enabled FSU has been proposed for efficient and flexible spectrum allocation in multi operator domain. The concept is based on cognitive radio cycle, where the decision making is assisted by a policy, where the policy refers to a set of rules agreed among operators to facilitate FSU. The FSU study has been primarily focused within the same radio access technology in the licensed frequency band.

Dansk Resumé

Dette ph.d.-studium sigter mod at udforske teknikker til effektiv udnyttelse af frekvensspekteret ifm. den næste generation af mobilkommunikationsnetværk. "Long Term Evolution" (LTE) og "LTE-Advanced" (LTE-A) systemer anvendes som eksempler. LTE er under udvikling ifm. "The 3rd Generation Partnership Project" (3GPP) og nærmer sig sin endelige standardiseringsfase. LTE sigter mod reduceret latens, større bruger datahastighed, forøget systemkapacitet og -dækning samt reducerede omkostninger for operatørerne. For øjeblikket arbejder den internationale telekommunikationsunion (ITU) på at specificere systemkravene for næste generation af mobilkommunikationssystemer benævnt "International Mobile Telecommunications-Advanced" (IMT-A). 3GPP sigter mod at videreudvikle LTE mod LTE-A med henblik på at opfylde eller overstige IMT-A kravene og som et led i sine egne bestræbelser mod at sikre LTE lang tids konkurrencedygtighed

Den første halvdel af ph.d.-studiet er hovedsageligt rettet mod LTE med særligt fokus på høj ordens sektorisation og hindring af inter-cell interferens til forbedring af systemets kapacitet og dækning. Tre antenner forventes typisk at skulle varetage tre sektorer ifm. LTE-afvikling. En udvikling til LTE-afvikling i seks sektorer er undersøgt. En blandet netværkstopologi - sammensat ved en kombination af afviklingerne i 3 og 6 sektorer - er også foreslået. Den blandede netværkstopologi har vist sig at præstere særligt høje ydelsesforbedringer m.h.t. cell-throughput og user-outage-throughput-performance, og den er derfor anbefalet som en potentiel løsning til imødekommelse af store datatrafikkrav i afgrænsede områder såsom hot spots.

LTE anvender Orthogonal-Frequency-Division-Multiple-Access (OFDMA) ifm. downlink med universal-frequency-reuse. Grundet OFDMA's særlige egenskaber tilføres der ikke intra-cell interferens, men omgivelserne indeholder fortsat interferens, der dog alene skyldes tilstedeværelsen af inter-cell interferens. Vores fokus i dette studium er at udvikle systemer til hindring af inter-cell interferens under små belastningsforhold. Små belastningsforhold optræder når alle ressourcerne ikke behøves på grund af begrænset celletrafik. Vi foreslår forskellige uafhængige systemer til hindring af inter-cell interferens, og som ikke kræver signalering mellem cellerne men tilvejebringer signifikante forbedringer i cellegennemgangen samt i bruger outage-throughput præstationerne.

Den anden halvdel af studiet er rettet mod LTE-A, som sigter mod at tilvejebringe topdatahastigheder af størrelsesordenen 1 Gbps i downlink og 500 Mbps i uplink for de nomadiske lokal-area/indendørs afviklinger. Sådanne høje datahastigheder kræver eventuelt høj spektral effektivitet og en stor båndbreddetildeling af størrelsesordenen 100 MHz. Store båndbreddetildelinger forudsætter eventuelt fleksibel spektrumsfordeling mellem operatørerne. For tiden fremstår Home e-nodeB (HeNB) som en potentiel løsning for tilvejebringelse af høje datahastigheder ifm. indendørs dækning med høj kvalitet. Potentielt forventes der I stor skala og ukoordineret en spektral fordeling af det fælles ra-

diospektrum mellem HeNB's, hvilket vil udløse alvorlige radio interferensproblemer. Der behøves en ny mekanisme til at sikre sameksistensen mellem HeNB's indenfor det givne område. Konceptet: "Flexible Spectrum Usage" (FSU), der betragtes som en nøgle hertil, tillader spektrumstildeling fra en fælles pulje og sikrer en sameksistens. "Spectrum Load Balancing" (SLB) og "Resource Chunk Selection" (RCS) algoritmerne er foreslået af FSU blandt diverse HeNB's og sikrer sameksistens ved delvist eller helt at afværge indbyrdes interferens i det fælles spektrum, og det tilfører samt selvkonfigurerer endvidere løsninger til brug for en ukoordineret HeNB-afvikling. Rammen for FSU-studiet udvides endvidere med et uafhængigt component-carrier-selection system, der endvidere tillader ukoordineret HeNB-udnyttelse uden en forudgående radio-netværksplanlægning. Endvidere foreslås der et strategisk light-cognitive radio styret FSU til effektiv og fleksibel allokering af spektrum i et multioperator domæne. Konceptet baseres på en cognitive radio cyclus, hvor beslutningsforløbet støttes af en strategi med reference til et regelsæt, som operatørerne har vedtaget med sigte på at lette FSU. FSU-studiet har primært været rettet mod en og samme radio access technologi i det licensbehæftede frekvensbånd.

Preface and Acknowledgments

This dissertation is the result of a three years research project carried out at the Radio Access Technology (RATE) section, Center for TeleInFrastruktur (CTIF), Institute of Electronic Systems, Aalborg University, Denmark, under the supervision and guidance of Professor Ramjee Prasad (Director, CTIF, Aalborg University, Denmark) and Professor Preben E. Mogensen (Aalborg University, Denmark). The dissertation has been completed in parallel with the mandatory course work, teaching, and project work obligations in order to obtain the PhD degree. This research project has been co-financed by Birla Institute of Technology, Ranchi, India and Radio Access Technology (RATE) section, Center for TeleInFrastruktur (CTIF), Aalborg University, Aalborg.

First of all, I express my sincere gratitude to my supervisors Professor Ramjee Prasad and Professor Preben E. Mogensen for their constant encouragement and support. Their extremely rich technical experience and clear understanding about the research direction have always made me confident towards my research work. More importantly, their human understanding on personal issues always made me optimistic and comfortable even in times of difficult situations. They have always given me courage to continue and complete the work. It has been a privilege for me to work with such supervisors. I am highly indebted for their guidance, support and co-operation. I shall always remain grateful to them.

I would like to thank Professor S.C. Goel of Birla Institute of Technology, Ranchi, India for giving me this opportunity to come to Aalborg University for research work. I thank Professor Nisha Gupta for her initiative in this project and constant support. I would like to thank Professor R. Sukesh Kumar for giving me encouragement and advice. I thank Professor PK Barhai, Vice Chancellor, Birla Institute of Technology for providing me all the needed support to complete the work. I also thank Professor H. C. Pande, Vice Chancellor Emeritus, Birla Institute of Technology for being a constant source of inspiration. I would like to thank all my colleagues and all the members of the Department of Electronics and Communications Engineering, Birla Institute of Technology, Ranchi India.

I worked in close association with Klaus I. Pedersen and Istvan Z. Kocavs of Nokia Siemens Networks, Aalborg for a considerable part of my research work. Their clear vision and expertise in the area of research gave me an invaluable learning experience. I am extremely thankful for their understanding and cooperation. I thank Troels Kolding, Mads Brix and Frank Frederiksen of Nokia Siemens Networks, Aalborg for all the administrative and technical support. I also thank all the colleagues at Nokia Siemens Networks, Aalborg for their cooperation and friendly support.

I am extremely thankful to Troels B. Sorensen, who introduced to me about the research activities at RATE section and also for his willingness to help whenever needed. I

am grateful to Flemming B. Frederiksen for his sincere concern for me and also for translating the abstract into Danish. I would be extremely pleased to thank Nicola Marchetti for his constant support, feedback and cooperation during a considerable part of the PhD work.

I very well appreciate and extend my thanks to the caring and sincere secretaries Lisbeth Schiønning Larsenand, Inga Hauge, Sussan Norrevang and Jytte Larsen for making my stay free from administrative worries. I thank Jytte Larsen also for providing feedback on the language of the thesis.

During the PhD study I was fortunate to work in close cooperation with my fellow researchers Guillaume Monghal, Yuanye Wang, Luis Garcia and Gustavo Costa. I thank them for their sincere collaboration. I would like to thank Andrea Fabio Cattoni, Mohmmad Anas, Francesco D. Calabrese, Naizheng Zheng, Oumer M. Teyeb, Gilberto Berardinelli and Carles N. Manchon for making my stay pleasant in Aalborg. I would like to thank former RATE colleagues Suvra Shekar Das, Mohammad Imadur Rahman, and Akhilesh Pokhariyal for inspiration and fruitful discussion at the early stage of my PhD work. I would also like to express my gratitude to all the colleagues at Radio Access Technology section and CTIF, Aalborg University for their friendly support.

I will never forget to thank Professor H.K. Grewal, my master thesis supervisor for her trust in me and introducing me into the noble world of teaching and research after my retirement from the defense services. I also thank my master project students for their interest and involvement in the project and their hard work.

It is the boundless blessings of my parents, endless sacrifice of my wife Babita, my daughter Shraddha and son Nitin, which gave me enough strength to complete the work. They have shown extreme patience and supported me in every possible way. Words alone can never express my gratitude to them. I express my thanks to my uncle and aunts, all the relatives and friends for their blessings and encouragement for my academic pursuit.

Finally, I thank the ultimate source of energy of every particle in the universe, the Almighty, for giving me enough energy to complete the work.

Sanjay Kumar, June, 2009.

Abbreviations

AMC	Adaptive Modulation and Coding
ARQ	Automatic Repeat ReQuest
AVI	Actual Value Interface
BLER	BLock Error Rate
CP	Cyclic Prefix
CQI	Channel Quality Information
DL	Downlink
DL-SCH	Downlink Shared Channel
eNode-B	Evolved Node B
EPC	Evolved Packet Core
EPS	Evolved Packet System
E-UTRAN	Evolved Universal Terrestrial Radio Access Network
FD	Frequency-Domain
FDD	Frequency Division Duplex
FDM	Frequency Domain Multiplexing
FDPS	Frequency-Domain Packet Scheduling
FEC	Forward Error Correction
HARQ	Hybrid Automatic Repeat reQuest
ISI	Inter-Symbol Interference
LA	Link Adaptation
LTE	Long Term Evolution
MAC	Medium Access Control
MCS	Modulation and Coding Scheme
MIMO	Multiple Input Multiple Output

MRC	Maximal Ratio Combining
OFDM	Orthogonal Frequency Division Multiplexing
OFDMA	Orthogonal Frequency Division Multiple Access
OLLA	Outer Loop Link Adaptation
PAPR	Peak-to-Average Power Ratio
PDCP	Packet Data Convergence Protocol
PDP	Power Delay Profile
PF	Proportional Fair
PF	Proportional Fair
PHY	Physical Layer
PRBs	Physical Resource Blocks
QAM	Quadrature Amplitude Modulation
QPSK	Quadrature Phase Shift Keying
RLC	Radio Link Control
RR	Round Robin
RRC	Radio Resource Control
RRM	Radio Resource Management
SC-FDMA	Single-Carrier Frequency Division Multiple Access
SINR	Signal-to-Interference-plus-Noise Ratio
SISO	Single Input Single Output
TDD	Time Division Duplex
TD	Time-Domain
TDPS	Time-Domain Packet Scheduling
TTI	Transmission Time Interval
UL	Uplink
UTRAN	Universal Terrestrial Radio Access Network
CN	Core Network
DwPTS	Downlink Pilot Time Slot
EPC	Evolved Packet Core
EPS	Evolved Packet System

GP	Guard Period
HeNB	Home eNode-B
HeNBs	Home eNode-Bs
IRC	Interference Ratio Combining
LA	Link Adaptation
LTE	Long Term Evolution
LTE-A	LTE-Advanced
MME	Mobility Management Entity
MUD	Multi User Diversity
PRB	Physical Resource Block
PCC	Primary Component Carrier
P-GW	PDN Gateway
RAN	Radio Access Network
SINR	Signal to Interference plus Noise Ratio
SCC	Secondary Component Carrier
S-GW	Serving Gateway
UpPTS	Uplink Pilot Time Slot
WINNER	Wireless World Initiative New Radio

Contents

Chapter 1

Thesis Introduction

1.1 Introduction

In the world of telecommunications, people today are more connected and more mobile than ever. We have more devices and more ways of staying in touch with one another [1]. In recent years the cellular operators across the world have seen a rapid growth in the number of mobile broadband subscribers as well as a constant increase in the traffic volume per subscriber. The users are demanding huge amount of data while on move. An increase of 6-14 times mobile data usage was reported in 2007 and 30-50 times in 2008 compared with 2006 [1]. The increasing demand for mobile data access to multimedia and internet applications and services presents a challenge for the mobile network operators as their existing network becomes capacity constrained. Operators need to upgrade their network to offer more compelling user experience. Users expect the network to originate, terminate and maintain a session while the user is moving and roaming. The services have to be delivered to the users based on their preferences. The requirements on the radio technology include improved performance as well as reduced system and device complexity. Over the last few years this has created new interest among existing and emerging operators to explore new technologies and network architecture to offer such services at low cost [2]. What is needed is a solution that offers a lower cost per bit, higher capacity and higher data rates.

This chapter is organized as follows. The evolution of 3GPP standards is presented in section 1.2, with the purpose of highlighting the recent historical development leading up to Long Term Evolution (LTE) and LTE-Advanced (LTE-A) systems, where the technological requirements and the main considerations for the future mobile communication systems are also discussed briefly. Section 1.3 outlines the main motivations behind this PhD study, and the key issues identified for study and investigation. The scientific methodologies for system level investigations are discussed in section 1.4, whereas section 1.5 brings into light the novelty of this research work and the main contributions made towards the scientific community. Finally section 1.6 presents the organization of this PhD thesis.

1.2 Evolution of 3GPP Standards

The wireless industry has rapidly grown through the development of multiple standards and technologies. Each wireless standard has evolved with its specialized service such as voice, video streaming, wireless internet access, or email services. Presently we are aiming for the 4th generation of mobile communication systems.

The 3rd Generation Partnership Project (3GPP) was established in December 1998 with the purpose of producing globally applicable Technical Specifications and Technical Reports for 3rd Generation Mobile System based on evolved GSM core networks [3]. Figure 1.1 presents the evolution of 3GPP standards since then. 3GPP started specification of Universal Mobile Telecommunications systems (UMTS) in 1998 based on Global System for Mobile (GSM) specifications. It introduced a new RAN called UTRAN together with a new air interface called Wideband Code Division Multiple Access (WCDMA) in the first release (Release'99) in 2002 [3].

WCDMA is a wideband spread-spectrum 3G mobile telecommunication air interface that utilizes code division multiple access. It provides simultaneous support for a wide range of services with different characteristics on a common 5 MHz carrier [3]. It provides new service capabilities, increased network capacity and reduced cost for voice and data services. It supports 384 Kbps with wide area coverage and 2 Mbps with local coverage. WCDMA allows flexible usage of the spectrum based on Link Adaptation (LA) and power control techniques. The term WCDMA also refers to one of the International Telecommunications Union's IMT-2000 standards, a 3G cellular network.

The evolution of WCDMA addressed the operators' needs for efficiency and the users' demands for enhanced experience. The further steps of this evolution are High Speed Downlink Packet Access (HSDPA) and High Speed Uplink Packet Access (HSUPA), which belongs to the High Speed Packet Access (HSPA) family, also called 3.5G. The Release '5 specifies the first phase of HSDPA [3],[4]. It supports 14.4 Mbps DL data rate. The second phase of HSDPA is specified in the Release'7 and has been named HSPA Evolved. It can achieve DL data rates of up to 42 Mbit/s. High-Speed Uplink Packet Access (HSUPA) is specified in Release'6, and it supports UL data rate up to 5.76 Mbps [3]. A further Evolution of HSPA (also known as HSPA+) is specified in release 8.

3GPP Long Term Evolution (LTE)

The 3GPP aims to continuously evolve its systems to meet the emerging needs of customers and to integrate state of the art technologies. With enhancements such as HSDPA and Enhanced Uplink, the 3GPP radio access technology will be highly competitive for several years. However, to ensure competitiveness in an even longer time frame 3GPP started specification of LTE parallel with the HSPA evolution.

In December 2004 3GPP started a feasibility study on LTE with the objective to develop a framework for the evolution towards a high data rate, low-latency and packet optimized radio access technology. The standardization of LTE has recently been completed and is defined in 3GPP Release'8. The LTE is commonly called 3.9 G and prepares

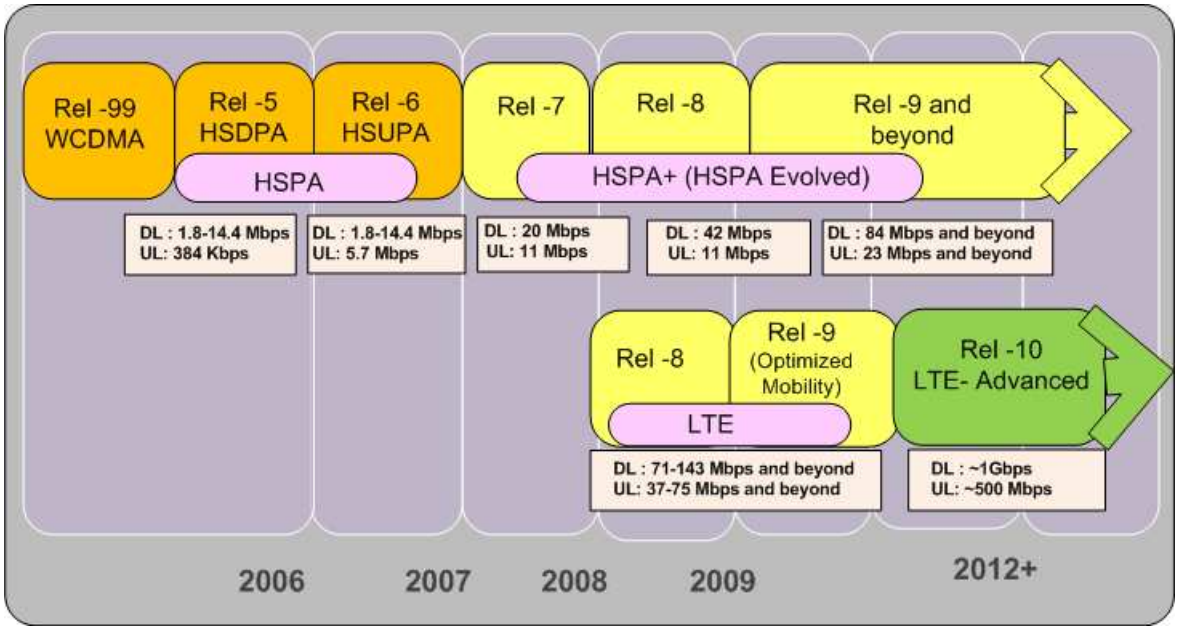

Figure 1.1: Evolution of 3GPP standards

the way forward towards 4G systems with a new simplified core network and radio access network (RAN) architecture, to reduce latency for a packet based network. LTE aims for reduced latency, higher user data rates, improved system capacity and coverage, and reduced cost for the operators. The first LTE product is expected to be available in 2010 [1].

The new LTE RAN is called E-UTRAN, which is composed of only one node, called Evolved Node-B (eNode-B) [5]. The radio interface of LTE uses Orthogonal Frequency Division Multiple Access (OFDMA) in the DL and Single-Carrier Frequency Division Multiple Access (SC-FDMA) in the UL. LTE standards have been defined with as much flexibility as possible so that the operators can deploy them in all current and existing frequencies as well as new spectrum. The physical layer of the LTE is defined in a bandwidth-agnostic way and supports various system bandwidth (1.4 to 20 MHz) in both FDD and TDD modes [3]. OFDMA multiplexes different users in time and frequency domain. The time and frequency domain adaptation of OFDMA is a key feature for increasing cellular capacity. The radio resource is subdivided into PRBs consisting of 12 subcarriers with 15 KHz spacing and a time duration of 1 ms [3]. PRBs are dynamically allocated to users in order to realize multi-user diversity gain in both time and frequency domains, leveraging adaptive modulation and coding with hybrid automatic repeat request (HARQ). To meet the performance requirements, the LTE Release'8 relies on MIMO transmission and reception techniques, with 2x2 MIMO as the baseline for DL and 1X2 MIMO for UL. However, higher order antenna configurations are also supported [5].

LTE is an all IP technology and supports full mobility and global roaming. LTE also facilitates gradual deployment ensuring smooth migration from the existing networks and offers deployment in existing and new FDD spectrum bands. LTE will be the technology

of choice for most of the existing 3GPP networks. The research forecasts more than 32 million LTE subscribers by 2013 despite the fact that LTE network will not be commercial until 2010 [1].

3GPP Long Term Evolution-Advanced (LTE-A)

The International Telecommunications Union (ITU) is currently working on specifying the system requirements towards next generation mobile communication systems called International Mobile Telecommunications-Advanced (IMT-A). The deployment of IMT-A systems is believed to take place around year 2015 at mass market level. IMT-A systems are expected to provide peak data-rates in the order of 1 Gbps in downlink and 500 Mbps in uplink [6], [7]. The 3GPP aims to further evolve the LTE towards LTE-A systems in order to meet or exceed the IMT-A requirements as well as its own requirements for advancing LTE for long term competitiveness [6]. The following performance targets are set for LTE-A to meet the IMT-A requirements, while maintaining the backward compatibility with LTE release'8 [6], [8].

LTE- A Performance Targets

- Average spectral efficiencies of up to 3.7 b/s/Hz/cell in the DL (with 4×4 antenna configuration) and 2.0 b/s/Hz/cell in UL (2×4).
- Cell edge spectral efficiencies of 0.12 b/s/Hz in the DL (4×4) and 0.07 b/s/Hz in the UL (2×4).
- Peak data rates of up to 1Gb/s in the DL and 500 Mb/s in the UL.
- Peak spectrum efficiencies of 30 b/s/Hz in the DL and 15 b/s/Hz in the UL using antenna configurations of 8×8 in DL and 4×4 in the UL.
- Low cost of infrastructure deployments and terminals and power efficiency in the network and terminals.

1.3 Thesis Motivation and Objectives

The network operators need to maximize the utilization of spectral resources in order to meet the ambitious data rate targets of the next generation communication systems. Hence, there is a need to develop solutions allowing for a more efficient utilization of the available spectrum. The aim of the PhD study is to investigate the potential techniques for efficient usage of the spectrum keeping in view the requirements of the next generation mobile communication systems. The overall objective of this PhD study is identified to answer the question, "How to enhance the efficiency of spectrum usage for the next generation mobile communication systems?" The LTE and LTE-A are taken as the example cases for next generation systems. Our focus is on Wide Area (WA) outdoor and Local Area (LA) indoor cellular deployment scenarios. For WA outdoor deployment the study is focused on LTE, whereas for LA indoor deployment scenario the study is focused on

LTE-A system. Our focus is on developing system level solutions and their performance evaluation.

The spectrum efficiency (amount of information bits per unit of spectrum per unit of area) is often used as figure of merit. The spectrum efficiency determines the required amount of spectrum to meet the service requirements. It directly relates to the operators' economies, cost of service delivery, and users' experience [9].

Two main approaches could be used to improve spectral utilization. The first approach relies on squeezing a larger number of bits/second/Hz in the allocated spectrum. This can be accomplished by using higher order modulation and MIMO techniques at the physical layer. The second approach relies on aggressive spatial reuse of assigned spectrum. This involves breaking large cells into smaller cells and deploying more base stations using lower peak power [9].

This PhD study is motivated by the second approach for the following reasons:

- The growth in wireless capacity is exemplified by following observation of Martin Cooper: "The wireless capacity has doubled every 30 months over the last 104 years". This translates into an approximately million fold capacity increase since 1957. Breaking down these gains shows a 25x improvement from wider spectrum, a 5 x improvement by dividing the spectrum into smaller slices, a 5x improvement by designing a better modulation scheme, and a 1600x gain through reduced cell sizes and transmit distance. The enormous gains reaped from smaller cell sizes arise from efficient spatial reuse of the spectrum or, alternatively, higher area spectral efficiency [10].
- So far plenty of efforts have been dedicated for improving the spectral efficiency using physical layer techniques. The research studies show that the physical layer techniques have nearly reached their capacity limits, and the improvements in spectrum usage could be only marginally improved at reasonable cost, whereas the system level approaches have not been fully exploited towards improving system capacity.

We identified the following open issues for investigation:

The first issue we need to address is the higher order sectorization (HOS). In order to increase the spectrum utilization, HOS is considered in the DL of LTE system. Typically three sectors per site deployment are considered for the LTE systems. A migration to six sectors per site deployment is considered in this study. The scope of study also includes a mixed network topology consisting of a combination of three and six sectors per site. The HOS provides a means to improve the coverage and capacity per unit area and therefore improves the efficiency of spectrum utilization.

The second critical issue is Inter-cell Interference Avoidance (ICIA)for LTE, which is an important aspect for improving system capacity and coverage. Inter-cell interference coordination (ICIC) has been extensively considered in LTE for controlling the interference between cells in order to further improve the so-called cell-edge user performance.

The ICIC schemes primarily rely on frequency domain sharing between cells and adjustment of transmission power. This PhD study aims to develop mechanisms for ICIA under fractional load conditions. The fractional load conditions arise when there is no enough traffic in the cell and all the resources are not required to be used. Under this condition the mechanisms can be developed to efficiently use the required amount of spectrum to improve the experienced SINR condition and in turn to improve the coverage and capacity over the given amount of spectrum.

Another research topic is concerning LTE-A, which is expected to provide 1Gbps in DL. Such high data rate requires high bandwidth as well as high efficiency of spectrum usage. The surest way to increase capacity of a wireless link is by getting the transmitter and receiver closer to each other, which create the dual benefits of higher quality link and more spatial reuse. In a network with nomadic users, this inevitably involves deploying more infrastructures, typically in the form of micro cells, hot spots, distributed antennas or relays. A less expensive alternative is the recent concept of home base stations, which are data access points installed by home users to get better indoor voice and data coverage [10]. Due to their short transmit -receive distance, home base stations can greatly lower transmit power and achieve a higher SINR. This translates into improved reception and higher capacity, and therefore improved spectrum utilization.

When several operators will deploy home base stations in the given geographical area, sharing over the same spectrum pool, then policies become mandatory to ensure fair and efficient usage of the spectrum. Moreover, the Home base stations are expected to be user deployed, self configurable and self adjustable according to the radio environment, therefore a degree of cognitivity is also assumed. Keeping these perspectives in view this PhD study also investigates the concept of policy and the cognitive aspects of the devices.

In summary the detailed objectives explained above can be boiled down into the following fundamental task: "Improvement in system capacity and coverage over the given spectrum with minimum increase in system complexity and signaling requirements".

1.4 Scientific Methodology Employed

The main objective of this PhD study is to provide an understanding at the system level performance, hence a system level approach is used. In fact the system level performance can be analyzed by various means such as analytical approach based on system model, computer aided simulation and field trial in operational network. Analytical approach may provide a viable approach when the system model is simple, but it becomes infeasible for modern cellular systems which are complex and involve numerous assumptions and constraints. The system level performance of modern cellular systems depends on a large number of parameters whose behavior cannot be predicted beforehand, making it tedious to formulate a theoretical framework. Consequently, a closed form analytical expression characterizing system performance is seldom possible. On the other hand field trial requires the availability of the network, which may not always be feasible (e.g. the LTE and LTE-A operational networks are not yet available). Under such circumstances

the computer aided simulation approach presents a suitable option. If the metrics are meaningful and the methodology reflects realistic networks, computer aided simulation is a good way to compare different concepts and predict the network performance [8]. For this reason a computer aided system level simulation has been used in this PhD study as the main performance assessment methodology, sometimes supported by the theoretical analysis to understand the simulation results more accurately.

The work in this thesis is divided in two phases. The first phase provides the performance results for LTE system in the DL. A quasi-dynamic system level simulator built in C++ is employed, which uses the 3GPP LTE system model as described in [11]. The system model includes detailed implementation of Link Adaptation (LA) based on Adaptive Modulation and Coding (AMC), explicit scheduling of Hybrid Automatic Repeat reQuest (HARQ) processes including retransmissions, link-to-system mapping techniques suitable for OFDMA. The study included development of the system level simulator for six sector implementation and performance evaluation in typical urban macro cellular environment.

The second part of the study involves LTE-A indoor deployment, which is based on a quasi dynamic system level simulator built in Matlab. The system model uses most of the features for IMT-A system recommended for local area scenario. The simulator is still in the development phase. The simulator provides features for fully configurable room/apartment/ wall/corridor/floor for indoor layout. It supports randomized users generation and distribution, different synchronization cases, i.e. fully, loose, non-synchronized, and several other features to support the LTE-A system requirements. The simulator is further developed to support the features of the proposed algorithms.

1.5 Novelty and Contributions

This PhD study mainly contributes towards providing a system level understanding of various mechanisms for improving the efficiency of spectrum utilization. The LTE and LTE-A systems are mainly considered for such study. The considered mechanisms in this study involved conceptual design, system modeling, software development, implementation and performance evaluation.

The first topic of research is related to Higher Order Sectorization, where we consider 6 sector site deployment for LTE DL. My main contribution in this regard is implementation and performance evaluation of 6 sector site network deployment. In addition to this my contribution also lies in proposal, implementation, and performance evaluation of mixed network topology. A mixed network topology consists of a combination of 3 and 6 sector site deployment. A significant system capacity gain is realized by 6 sector over the typically assumed 3 sector deployment. The realized gain is further improved by mixed network topology. The main contribution and novelty of this PhD study lies in the fact that no such performance study was available in the open literature for LTE; therefore this study fills the gap in the literature in this regard. The results of this study have been published in the following article:

- " Sanjay Kumar, I. Z. Kovacs, G Monghal, K. I. Pedersen, P. E. Mogensen "Performance Evaluation of 6 Sector Cell Lay Out For 3GPP Long Term Evolution", IEEE VTC, Calgary, Canada, 21-24 Sep, 2008.

The second topic of research is related to the Inter-Cell Interference Avoidance (ICIA) under Fraction Load (FL) conditions for LTE DL. Numerous studies are available on Inter-Cell Interference Coordination (ICIC) at full load conditions, but only few studies are available on FL. In this study we propose several algorithms for ICIA and recommend that the ICIA algorithm needs to be integrated with the packet scheduler functionalities in order to improve the average experienced SINR, leading to improved coverage and capacity. Part of the discussion and the results presented in this study is an outcome of a collaborative work with a fellow researcher and joint supervision of master thesis at Aalborg University in collaboration with Nokia Siemens Networks, Aalborg. My contribution is in jointly developing the algorithm, planning simulation methodology and adaptation to the system level simulator. The results of this contribution are published in the following article:

- " Sanjay Kumar, G. Monghal, Jaume Nin, Ivan Ordas, K. I. Pedersen, P. E. Mogensen, "Autonomous Inter Cell Interference Avoidance under Fractional Load for Downlink Long Term Evolution", IEEE Vehicular Technology Conference, Barcelona, Apr 26-29, 2009.

In addition, the following article in this area of study is also co- authored:

- " Guillaume Monghal, Sanjay Kumar, K. I. Pedersen and P. E. Mogensen, " Integrated Fractional Load and Packet Scheduling for OFDMA Systems ", (Submitted to ICC for International Workshop on LTE Evolution,June 2009, Dresden, Germany.

The third topic of research presented in this study is related to Flexible Spectrum Usage (FSU) in local area indoor deployment for LTE-A. The work was undertaken together with the fellow researchers at Aalborg University as part of the Spectrum Sharing project. In this regard our effort was directed to develop an autonomous, self-configurable and scalable solution for such deployment scenario. My personal contribution in this regards was proposal, development and performance evaluation of a novel Spectrum Load Balancing (SLB) algorithm. The SLB algorithm ensures coexistence in the given geographical area by partially or completely preventing mutual interference over the shared spectrum. Further, an Resource Chunk Selection (RCS) algorithm was developed in collaboration with a fellow researcher, where my personal contribution lies in jointly developing the concept of the algorithm and evaluation of the performance in the given scenario. Presently, the research in this area is in the evolving phase, therefore the proposed concepts and algorithms can be regarded as significant contributions in this emerging area of research. The results of this study are published in the following article:

- " Sanjay Kumar, Y. Wang, N. Marchetti, I. Z. Kovács and P. E. Mogensen, "Spectrum Load Balancing for Flexible Spectrum Usage in Local Area Deployment Scenario" IEEE Symposium on Dynamic Spectrum Access 2008 (DySPAN 2008), Chicago, USA, Oct 14-17, 2008

In addition, the following article has been also published, which is an outcome of joint work with fellow researchers during the initial phase of study on flexible spectrum usage.

- " Sanjay Kumar, G. Costa, S. Kant, Flemming B. Frederiksen, N. Marchetti and P. E. Mogensen, "Spectrum Sharing for Next Generation Wireless Communication Networks", First International Workshop on Cognitive Radio and Advanced Spectrum Management (CogART'08), Aalborg, Feb. 14, 2008.

Also, the following article has been co-authored during the study on local area deployment and flexible spectrum usage.

- " Yuanye Wang, Sanjay Kumar, Luis Garcia, K. I. Pedersen, I. Z. Kovács, Simone Frattasi, Nicola Marchetti, P. E. Mogensen and T. B. Sørensen "Fixed Frequency Reuse for LTE-Advanced Systems in Different Scenarios", IEEE Vehicular Technology Conference, Barcelona, Apr 26-29, 2009.

The fourth topic presented in this thesis is on Autonomous Component Carrier Selection in uncoordinated deployment for local area of LTE-A. This is a joint work with fellow researcher at Aalborg University and Nokia Siemens Networks colleagues in Aalborg. My main contribution in this study is related to jointly developing primary component carrier selection scheme, quality monitoring of primary component carrier and recovery action. The concept and the outcome of the results of this study are presented in the following 3GPP contributions:

- " 3GPP, R1-090735, "Primary Component Carrier Selection, Monitoring, and Recovery– Nokia Siemens Networks, Nokia", TSG RAN WG1 Meeting , Athens, Greece, February 9-13, 2009.
- " 3GPP, R1-084321, "Algorithms and Results for Autonomous Component Carrier Selection for LTE-Advanced- Nokia Siemens Networks, Nokia", TSG RAN WG1 Meeting Prague, Czech Republic, November 10-14, 2008.
- " 3GPP, R1-083103, "Autonomous Component Carrier Selection for LTE-Advanced –Nokia Siemens Networks, Nokia", TSG RAN WG1 Meeting, Jeju Island, Korea, August 18-22, 2008

The fifth and the last topic of study presented in this thesis is related to multi operator FSU, where the deployment by several operators in the given geographical area is considered. In this regard a novel concept 'Policy Assisted Light Cognitive Radio enabled FSU'

is presented in the thesis. The work and my contribution in this chapter includes proposal of the concept, algorithm development and implementation, and performance evaluation for the given scenario. However, during the implementation phase the support by master students at Aalborg university, whom I co-supervised, is also recognized.

- " Sanjay Kumar, V. Palma, E. Borgat, N. Marchetti, and P. E. Mogensen "Light Cognitive Radio for Flexible Spectrum Usage in Local Area Deployment" IEEE Vehicular Technology Conference 2009 (VTC 2009), Barcelona, Apr 26-29, 2009.

In addition the following article has been published, which provides an overview of the existing state of the art concerning the technical requirements and technological solutions for IMT-A systems.

- " Sanjay Kumar and Nicola Marchetti, "IMT-Advanced : Technological Requirements and Solution Components", International Conference on Wireless VITAE, Aalborg, 17-20 May 2009

Apart from the above contributions, the following articles have also been published during the PhD study. These are the outcome of the preliminary directions at the outset of the PhD study, and are not included in the PhD thesis.

- " Sanjay Kumar, S. S. Das and Ramjee Prasad, "Proportional Fair Scheduling With QoS Constraints in the Downlink of OFDMA Systems," Symposium on Wireless Personal Multimedia Communications (WPMC), Jaipur, India, Dec 3-6, 2007.
- " Nicola Marchetti, Muhammad Imadur Rahman, Sanjay Kumar and Ramjee Prasad, "OFDM: principles and challenges", chapter in the book 'New Directions in Wireless Communications Research', Springer Publications, in press.

1.6 Thesis Outline

The PhD thesis is organized as follows:

Chapter 2: System Description.
This chapter provides a general description of LTE and LTE-A systems. The Architecture, Radio Resource Management (RRM) functionalities, Multiplexing and Duplexing schemes of LTE are discussed. A general system model of LTE under consideration is outlined. Also, a general system model of LTE-A and various assumptions for local area indoor deployment scenario are presented in this chapter.

Chapter 3: Higher Order Sectorization for LTE DL.
This chapter introduces briefly the concept and benefits of higher order sectorization. It

includes the antenna pattern and different network topologies used for performance evaluation of 6 sector site deployment for LTE DL. The proposed mixed network topologies and their performance evaluation are also presented in this chapter.

Chapter 4: Inter-cell Interference Avoidance under Fractional Load for LTE DL.
This chapter provides a brief account of the Inter-Cell Interference Coordination (ICIC) for LTE DL and afterwards provides a discussion on the concept of Inter-Cell Interference Avoidance (ICIA) under fractional load conditions. The description of the various schemes proposed for ICIA are given, and their performance results are presented in this chapter.

Chapter 5: Flexible Spectrum Usage for LTE-Advanced.
This chapter discusses the relevance of Flexible Spectrum Usage in the context LTE-A local area deployment scenario. The proposed Spectrum Load Balancing (SLB) and Resource Chunk Selection (RCS) algorithms for FSU are described in this chapter. The performance analysis of the proposed schemes are presented, and a self-configurable solution for local area indoor deployment scenario is suggested in this chapter.

Chapter 6: Autonomous Component Carrier Selection for IMT-A.
This chapter presents the concept of carrier aggregation as a means to achieve wider bandwidth for the LTE-A system. A concept of primary and secondary component carriers is provided. A description of the overall primary states, quality monitoring and recovery action are discussed in this chapter. A self-adjustable solution for LTE-A uncoordinated local area deployment is suggested by means of autonomous component carrier selection mechanism.

Chapter 7: Policy Assisted Light Cognitive Radio for FSU.
This chapter describes the concept of FSU in multi operators' domain and highlights the importance of policy and the concept of cognitive radio for fair, flexible and efficient spectrum allocation among the operators deployed in the given geographical area. In this respect a concept of Policy Assisted Light Cognitive Radio for FSU is presented.

Chapter 8: Conclusions and Recommendations.
This chapter provides the summary of overall study and discusses future research issues.

Chapter 2

System Description

2.1 Introduction

This chapter provides a description of the systems under consideration. Different assumptions are outlined and their relevance to the study is discussed. The Long Term Evolution (LTE) and LTE-Advanced (LTE-A) are considered as the case study, therefore the descriptions provided in this chapter are mostly relevant to these systems.

The chapter is organized as follows: Section 2.2 provides an overview of the LTE architecture and a discussion on its main components. Section 2.3 gives a description of the Radio Resource Management (RRM) functionality in LTE. The duplexing scheme and LTE frame structures are illustrated in section 2.4. The LTE and LTE-A system models under consideration are outlined in section 2.5 and 2.6 respectively.

2.2 LTE Architecture

The LTE architecture has two distinct components: Core Network (CN) and Radio Access Network (RAN). The CN is called Evolved Packet Core (EPC) and the RAN is called Evolved Universal Terrestrial Radio Access Network (E-UTRAN). The EPC and E-UTRAN together constitute the Evolved Packet System (EPS). Figure 2.1 gives a pictorial representation of the LTE architecture.

Evolved Packet Core (EPC)

The EPC is based on the internet protocol and provides one common packet core network for 3GPP radio access (LTE, 2G and 3G), non 3GPP radio access (WLAN and WiMAX), and fixed access (Ethernet, DSL, cable and fiber). The main characteristic of EPC is its simplified architecture. The network latency and complexity are reduced in EPC as there are fewer hopes in both the control and data planes. It has three main

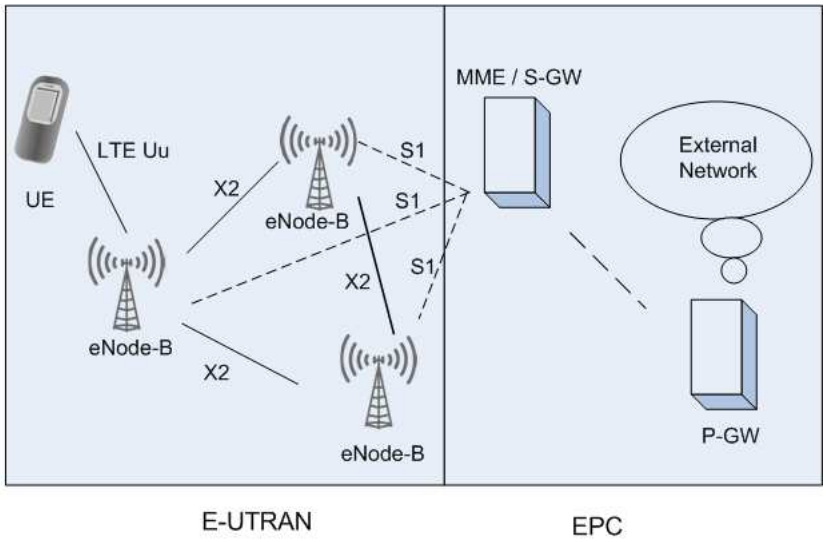

Figure 2.1: Pictorial representation LTE architecture.

nodes; Mobility Management Entity (MME), Serving Gateway (S-GW) and the PDN Gateway (P-GW). MME enables the transfer of subscription and authentication data for authenticating/authorizing users' access. S-GW routes and forwards user data packets, while also acting as the mobility anchor for the user plane during inter-eNode-B handovers and as the anchor for mobility between LTE and other 3GPP technologies. The P-GW provides connectivity for the UE to external packet data networks by being the point of exit and entry of traffic for the UE.

E-UTRAN

It consists of just one node, the Evolved Node B (eNode-B), which performs all the Radio Resource Management (RRM) as well as radio functions. The eNode-B interacts to MME on the signaling plane and directly to the S-GW on the data plane. The eNode-B hosts the Physical Layer (PHY), Medium Access Control (MAC), Radio Link Control (RLC), Packet Data Convergence Protocol (PDCP) and Radio Resource Control (RRC) layers. The RRM functionalities of E-UTRAN are discussed in section 1.4.

The E-UTRAN is based on Orthogonal Frequency Division Multiplexing (OFDM) and Single-Carrier Frequency Division Multiple Access (SC-FDMA) technologies [12]. The OFDM is briefly described below.

2.2.1 Orthogonal Frequency Division Multiplexing

The OFDM has been adopted as the transmission scheme for the LTE, and is also used for several other radio technologies, e.g. WiMAX [13], [3] and DVB broadcast technologies [14].

OFDM is used as a digital multi-carrier modulation scheme. In OFDM the total system bandwidth is divided into a large number of closely-spaced, spectrally overlapping, but mutually orthogonal subcarriers [15]. These closely-spaced orthogonal sub-carriers are used to carry parallel data streams. Each sub-carrier is modulated with a conventional modulation scheme, such as Quadrature Amplitude Modulation (QAM) or Quadrature Phase Shift Keying (QPSK)[16].

The primary advantage of OFDM is its ability to cope with severe channel conditions, narrowband interference and multipath fading. The channel equalization is simplified because OFDM can be viewed as using many slowly-modulated narrowband signals rather than one rapidly-modulated wideband signal. Due to slow symbol rate in OFDM, the guard interval between the symbols is effectively used to handle time spreading and to eliminate Inter-Symbol Interference (ISI). Figure 2.2 shows the OFDM transmission technique.

In OFDM the number of subcarriers can range from less than one hundred to several thousands, with the subcarrier spacing ranging from several hundred kHz down to a few kHz. What subcarrier spacing to use depends on the type of environment the system is to operate in, including such aspects as the maximum expected radio channel frequency selectivity (maximum expected time dispersion) and the maximum rate of channel variations (maximum expected Doppler spread). Once the subcarrier spacing has been selected, the number of subcarriers can be decided based on the assumed overall transmission bandwidth, taking into account acceptable out-of-band emission [3]. The OFDM allows the possibility of flexible bandwidth allocation by varying the number of sub carriers used for transmission, while keeping the subcarrier spacing unchanged. LTE supports the operation of spectrum allocations of 1.4, 3, 5, 10, 15 and 20 MHz [3].

The basic OFDM parameters that need to be configured are; subcarrier spacing, number of subcarriers and Cyclic Prefix (CP) length. The LTE uses a basic subcarrier spacing of 15 kHz. The number of sub carriers depends on the transmission bandwidth. As an example, 600 subcarriers are considered over a 10 MHz system bandwidth [11]. The E-UTRAN multiple access techniques, i.e. OFDMA and SC-FDMA, are described in the following subsections.

2.2.2 Orthogonal Frequency Division Multiple Access

In OFDMA the multiple access is achieved by assigning subsets of subcarriers to individual users. In principle, fully flexible allocation of the subcarriers to different users can be supported in OFDMA. However, a subcarrier level granularity in resource allocation is difficult due to practical limitations. Therefore, the resources are partitioned in time and frequency domain resource blocks to minimize signaling and simplify resource allocation. LTE defines a Physical Resource Block (PRB) as the smallest resource allocation unit. A PRB is defined by N OFDM symbols in time domain and M consecutive subcarriers in the frequency domain thus a PRB consists of NxM resource elements [18]. A PRB consists of 12 consecutive sub carriers (180 kHz spectrum bandwidth) in frequency

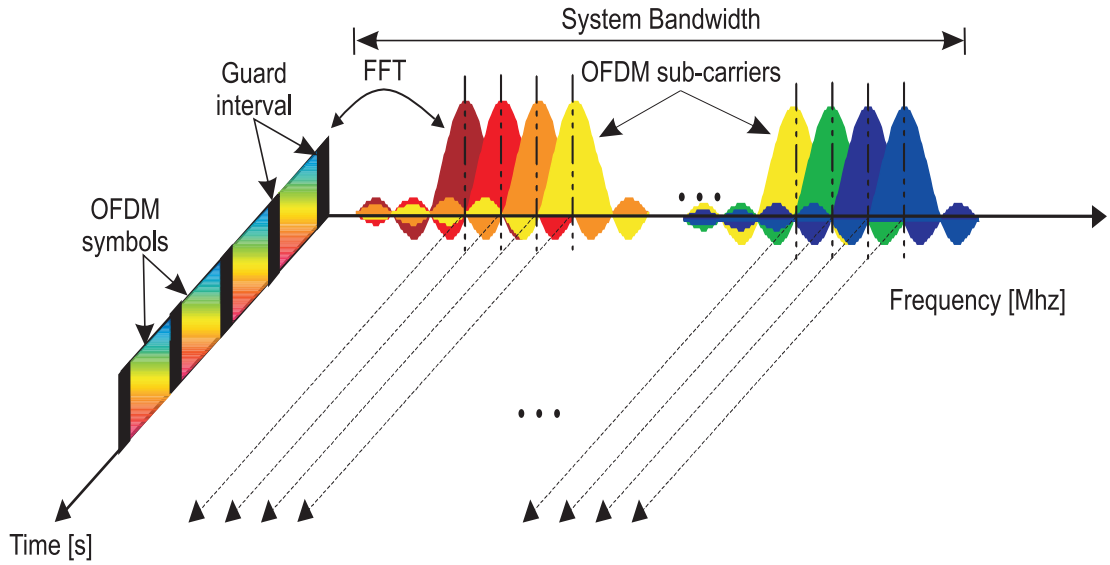

Figure 2.2: Illustration of the OFDM transmission technique [17].

domain and 14 adjacent OFDM symbols (1 ms duration) in time domain for short cyclic prefix configuration. The time domain allocation unit is also called Transmission Time Interval (TTI) in LTE.

Based on the instantaneous channel conditions in frequency domain, the different sub-carriers can be allocated to different users using OFDMA. The OFDMA also allows the dynamic adjustment of the bandwidth usage and therefore supports adaptive resource allocation in multi user scenario. An example of time and frequency domain resource allocation to two users is presented in Figure 2.3.

2.2.3 Single-Carrier Frequency Division Multiple Access

The main disadvantage of OFDM is the high Peak-to-Average Power Ratio (PAPR) due to multi carrier transmission. High PAPR implies lower power amplifier efficiency and higher mobile terminal power consumption. Therefore,instead of OFDMA, the SC-FDMA is used in the UL of LTE. While retaining most of the advantages of OFDM, SC-FDMA also exhibits significantly lower PAPR resulting in reduced power consumption for UE and improved coverage. However, the benefit of lower PAPR is at the cost of single carrier constraint, i.e. it requires that the subcarriers to be allocated to a single user should be adjacent. SC-FDMA has similar throughput performance and essentially the same overall complexity as OFDMA [19].

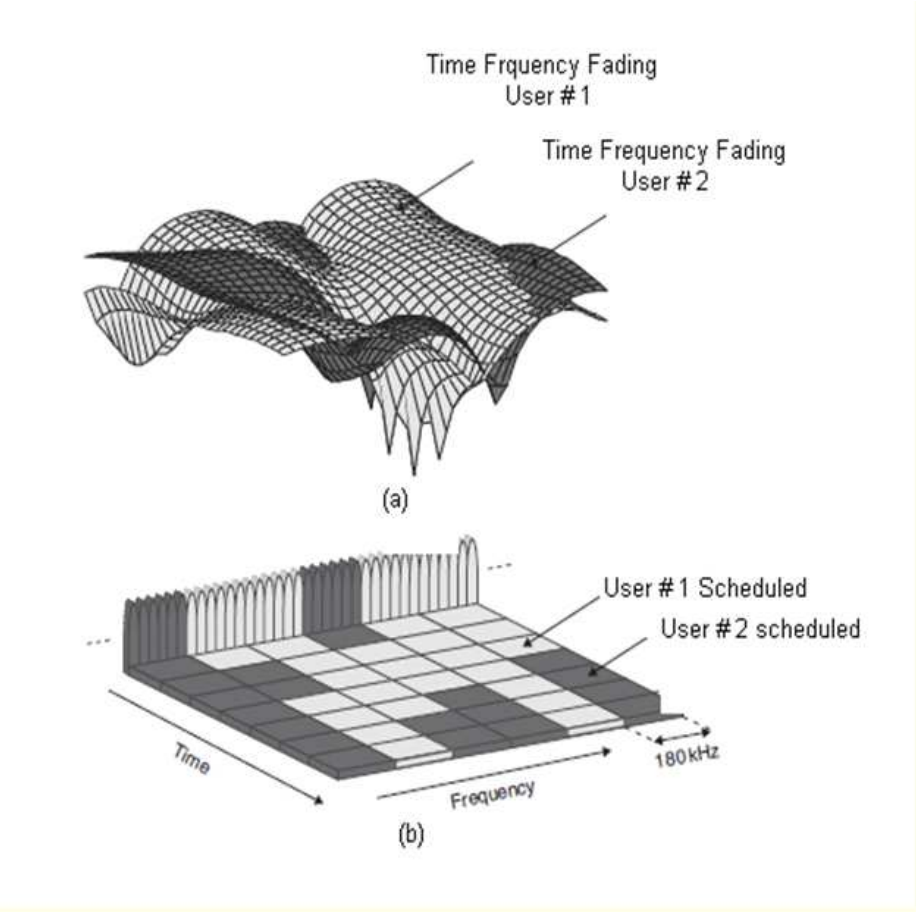

Figure 2.3: Example of time and frequency domain resource allocation using OFDMA [5].

2.3 RRM Functionality

RRM involves strategies and algorithms for controlling interference, transmit power, modulation schemes etc., in order to utilize the radio resources as efficiently as possible. The wireless channel experiences variations due to frequency selective fading, shadow fading, distance dependent path loss and interference. These variations could be exploited favorably to improve system performance by means of channel dependent scheduling. The channel dependent scheduling takes the channel variations into account to achieve efficient resource allocation. The Link Adaptation (LA) is closely related to the channel dependent scheduling. The LA deals with setting the transmission parameters of a radio link to handle variation of the radio link quality. The channel dependent scheduling together with LA aim to adapt the channel variations prior to transmission. However, a perfect adaptation to instantaneous radio link quality is not realized, due to the random channel variations. The data may be received in error. Therefore, a Hybrid Automatic Repeat reQuest (HARQ) scheme is employed, which requests retransmission of erroneously received data. In this way HARQ complements channel dependent scheduling and LA after transmission.

2.3.1 Packet Scheduling

The packet scheduler is basically responsible for selection of users to be scheduled, and also scheduling of HARQ retransmissions. During the decision making, the packet scheduler interacts closely with the LA unit. The information about the Downlink (DL) channel conditions, necessary for channel dependent scheduling, is fed back from users to the eNode-B via channel quality reports. The channel quality reports, also known as Channel Quality Information (CQI), include information about the instantaneous channel quality in the frequency domain. The PS in LTE dynamically determines, in each 1 ms interval, which users are supposed to receive Downlink Shared Channel (DL-SCH) transmissions and on what resources. The one millisecond basis for PS in LTE is used in order to adapt to fast channel variations and therefore take advantage of the Multi User Diversity (MUD) gain, where the gain obtained by transmitting to users with favorable channel conditions is called MUD gain.

In addition to the CQI, the packet scheduler also takes into account the buffer status, QoS parameters of different users and priorities, HARQ status and ACK/NAK reports in the scheduling decisions. Interference coordination, which tries to control the interference, is also part of the packet scheduler functionality. In our study we used decoupled time and frequency Domain Packet Scheduler [20], briefly explained below.

Decoupled Time and Frequency Domain Packet Scheduler

Figure 2.4 presents the basic architecture of the decoupled time and frequency Domain PS. It consists of two main entities : Time-Domain Packet Scheduling (TDPS) and Frequency-Domain Packet Scheduling (FDPS). The Time-Domain (TD) scheduling is first performed followed by Frequency-Domain (FD) scheduling. For each TTI the TDPS selects N users for Frequency Domain Multiplexing (FDM). The FDPS then decides how to multiplex those users on the available Physical Resource Blocks (PRBs). This PS offers simple, flexible and low complexity framework for time and frequency domain packet scheduling. Both the TDPS and FDPS entities take input from the LA unit in order to take the radio channel conditions into account in the scheduling decision.

Packet Scheduling Strategies

Different strategies could be used for packet scheduling. The scheduling of the users with the best channel condition is referred to as max-C/I (maximum rate scheduling), which can be expressed as scheduling user k given by:

$$k = argmax_{(i)} R_i \tag{2.1}$$

where R_i is the instantaneous data rate for user i. This leads to high multiuser diversity gain and hence high system capacity. The high MUD gain is realized when the number of users is large and the channel variations are high. However, a pure max-C/I scheduling may starve the users in bad channel conditions, and therefore this scheduling does not provide a fair strategy. An alternative to max-C/I is Round Robin (RR) scheduling, which allows the users to take turns in using the resource, without taking the instantaneous

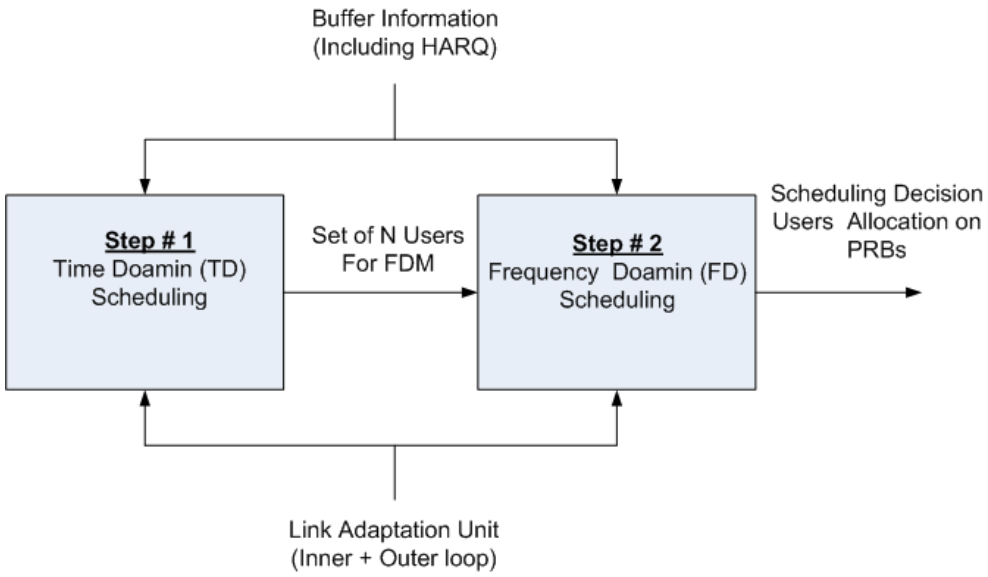

Figure 2.4: The decoupled time and frequency domain packet scheduler.

channel conditions into account. The RR scheduling can be seen as a fair scheduling in terms of the the amount of resource allocation to each user. However, it cannot be fair in the sense of providing the same throughput due to different channel conditions. This scheduling strategy results in overall low system performance [3].

A practical scheduler should run in between the max-C/I and RR scheduler, that is try to utilize fast variations in channel conditions as much as possible while still satisfying some degree of fairness among the users. one example of such scheduler is Proportional Fair (PF) scheduler , which assigns the resources to the user with the relatively best radio link conditions, i.e. at each time instant user k is scheduled for transmission according to [3]:

$$k = argmax_{(i)} \frac{R_i}{\bar{R}_i} \tag{2.2}$$

where R_i is the instantaneous data rate for user i, and $\bar{R}_i$ is the average data rate of user i. The average is obtained over a certain averaging period. The averaging period is selected to ensure efficient usage of the short term channel variations and at the same time limit the long term differences in the channel quality [3]. The considered scheduler uses proportional fair strategy in both time and frequency domain.

2.3.2 Link Adaptation

In wireless communications, the channel capacity can be maximized if the transmitter adapts it transmit power, data rate, modulation, and coding scheme according to the channel variations. The dynamic transmit power control, used to compensate the variations in the instantaneous channel conditions, can be seen as a kind of link adaptation. An alter-

native to dynamic transmit power control is dynamic rate control, where the data rate is dynamically adjusted to compensate for the varying channel conditions. The data rate is controlled by adjusting the modulation scheme and/or channel coding rate, and therefore, sometimes referred to as Adaptive Modulation and Coding (AMC)[3].

LTE supports fast adaptive LA, performed on millisecond basis. The LA is based on the CQI reports and aims to ensure that the most suitable Modulation and Coding Scheme (MCS) is always used. The PS interacts with LA unit in order to make scheduling decisions. The LA unit consists of an inner loop algorithm and an outer loop algorithm. The inner loop algorithm is the primary unit, which estimates the transport block size and modulation scheme based on the CQIs reports. Whereas the Outer Loop Link Adaptation (OLLA) helps to maintain the desired BLock Error Rate (BLER) target.

2.3.3 Hybrid ARQ

In LTE HARQ, a combination of Forward Error Correction (FEC) and Automatic Repeat ReQuest (ARQ) is used to provide a robustness against transmission errors. HARQ uses FEC to correct a subset of all errors and relies on error detection to detect uncorrectable errors. Erroneously received packets are discarded, and the receiver requests retransmissions. In HARQ with soft combining, the erroneously received packet is stored in a buffer memory and later combined with the retransmission to obtain a single, combined packet which is more reliable than its constituents. The HARQ with soft combining is usually categorized with the chase combining and incremental redundancy. In chase combining the retransmissions consist of the same set of coded bits as the original transmission. In incremental redundancy, each retransmission need not to be identical with the original transmission.

LTE employs HARQ with soft combining. The HARQ protocol is part of the MAC layer, while the soft combining is handled at physical layer. In LTE the HARQ protocol uses multiple parallel stop and wait processes. The current assumption in LTE is asynchronous and adaptive HARQ for the DL. This implies that the PS has the freedom to freely schedule pending HARQ retransmissions in both the frequency and time domain.

2.3.4 Channel Quality Indicator

The information about the DL channel conditions, necessary for link adaptation and channel dependent scheduling, is fed back from users to the eNode-B via channel quality reports. The channel quality reports also known as CQI, include information about the instantaneous channel quality in the frequency domain. The basis of CQI report is measurement on the DL reference signals.

The PS and LA entities employ CQI feedback. The inner loop LA unit determines the modulation scheme for the different users based on CQI feedback. The CQI consists of a set of values corresponding to an estimate of the Signal to Interference plus Noise

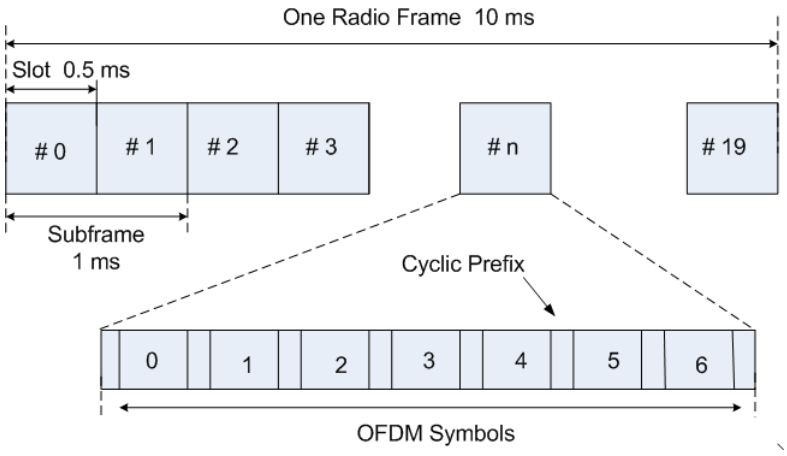

Figure 2.5: The LTE type 1 frame structure, applicable for both full and half duplex FDD [18]

Ratio (SINR) on each CQI block. A CQI block consisting of 2 PRBs is considered in our LTE study. The receiver imperfections are modeled by adding a zero mean Gaussian error of 1 dB standard deviation to the ideal CQI as in [21]. The CQI is further quantified with a 1dB step. A processing delay equivalent to 2 TTI is considered.

2.4 Duplexing Scheme and LTE Frame Structure

LTE supports both Frequency Division Duplex (FDD) and Time Division Duplex (TDD) schemes. DL and UL transmissions are organized in radio frames with 10 ms duration. Two frame structures are supported. Type 1 applicable to FDD and Type 2 applicable to TDD [18].

Frame Structure Type 1

This is applicable to both full duplex and half duplex FDD. Each LTE frame consists of $10\ ms$ duration. They are divided into 10 subframes, each subframe is further divided into two slots, each of $0.5\ ms$ duration. A slot consists of either 6 or 7 OFDM symbols, depending on whether a short or long cyclic prefix is used. Subframe is defined as two consecutive slots where subframe i consists of slots $2i$, and $2i + 1$. Figure 2.5 shows the frame structure.

Frame Structure Type 2

This is applicable to TDD. Each radio frame consists of two half-frames each with the length of $5\ ms$. Each half-frame consists of eight slots of length $0.5\ ms$ and three special fields, Downlink Pilot Time Slot (DwPTS), Guard Period (GP), and Uplink Pilot Time Slot (UpPTS). The lengths of DwPTS and UpPTS are configurable subject to the total length of DwPTS, GP and UpPTS being equal to $1\ ms$. Subframe $\#1$ and $\#6$ consists of DwPTS, GP and UpPTS, all other subframes consist of two slots. Both $5\ ms$ and $10\ ms$

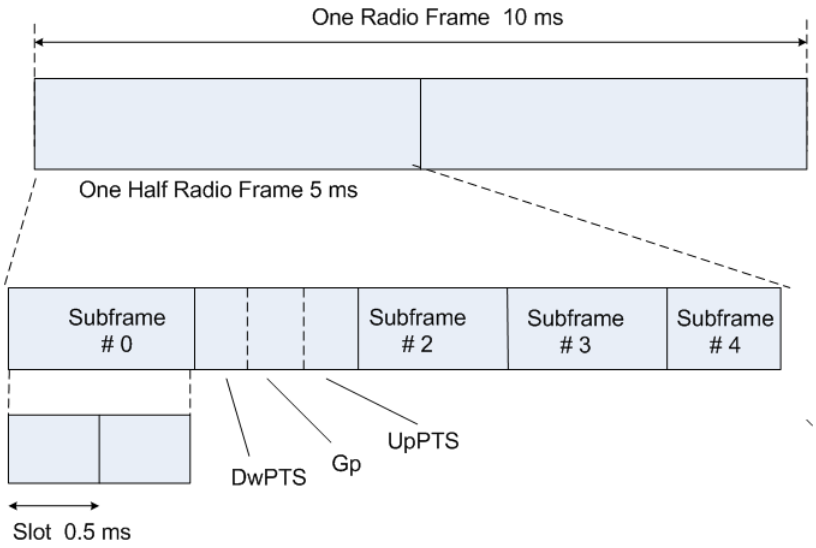

Figure 2.6: The LTE type 2 frame structure, applicable for TDD [18]

switch-point periodicity are supported. Figure 2.6 shows the structure of frame type 2.

2.5 LTE System Model

Figure 2.7 represents a general system model under consideration. The system model used for performance evaluation follows the 3GPP LTE recommendations [11]. A cellular layout of 19 hexagonal sites is considered. Each site typically consists of 3 sectors. Each sector is covered by a sectorized antenna. Only the centre site has been simulated with active User Equipments (UEs), where the locations of UEs are randomly assigned with a uniform probability distribution. All other sites in the assumed network are considered as interfering sites. Once a UE is dropped, the links are created with all the sectors. Each link is associated with shadow fading, antenna gain and path gain. A quasi-dynamic simulation approach is used, where a UE remains in the same location until the end of the session, implying that the shadow fading, antenna gains and path gains remain unchanged. But the fast fading variations are taken into account. For this, the users are assumed to move with a certain speed and the corresponding variations in fast fading due to movement is considered. It is assumed that the users move around the same approximate locations. The multipath model used is ITU Typical Urban (TU) 20 paths (explained in appendix A).

2 GHz carrier frequency and 10 MHz operating system bandwidth is considered. Frequency Division Duplex (FDD) is employed. Shadowing is fully correlated between the cells of the same site, whereas the correlation is assumed to be 0.5 between sites.

Link-To-System Performance Mapping Function

In OFDMA each subcarrier may experience a different SINR. An effective SINR metric is needed to compress a set of SINR values at the link level to represent an effective

SINR for system level simulations. This link to system level mapping is based on the exponential effective SINR mapping (EESM) model [22]. The EESM model maps the instantaneous channel state experienced by the OFDM subcarriers within the code-block into a single scalar value, an effective SINR, which is then used to find an estimate of the BLER for this specific channel state. In the general form, the EESM model is given as :

$$SINR_{eff} = -\beta \cdot \ln\left(\frac{1}{N}\sum_{i=1}^{N} e^{\frac{SINR_i}{\beta}}\right) \tag{2.3}$$

where $SINR_i$ denotes the SINR of the i^{th} subcarrier, and β is a parameter, which is obtained from link level simulations and is adjusted for each MCS separately. N denotes the number of active OFDM subcarriers.

Traffic Modeling

The infinite buffer and the finite buffer traffic models have been employed in this study. These models differ in terms of the session time of the users. In the infinite buffer model all users experience equal session time irrespective of their location within the cell. This implies that the users close to the eNode-B download a much larger amount of data in comparison to those located near the cell edge (due to superior SINR conditions near the cell center). The cell and user throughput statistics are collected over several simulation runs, each of a fixed duration. In each run a fixed number of user locations within the coverage area are sampled. Since the UEs have infinite buffer at the eNode-B to download, therefore the UE session ends with the end of the run. The new UEs are generated at the start of the next simulation drop [23]. The infinite buffer simulations are easy to analyze since the number of UEs and the time spent by each UE in the network is fixed.

The finite buffer model allows each user to download the same amount of data. Once the download is finished the session is terminated, and the UE is replaced by another UE in the same cell so that the number of UEs remains constant. Hence, the session time is proportional to the experienced data rates. Thus, users close to the cell edge are expected to stay longer in the system in comparison to the users located near the cell center. The data rates delivered to the cell edge users will dominate the resultant cell throughput. Only a single simulation run is performed in this case, which is of a relatively long duration, in order to collect sufficient user statistics. This is also required to sample most of the locations within the coverage area of a cell. For both traffic models it is assumed that data is always available in the eNode-B buffers, waiting to be served by the PS. The finite buffer call arrival mode is more fair and realistic than the infinite buffer model.

Reference Antenna Schemes

The antenna schemes considered are the following:

1. 1×1 , representing a Single Input Single Output (SISO) antenna scheme, which does not include any transmit or receive diversity.

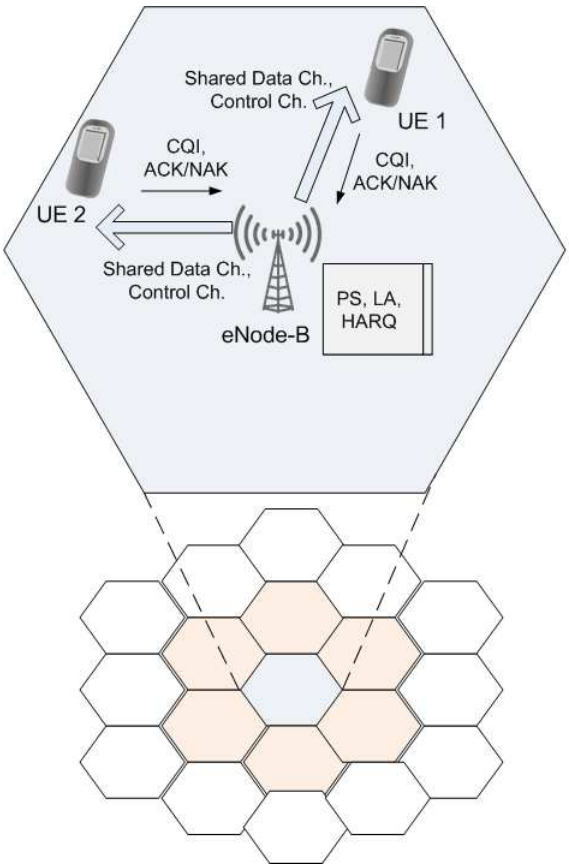

Figure 2.7: LTE system model under consideration.

2. 1×2 Maximal Ratio Combining (MRC), which includes two-branch receive diversity. The signal combining is performed by using the Maximum Ratio Combining (MRC) technique.

3. 1×2 IRC, which includes two-branch receive diversity. The signal combining is performed by Interference Ratio Combining (IRC) technique. We also assume that multiple antennas are uncorrelated, and therefore the fading over the different Tx-Rx pairs are independent with respect to each other.

The detailed simulation assumptions and parameters are given in the respective chapters.

2.6 LTE-A System Model

The LTE-A is an evolution of LTE, and it is desirable to reuse LTE Release'8 solutions for LTE-A as much as possible [24], therefore it is expected that many LTE features will be applicable to LTE-A as well. However, the LTE-A has increased focus on indoor corporate (office) and indoor residential (home) deployment scenarios with uncoordinated

deployment of the Home eNodeB (HeNB) [6] and [25]. Therefore, the relevant considerations for such scenarios are outlined in this section. More specific assumptions and evaluation parameters are presented in the respective chapters.

2.6.1 Deployment Scenario

Figure 2.8 shows an example of indoor corporate deployment scenario with 4 HeNBs providing a coverage area of $100m \times 50m$ in the same building floor. The HeNBs may be deployed by a single operator or several operators. Each HeNB is expected to provide coverage in an area $1/4$ of the total floor area ($50 \times 25m$, 10 rooms), considering the simple case with 4 equal coverage areas. The locations of HeNBs are shown in the centre of the corridors in Figure 2.8. In case of a single operator deployment for corporate scenario, the location of the HeNBs could potentially be planned, but this may not always be essentially true. Figure 2.9 shows a similar 4 HeNBs deployment in the residential scenario. As opposed to the corporate scenarios, the 4 coverage areas in the residential scenario are smaller ($10 \times 10m$, 4 rooms) and are separated by walls with higher attenuation ($10\ dB$). Figure 2.9 also exemplifies a typical scenario where the HeNBs in neighboring residences could be placed in strongly interfering locations, as can be seen in case of HeNBs placed in blue and red residential coverage areas [26].

An uncoordinated HeNB deployment is assumed without prior radio network planning. In this context, uncoordinated deployment refers to cases where HeNBs are more or less installed randomly to get coverage/capacity in one particular area, without considering the impact on/from potentially existing HeNBs' radio performance in the immediate surroundings.

To simplify the evaluation scenario, the serving cell selection for a given UE location is performed based on the 'no RAN sharing' principle, i.e. UEs in the coverage area of one HeNB cannot be served by the other HeNB(s).

To facilitate performance evaluation a quasi-dynamic multi-cell system level simulator built on Matlab is used. The simulation assumptions are largely based on IMT-A requirements for local area indoor scenario, described in [27].

2.6.2 Multiple Access Scheme

OFDMA is used as the multiple access schemes in the DL, and the SC-FDMA is used in the UL (the OFDMA and SC-FDMA are briefly described in subsections 2.2.1 and 2.2.2)

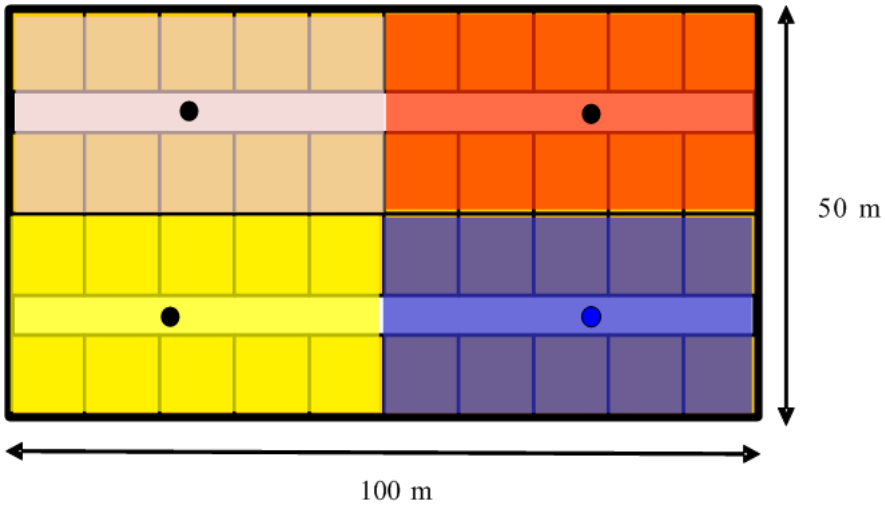

Figure 2.8: Indoor regular corporate scenario with equal coverage areas of 4 HeNBs. The locationS of HeNBs are shown at the center of the corridors [26].

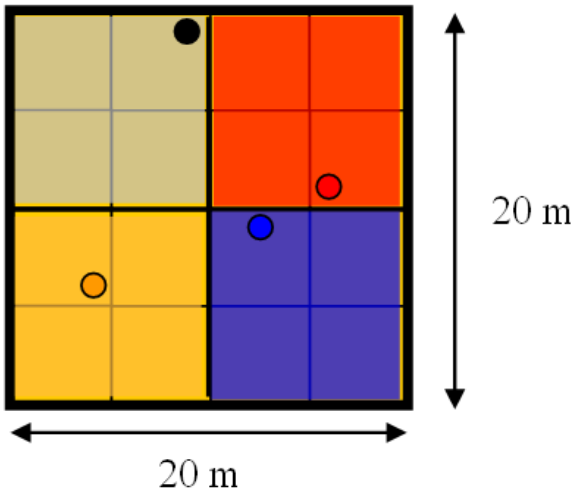

Figure 2.9: Regular residential scenario with 4 HeNBs covering equal area with random deployment [26].

2.6.3 Duplexing Schemes

The TDD is considered as the duplexing scheme. A radio frame duration of $10\ ms$ is assumed based on the latest 3GPP specifications, where DL to UL switching can be applied with a full frame periodicity ($10\ ms$) or with only a half-frame periodicity ($5\ ms$) [18]. A brief description of the frame structure is given in section 2.4 and shown in figure 2.6

2.6.4 Physical Resource Block

The Physical Resource Block (PRB) definition given in [36.211] is used. However, considering 100 MHz system bandwidth, we assume 1500 subcarriers with 60 kHz subcarrier spacing. A group of 12 subcarriers constitutes one PRB in frequency domain, therefore we have a total of 125 PRBs. In time domain we consider 0.5 ms subframe duration, which consists of 28 OFDM symbols including cyclic prefixes between the symbols.

2.6.5 Propagation model

Path Loss (PL) Model

The indoor path loss models used are based on A1-type generalized path loss models for the frequency range 2-6 GHz developed in WINNER and also proposed to ITU-R for evaluations of IMT-Advanced [28]. The Applicability Range of this model is from $3m$ to $100m$, and the antenna height default values for HeNBs and UEs are $1m$ to $2.5m$. The specified PL models are given below:

Line Of Sight (LOS)

$PL = 18.7log10(d[m]) + 46.8 + 20log10(f[GHz]/5.0)$

Non Line Of Sight (NLOS)

$PL = 20log10(d[m]) + 46.4 + nw.L_w + 20log10(f[GHz]/5.0)$

where, d = direct-line HeNB-UE or UE-UE distance [m],
f = carrier frequency [GHz],
nw = number of walls between transmitter and receiver,
L_w = wall attenuation loss [dB]

Shadow Fading Standard Deviation

LOS: 3 [dB]

NLOS : Light Wall : 6 [dB], Heavy Wall : 8 [dB]

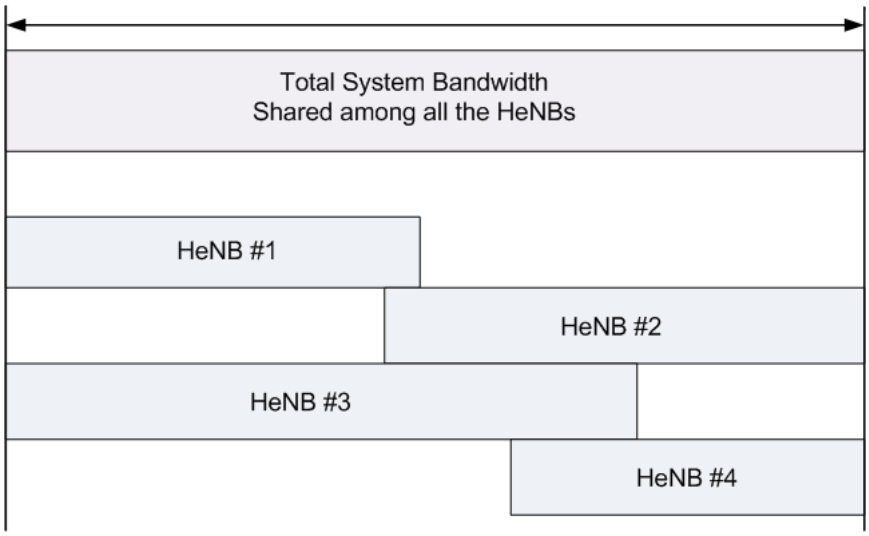

Figure 2.10: Sharing of system bandwidth by 4 HeNBs with spectrum overlap. The system bandwidth is assumed to be 100 MHz

Multipath Channel Model

The multipath channel model to be used in the corporate/residential scenarios for the HeNB-UE, HeNB-HeNB and UE-UE links is based on the A1-type indoor Cluster Delay Line (CDL) models for the frequency range 2-6 GHz developed in WINNER II [29]. The multipath channel is not modeled in the simulations performed.

2.6.6 System Bandwidth and Traffic Models Used

The system bandwidth considered is 100 MHz, which is shared among all the HeNBs in non orthogonal manner as shown in figure 2.10. The model for the calculation of traffic load is shown in figure 2.11, where it is shown that at first the number of PRBs per UE is specified, and then the average number of UEs per HeNB is estimated. Finally the product of the average number of UE at a HeNB and the number of PRB per UE gives the average traffic load at that HeNB in terms of number of PRBs. The number of PRBs per UE is varied in order to have different amounts of traffic loads at HeNB.

Power control is used neither in UL nor DL in the simulations. Multiple Input Multiple Output (MIMO) is not considered, only single input single output (SISO) antenna configuration has been assumed. The Key Performance Indicators (KPIs) used for performance evaluation are described in the respective chapters. The ideal Shannon throughput mapping of effective SINR is used for throughput estimation.

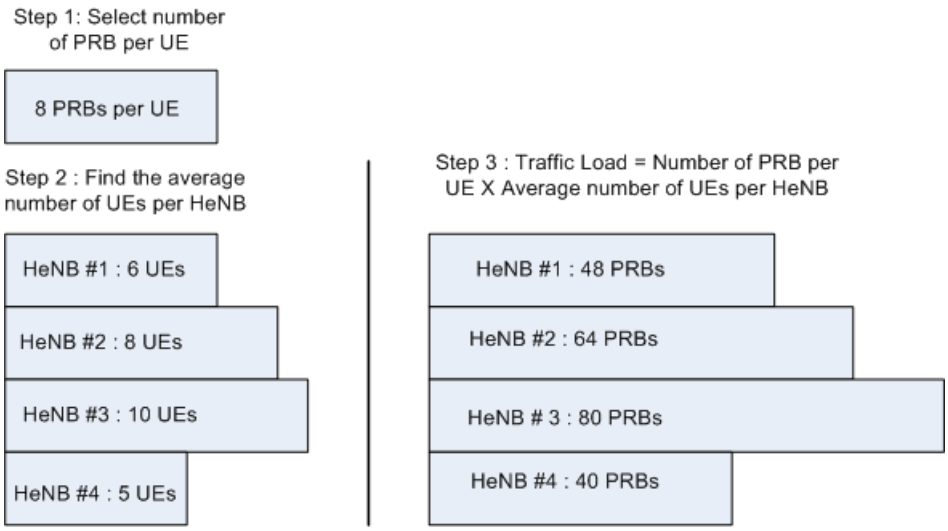

Figure 2.11: Scheme for the calculation of traffic load for different HeNBs.

Chapter 3

Higher Order Sectorization for UTRAN LTE

3.1 Introduction

The Universal Terrestrial Radio Access Network (UTRAN) LTE typically employs three antennas per site to render 3 sector deployment. A migration to Higher Order Sectorization (HOS), such as 6 sectors per site is considered a potential option to increase system capacity. This chapter provides investigations on 6 sector deployment and its performance evaluation for UTRAN LTE in the downlink.

The chapter is organized as follows. Section 3.2 provides a brief description of HOS. Section 3.3 presents the antenna pattern and different cell topologies under consideration for our study. Section 3.4 gives an account of the simulation environment and various parameters assumed to test the underlying concepts. Section 3.5 presents simulation results and their interpretations. Finally section 3.6 provides a summary of the conclusions.

3.2 Higher Order Sectorization

A key parameter for the performance evaluation of a cellular system is the capacity it offers. The capacity of a cellular system is expected to increase by exploiting the spatial dimension. There are several approaches to exploit the spatial dimension. Main concepts suggested are HOS, fixed beam switching concept and adaptive beam forming [30].

Our focus in this study will be on HOS. The network operators may need to install new sites to provide the necessary capacity. One way to increase the capacity without installing new sites is to migrate the existing sites with HOS antenna systems [31][32].

HOS provides a promising technique to increase system capacity by increasing the number of UEs supported in the system, because each antenna can serve almost the same

number of UEs, i.e. the number of UEs can be doubled if the number of sectors is doubled [33]. However, in practical systems this is not realized because the sectorized antenna beam pattern tends to be non-ideal, creating an overlapping region between the sectors and giving rise to inter-cell interference, which limits the system capacity [34].

The impact of HOS on cellular system has been extensively studied. The effect of sectorization on spectrum efficiency of a cellular system has been studied in [35], where it is also highlighted that the 6 sector system tends to perform better than the 3 sector system in a larger cell radius. The investigations on system level performance by comparing fixed and adaptive beam forming approaches with simple sectorization and evaluation of the system capacity in terms of a servable number of UEs are presented in [30].

HOS has been considered a promising feature for the evolving 3rd generation mobile telecommunication systems such as WCDMA [31]. A large number of studies are available in the literature on HOS for WCDMA. An investigation on WCDMA system capacity for different number of sectors per cell, different antenna operating angle and different antenna front to back ratios are presented in [33]. The impact of higher order sectorization on the performance of a capacity limited WCDMA macro cellular network is demonstrated in [36], where it is also shown that the higher order sectorization gives higher capacity, but the increase is not proportional to the number of sectors due to the overlap of the antenna radiation pattern.

The radiation pattern of a base station antenna is an important design parameter, since it has a strong influence on the interference distribution in the network. In practice the antenna pattern does not fit the sector area perfectly, and there is an overlapping of the two adjacent antenna patterns between sectors, generating additional interference [37], [38]. Selection of an optimal antenna beam width, which can optimize the system performance is an important consideration. The investigations for an optimal beam width under a wide range of operating conditions for 3 and 6 sector site deployment of WCDMA system are conducted in [39]. The studies presented in [36] conclude that the network performance can be significantly improved by higher order sectorization, but the more sectors are applied the more careful network planning has to be done. The studies presented in [40] indicate that using a proper hand off protocol is especially critical to the performance of the 6 sector configuration, because the increased number of sectors cause UEs to hand off more frequently. The effect of soft and softer handoffs on CDMA capacity have been evaluated in [38].

Currently, [31] studied the impact of HOS for WCDMA system and evaluated the system performance in realistic and non-homogeneous deployment and traffic scenario. However, presently no study is available in the open literature that evaluates the performance of the 6 sector site deployment for UTRAN LTE. One of the aims of the study presented in this chapter is to fill up this gap in the open literature.

The UTRAN LTE uses OFDMA in the downlink [41], therefore the intra-cell interference is ideally avoided by orthogonal allocation of the subcarriers to the scheduled users, but the environment still remains interference limited due to the presence of inter-cell interference. UTRAN LTE typically employs three antennas per site rendering 3 sector site

deployment. A migration to higher order sectorization such as 6 sector site deployment is considered as one possible option to increase capacity per unit area and enhance system capacity. This chapter documents the results of system level investigations on 6 sector site deployment for UTRAN LTE in the downlink.

At first, a comparison of the performance of 6 sector against the existing 3 sector deployment is presented. Thereafter, investigations on the behavior of 6 sector site deployment under various network conditions such as finite and infinite buffer traffic models, different degrees of antenna azimuth spreads, ideal and non-ideal serving cell selection, macro cell case #1 and case #3 deployment scenarios [11] are also outlined. Finally, deployment of mixed network topologies, with a combination of 3 and 6 sectors, is proposed, and their potential benefits are presented in this chapter.

3.3 The Antenna Pattern and Network Topologies

The antennas used in this study are characterized by the Half Power Beam width (HPBW) scaled proportionately to the number of sectors per site. We adopt the following 3GPP antenna pattern model specified in [11], [42]:

$$A(\theta) = -min\left[12\left(\frac{\theta}{\theta_{3dB}}\right)^2, A_m\right] \tag{3.1}$$

where, $-180 \leqslant \theta \leqslant 180$ and θ is defined as the angle between the direction of interest and the boresight of the antenna (the bore sight is defined as the direction in which the antenna shows the maximum gain). θ_{3dB} represents 3dB beamwidth in degrees, and A_m represents the considered maximum attenuation. Table 3.1 enumerates the values of the above parameters for 3 and 6 sector antennas.

Table 3.1: eNode-B Antenna Parameters

Parameters	**3 Sector Antenna**	**6 Sector Antenna**
θ_{3dB}	70^o	35^o
A_m	$20dB$	$23dB$
Boresight Gain	$14dBi$	$17dBi$

The antenna patterns are plotted in figure 3.1, where the region of inter-sector overlap in azimuth due to the presence of adjacent antenna beam is also shown. The maximum overlap between the two adjacent sectors is 60^o for 3 sector and, 40^o for 6 sector antennas. However, 6 sector site has twice the number of overlaps compared to the 3 sector site, resulting in a larger amount of total inter-sector overlap and hence high inter-cell interference. The maximum antenna gain, i.e. the gain in the direction of bore sight for 3 sector

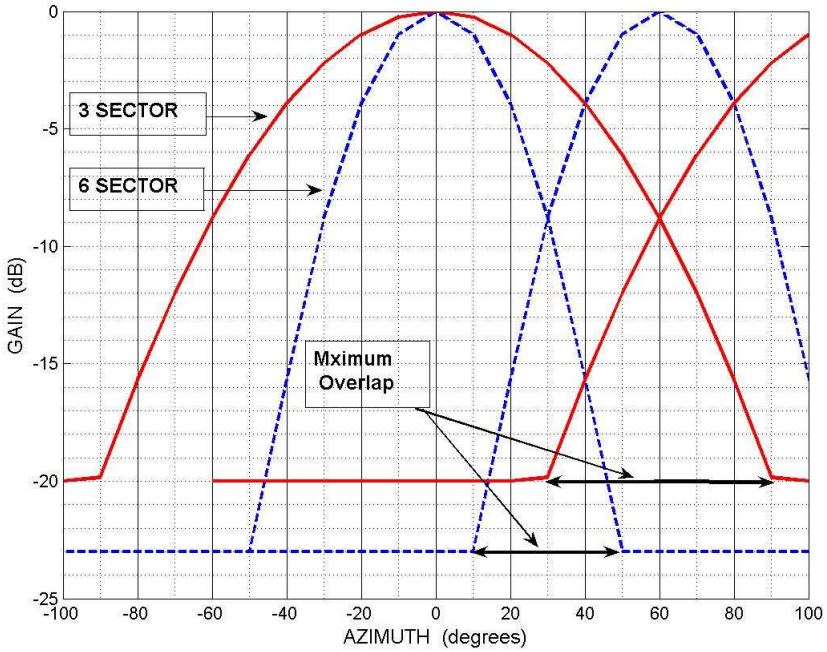

Figure 3.1: Antenna pattern of 3 and 6 sector site antennas, showing the region of inter-sector overlap.

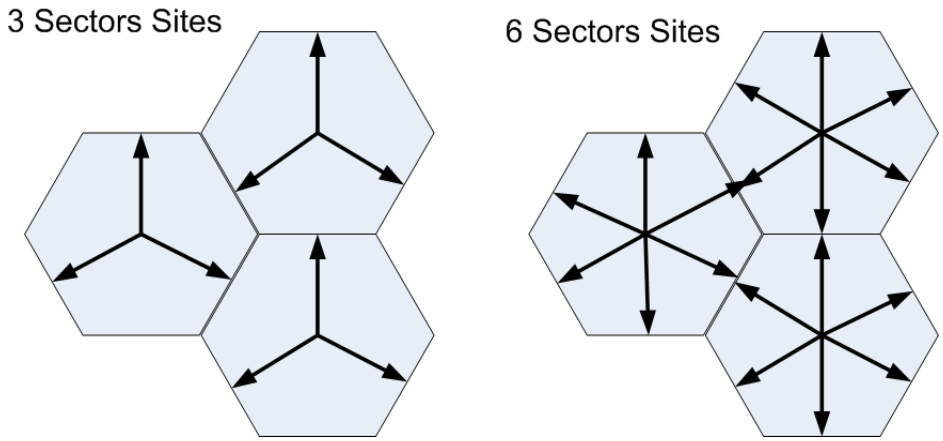

Figure 3.2: The antenna orientations for 3 and 6 sector antennas. The arrows indicate the boresight direction.

antenna with 70^o HPBW is $14dBi$ and for 6 sector antenna $17dBi$. This is 3 dB higher due to reduction in HPBW by half to 35^o compared to HPBW of 3 sector antenna. Figure 3.2 shows the orientations for 3 and 6 sector antennas, where the arrows pointing towards the sides of the hexagons represent the boresight direction.

In the homogenous network topologies of 3 or 6 sectors all the sites are composed of identically sectorized antennas over the assumed cellular network consisting of 19 sites. In addition to the homogeneous network topologies we propose mixed network topologies

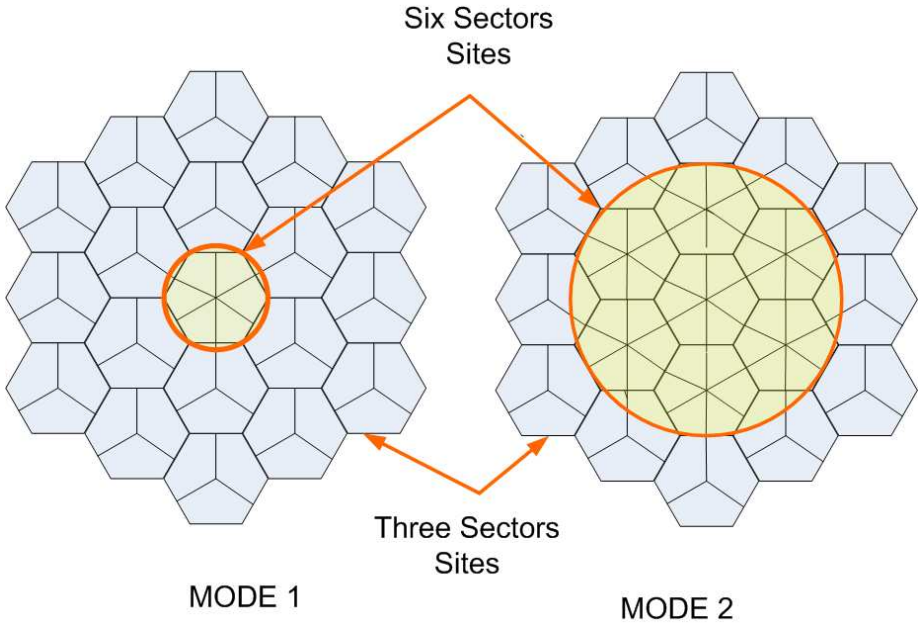

Figure 3.3: Proposed mixed network topologies

with the combinations of 3 and 6 sector sites within the network. Two different combinations, namely $mode1$ and $mode2$ are proposed. In $mode1$ the centre site is composed of 6 sectors, and all the other 18 sites are composed of 3 sectors. In $mode2$, the centre site and the sites within the first ring are composed of 6 sectors, and the remaining 12 sites of the outer ring are composed of 3 sectors. Figure 3.3 provides the pictorial representation of the proposed mixed network topologies.

3.4 Modeling Assumptions

3.4.1 Simulation Parameters

To facilitate the performance evaluation a quasi-dynamic multicell system level simulator has been used. The simulation assumptions are largely based on the 3GPP UTRAN LTE specifications [41]. The system model employed is as per the discussion in chapter 2 (section 2.5). Here more specific parameters and assumptions used for the performance evaluation are presented. The macro cell case #1 (inter-site distance of 500 meters) and case #3 (inter-site distance of 1732 meters) are employed [11]. In the considered hexagonal cellular layout of 19 sites, each site is composed of either 3 or 6 sectors per site based on the simulation requirements. The site refers to the area covered by a eNode-B, and the sector refers to the area covered by one of the sectorial antennas in that eNode-B.

The finite and infinite full buffer traffic models are considered. $2Mbit$ packet size is chosen as the buffer information for the finite buffer model. In infinite buffer model UEs

always have data to transmit. A total of 120 UEs per site is simulated, which is scaled per sector according to the number of sectors. This amounts to 40 UEs per sector for 3 sector and 20 UEs per sector for 6 sector sites. Link to system level mapping is based on exponential effective SINR model [43]. A decoupled time and frequency domain packet scheduler is considered. The maximum scheduling of $N = 12$ UEs per TTI is considered.

For 6 sector antennas the azimuth angle spread of 5^o and 10^o are considered, resulting in an increased effective HPBWs of 40^o and 45^o. For 40^o HPBW the maximum inter-cell overlap amounts to 60^o, and for 45^o HPBW this amounts to 80^o, resulting in increased additional inter-cell interference.

The ideal and non ideal serving cell selections are assumed. In ideal cell selection a UE is always connected to the cell with the minimum total path loss. In this context, the total path loss includes the effect of the distance dependent path loss, shadowing, minimum coupling loss, and antenna gains. A more realistic serving cell selection could be a non-ideal serving cell selection, assuming that sometimes UEs are not connected to the optimal cell, i.e. the cell with the minimum total path loss. In non-ideal serving cell selection the UE randomly selects one of the cells to be the serving cell with equal selection probability, out of the virtual active set of cells with a total path loss within the given handover window offset margin. The handover window offset margin explicitly includes effects from having UE measurement imperfections for serving cell selection. This assumption is taken to account for imperfections from the serving cell selection algorithm. Table 3.2 provides a summary of the main parameters and simulation assumptions.

3.4.2 Key Performance Indicators (KPIs)

Geometry Factor, Average User Goodput, Average Cell Throughput and Average Site Throughput are taken as KPI.

- **Geometry Factor** is defined as the ratio between the desired received signal power that a UE receives and the total amount of inter-cell interference plus white noise averaged over the fast fading, which is expressed as:

$$\text{Geometry Factor} = \frac{P_{Rx}}{P_{int} + P_{noise}} \tag{3.2}$$

  where, P_{Rx}, P_{int}, P_{noise} represent signal power, total amount of interference and noise received respectively.

- The **Average Cell Throughput** is described as :

$$\overline{TP}_{cell} = \frac{\text{Total bits correctly delivered}}{\text{Simulation time}} \quad , \tag{3.3}$$

  where the numerator is an aggregate of the correctly delivered bits over all the active sessions in the system [44]. The Average Site Throughput is defined as the product of Average cell throughput and the number of cells within the site.

Table 3.2: Main Parameters and Simulation Assumptions

Parameter	Settings
Standard Settings	
Carrier Frequency	2 GHz
System Bandwidth	10 MHz
Number of Subcarriers	600
Number of PRBs	50 (12 Subcarriers/PRB)
Subframe Duration	1 ms (14 OFDM Symbols)
Total eNode-B Transmit Power	46 dBm (1 Tx Antenna)
Shadowing Standard Deviation	8 dB
HARQ Model	Ideal Chase Combining
Ack/Nack Delay	2 ms
CQI Log Normal Std. Error	1dB
AMC	QPSK (1/5 to 3/4)
	16-QAM (2/5 to 5/6)
	64-QAM (3/5 to 9/10)
Specific Settings	
No. of Sectors per Site	3 or 6 Sectors per Site
No. of UEs	120 UEs per Site
Max. No. of UEs per TTI	12 UEs
UE Rx Antenna	2-Rx (IRC)
Power Delay Profile	ITU 20-Path Typical Urban
UE Speed	3 kmph
Min. UE to eNB Distance	35 m
CQI reporting resolution	1 dB
CQI Reporting Delay	2 ms
BLER Target	20 %
Cellular Layout	Hexagonal Grid 19 Sites
Traffic Model	Infinite and Finite Full Buffer
Inter-site Distance	500 m for Macro Case#1
	1732 m for Macro Case#3

- The **Average User Goodput** for the ith user is defined as:

$$\overline{TP}_i = \frac{\text{Total bits correctly received by user } i}{\text{Session time}} \quad . \tag{3.4}$$

  where the session time of the user depends on the traffic model.

- **Coverage** is denoted by $\overline{TP}_{cov}$ and is determined from the CDF of the average user Goodput taken over all the completed sessions. The 5^{th} percentile on the CDF of the user goodput is defined as the Coverage of the cell, which represents the minimum throughput achieved by 95% of UEs i.e., only 5% of the UEs experience a lower average data rate than the coverage rate, which can be expressed as:

$$prob(\overline{TP}_{users} < \overline{TP}_{cov}) = 0.05 \tag{3.5}$$

The coverage is used as an indicator to represent the throughput achieved by the users in cell-edge channel conditions, where the experienced inter-cell interference is high.

3.5 Simulation Results

Extensive simulations are conducted to evaluate the performance of 6 sector site deployment for UTRAN LTE. Initially the performance is compared against 3 sector site deployment, and then the investigations are carried out to evaluate the performance with various simulation assumptions, such as finite and infinite buffer traffic models, different degrees of antenna azimuth spreads, ideal and non-ideal serving cell selection, macro cell case $\#1$ and case $\#3$ scenarios. At the end the potential benefits of the proposed mixed network topologies are examined. The following subsections present the simulation results.

3.5.1 Comparison with 3 Sector Site Cellular Deployment

To compare the performance of 6 sector site against 3 sector site deployment, the simulations were conducted with macro cell case $\#1$, infinite full buffer traffic model, ideal serving cell selection, and assuming no spread in the antenna beam width.

Figure 3.4 compares the Geometry factor distributions of 3 and 6 sector sites homogeneous network deployments. The Geometry factor is approximately $0.5dB$ to $1dB$ worse for 6 sector site. The lower Geometry factor distribution is due to increased inter-cell interference because of a larger degree of inter-cell overlap. The CDF of user goodput distribution for 3 and 6 sector sites are presented in figure 3.5. At 50^{th} percentile (i.e. at the median value) the user goodput for 6 sectors is increased by 96%. Similarly the coverage gain is increased by 63% as can be seen at 5^{th} percentile on CDF of user goodput distribution. This gain is noticeable due to scaling of number of UEs assigned per sector. 40 UEs per cell for 3 sector and 20 UEs per cell for 6 sector are assumed to keep the total number of UEs fixed per site in both cases.

Figure 3.6 compares average cell and average site throughputs. The average cell throughput for 6 sector is 6% lower, but the average site throughput is 88% higher. However, the gain for 6 sectors is not exactly of the same proportion as the number of UEs because of the lower geometry factor distribution. Although 6 sector site deployment shows slightly lower per cell throughput but gives significantly higher per site throughput gain. This highlights the potential gains for 6 sectors site deployment to significantly enhance the capacity per unit area and hence to improve the spectrum utilization. These relative gain figures for LTE are in line with the findings from previous WCDMA studies reported in [31].

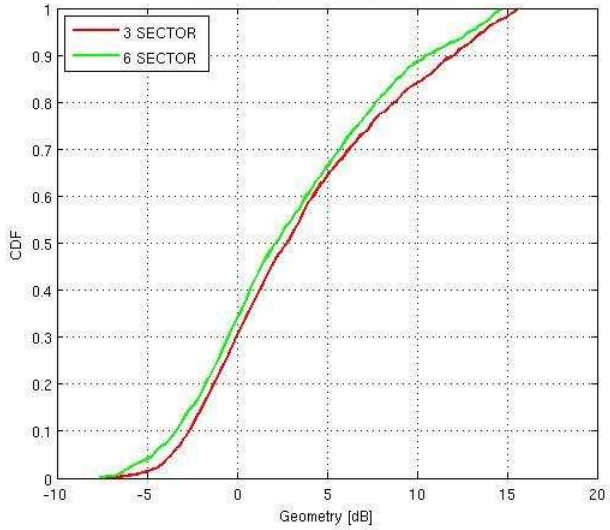

Figure 3.4: Geometry factor distributions for 3 and 6 sector sites homogeneous network deployments

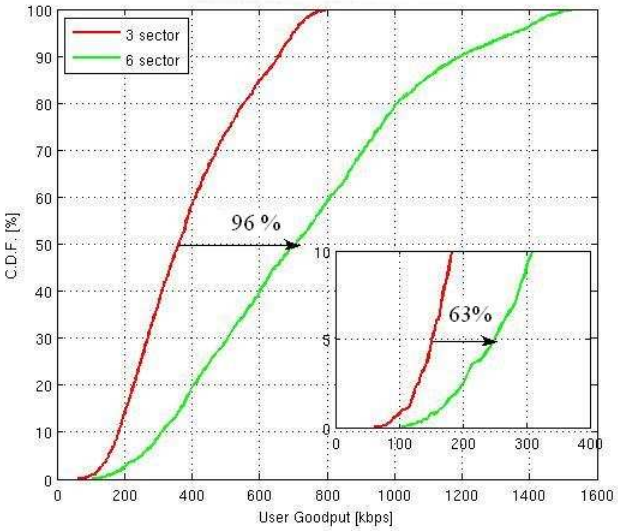

Figure 3.5: User Goodput distributions for 3 and 6 sector sites homogeneous network deployments

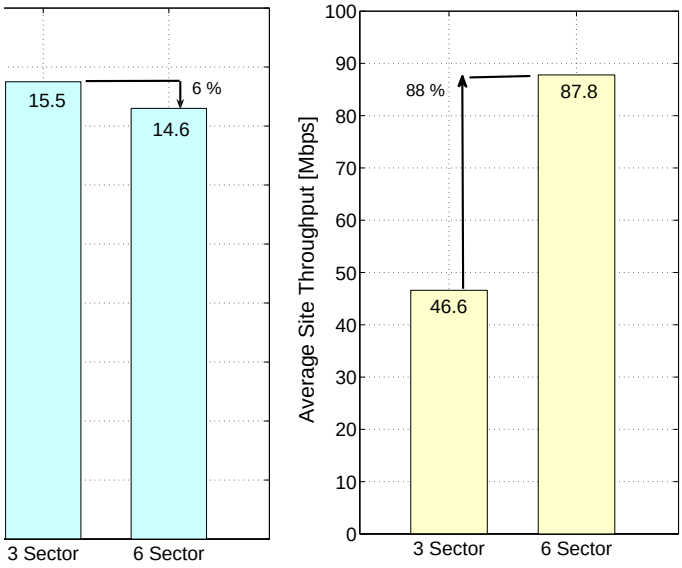

Figure 3.6: Comparision of average cell and average site throughputs for 3 and 6 sector sites homogeneous network deployments

3.5.2 Deployment under Different HPBWs

To investigate the impact of non-ideal sectorized antenna beam widths, the simulations were conducted for 6 sector site deployment with different degrees of azimuth angle spread, assuming macro cell case $\#1$, infinite full buffer traffic model, ideal serving cell selection and 20 UEs per site.

The motivation for presenting these results is that even though the raw antenna beam width under consideration is 35^o, the effective antenna beam width may be larger due to the radio channels azimuthal dispersion. The azimuthal dispersion is found to be on the order of $5^o - 10^o$ for typical urban macro cells [45]. Considering this, the antenna azimuth spreads of 5^o and 10^o are considered, resulting in an increased effective HPBWs to 40^o and 45^o, therefore the simulations were conducted assuming HPBWs of 35^o, 40^o, and 45^o.

The impact of azimuth angle spread on geometry factor distribution is presented in Figure 3.7. The geometry factor decreases with increasing effective beam width, which is especially visible for high geometry factor values. The reason for this is that increasing effective beam width increases the overlap area in the adjacent cells, resulting in higher amount of inter-cell interference. Figure 3.8 shows user goodput distribution, and Figure 3.9 presents the average site throughput performance. The main observation is that the relative 6 sector capacity gain decreases with increasing effective beam width. The average site throughput with antenna HPBW of 40^0 is 1% lower compared to 35^0 HPBW, and with 45^0 it is 4% lower, reducing the effective site throughput gain from 88% to 84%. However, a gain in the order of 80% from 6 sectors could be a realistic estimate. The consideration of the impact of azimuth spread is important to make a reasonable assumption about the capacity improvement.

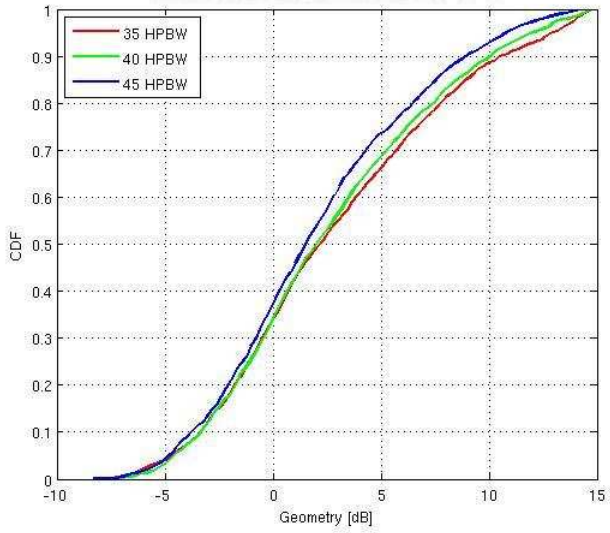

Figure 3.7: Geometry factor distributions of 6 sector site deployment under different amount of azimuth angle spreads

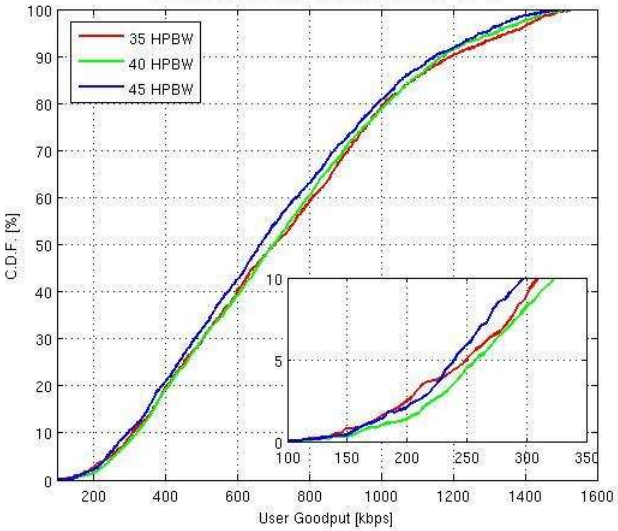

Figure 3.8: User goodput distributions of 6 sector site deployment under different amount of azimuth angle spreads

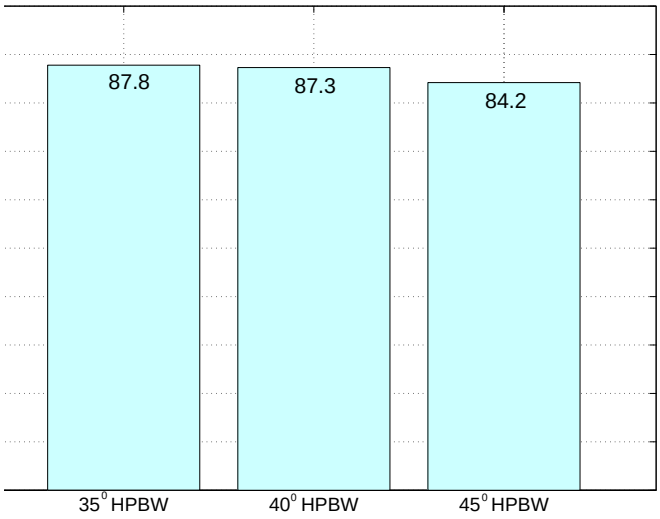

Figure 3.9: Site throughput performance of 6 sector site deployment under different amount of azimuth angle spreads

3.5.3 Comparison under Macro Cell Case $\#1$ and Case $\#3$

To find out the cell size sensitivity on 6 sector site deployment the simulations were conducted with macro cell case $\#1$ and case $\#3$ i.e. increasing the site-to-site distance from $500m$ to $1732m$, assuming infinite full buffer traffic model, ideal serving cell selection, no azimuth angle spread and 20 UEs per cell.

Figure 3.10 compares the geometry factor distribution. Macro cell case $\#3$ shows lower geometry below $10dB$. However, above $10dB$ there is no difference with case $\#1$. The difference is more pronounced towards the cell edge, which is expected due to larger cell size. The impact of geometry factor distribution is reflected in user goodput distribution presented in figure 3.11. For 10% of the UEs (at 90^{th} percentile and above) there is no difference in the good put distribution, which shows UEs at the cell centre, with good channel conditions. As the distance from the cell centre increases the goodput distribution for case $\#3$ becomes lower. At 50^{th} percentile CDF, this amounts to 8% and at the cell edge 18% lower compared to case $\#1$. Correspondingly the average site throughput achieved in case $\#3$ is 4% lower (figure 3.12).

3.5.4 Performance under Finite and Infinite Buffer Traffic Models

Simulations were conducted with infinite and finite buffer traffic models assuming macro cell case $\#1$, ideal serving cell selection, no azimuth angle spread and 20 UEs per cell.

User goodput distribution is shown in figure 3.13. Up to 50^{th} percentile on the CDF the user goodput is slightly higher for infinite buffer model; however, beyond this the finite

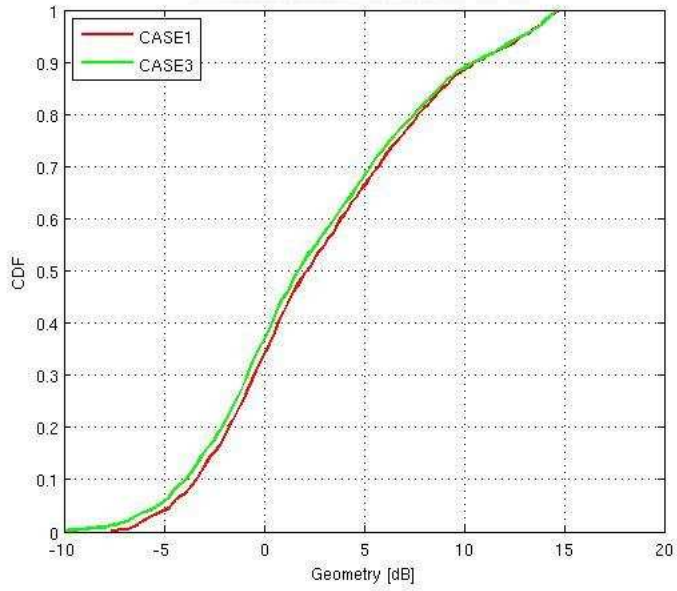

Figure 3.10: Geometry factor distributions of 6 sector site for macro cell case #1 and case #3

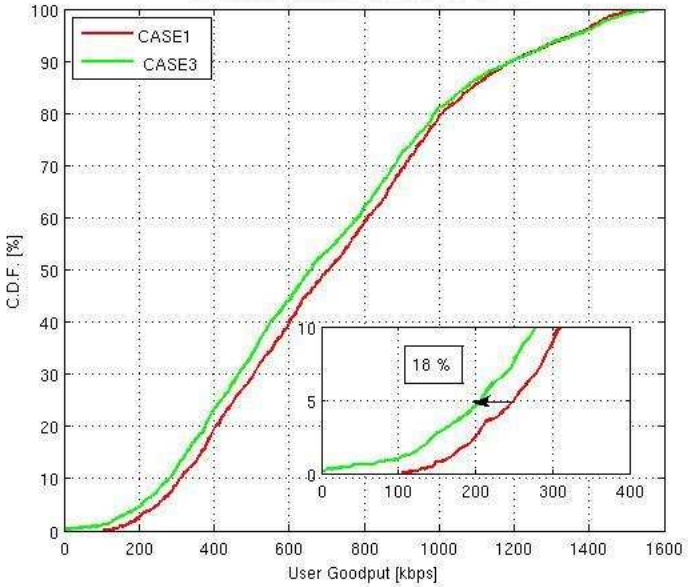

Figure 3.11: User goodput distributions of 6 sector site for macro cell case #1 and case #3

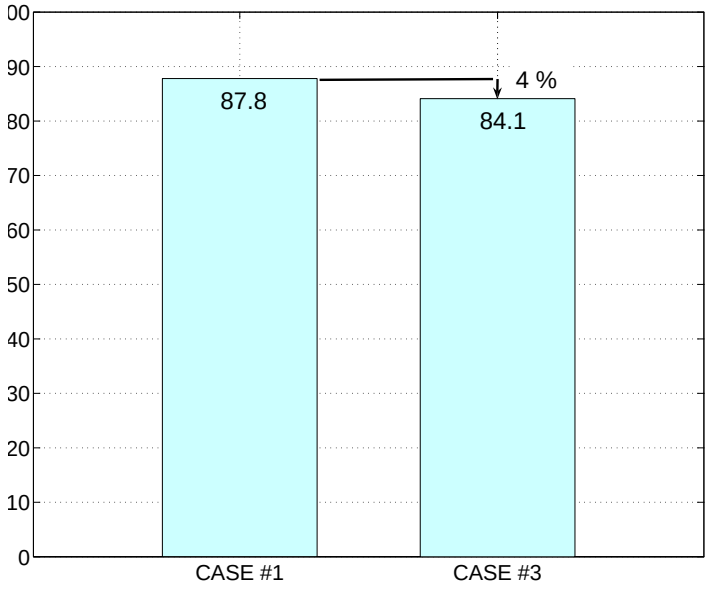

Figure 3.12: Site throughput performance of 6 sector site for macro cell case #1 and case #3

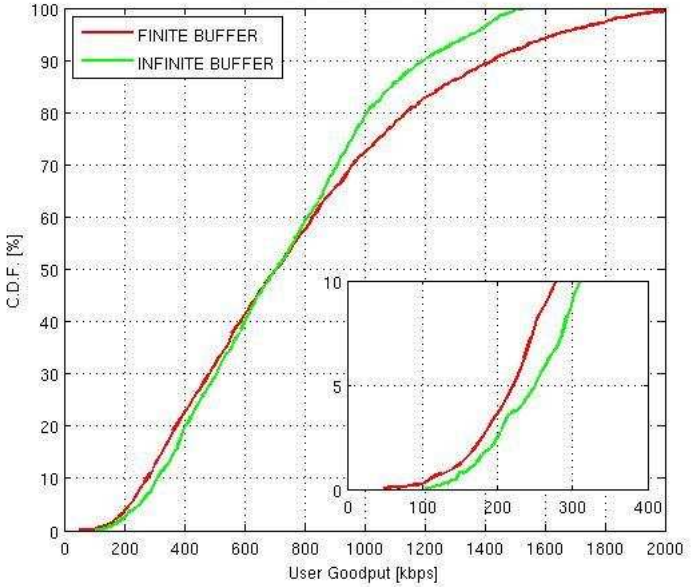

Figure 3.13: User goodput distributions of 6 sector site under finite and infinite buffer traffic models

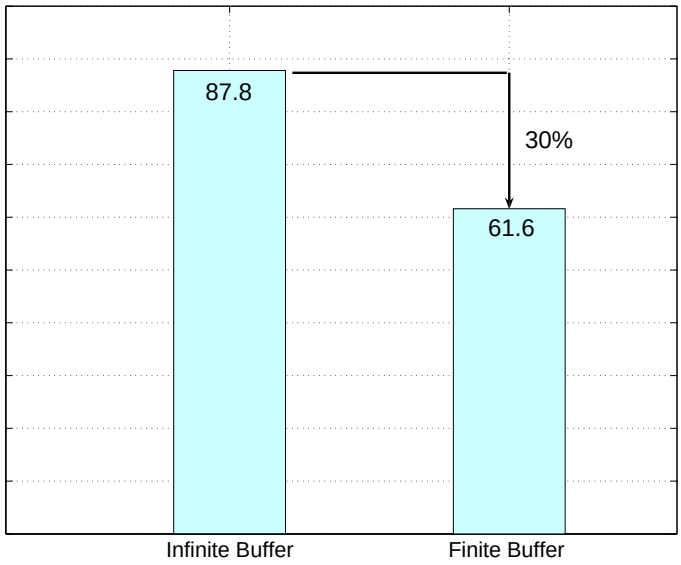

Figure 3.14: Site throughput performance of 6 sector site under finite and infinite buffer traffic models

buffer model shows higher user goodput distribution. In finite buffer model users at the cell edge remain alive until they download the specified amount of data; this requires more resource allocation, resulting in lower cell throughput. But in infinite buffer model cell edge users are terminated at the end of the simulation drop, and the users in good channel condition continue to download until they are terminated resulting in more throughput. Therefore the absolute capacity is 30% lower for finite buffer model (figure 3.14).

3.5.5 Performance with Ideal and non Ideal Serving Cell Selections

The performance of 6 sector site deployment is compared for ideal and non ideal serving cell selections to understand the impact of UE measurements imperfections. For non-ideal serving cell selection $1dB$, $2dB$ and $3dB$ handover window margins are considered, macro cell case $\#1$, infinite buffer traffic model, no azimuth angle spread, and 20 UEs per cell are assumed.

Only a marginal difference is observed in the geometry factor distribution for ideal and non ideal serving cell selections. In non-ideal case, the geometry factor is slightly shifted to the left and tends to result in longer tails towards the lower values (figure 3.15). At the cell edge non-ideal cell selection with $3dB$ handover window offsets gives slightly lower user goodput (figure 3.16). The main observation is that varying the HO window margin from $0dB$ to $3dB$ seems to impact the relative 6 sector capacity gains only marginally.

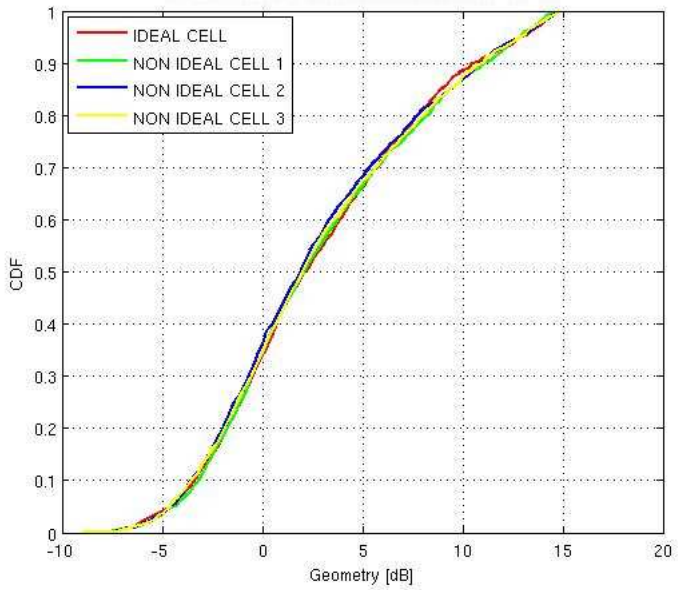

Figure 3.15: Geometry factor distributions of 6 sector site with ideal and non-ideal serving cell selections

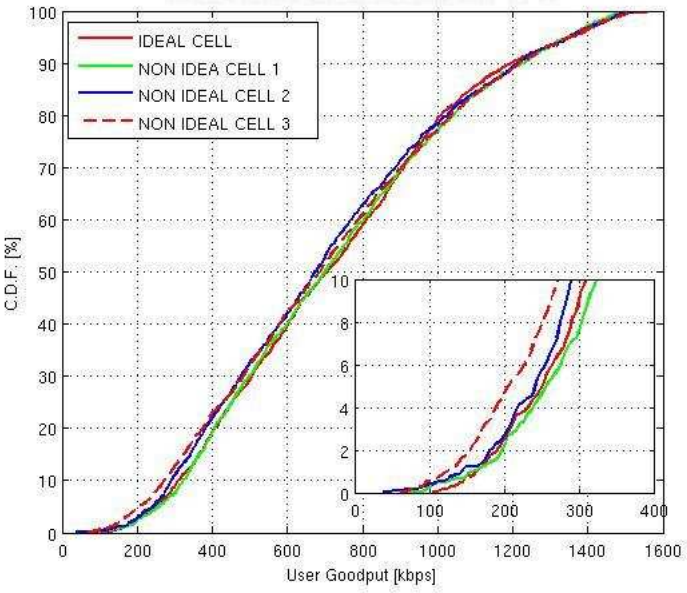

Figure 3.16: User goodput distributions of 6 sector site with ideal and non-ideal serving cell selections

3.5.6 Performance under Mixed Network Topologies

The performance of proposed mixed network topologies, namely; $mode1$ and $mode2$ is compared with homogeneous 3 and 6 sector sites deployments, assuming macro cell case $\#1$, infinite buffer traffic model, ideal serving cell selection, no azimuth angle spread, and 20 UEs per cell for 6 sectors and 40 UEs per cell for 3 sectors.

Geometry factor distributions are presented in figure 3.17. The 6 sectors homogeneous deployment gives the lowest geometry distribution, due to the largest degree of inter-cell overlap. The $mode1$ deployment yields the highest overall geometry distribution. At cell-edge the geometry in the $mode1$ is about $0.5dB$ higher compared to the 3 sectors homogeneous deployment, presenting the lowest interference scenario among all. The difference in geometry distribution for $mode2$ with 3 and 6 sectors homogeneous deployments is visible only towards the higher geometry factor values. Towards the cell edge $mode2$ geometry presents no significant difference with 6 sectors homogeneous deployment.

Figure 3.18 shows 122% and 102% higher user goodput for $mode1$ and $mode2$ at the cell edge compared to 3 sectors homogeneous deployment. The similar gains are observed at 50% CDF. The site throughput gains presented in figure 3.19 are 110% and 96% higher than 3 sector respectively, and are also higher than the 6 sector homogeneous deployment. This is an important finding, and the main observation is that the relative site capacity gain from upgrading existing 3 sector sites with 6 sector sites is comparatively larger for the single site upgrade ($mode1$), as compared to upgrading a cluster of sites ($mode2$). Therefore $mode1$ could provide a potential option to meet high traffic demands in a localized area such as hot spots. However, in practical setup the realized gain may be slightly lowered.

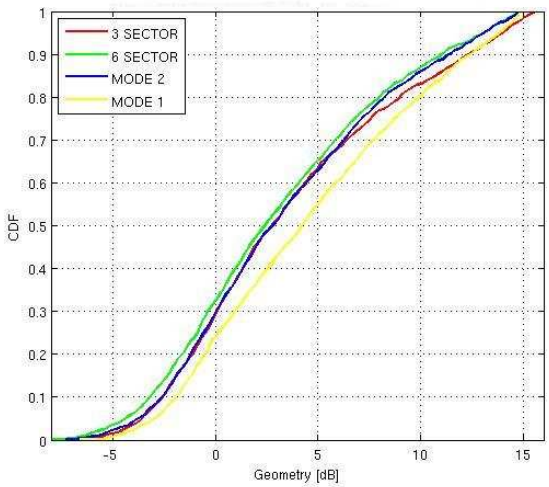

Figure 3.17: Comparison of geometry factor distributions for homogeneous and proposed mixed network topologies

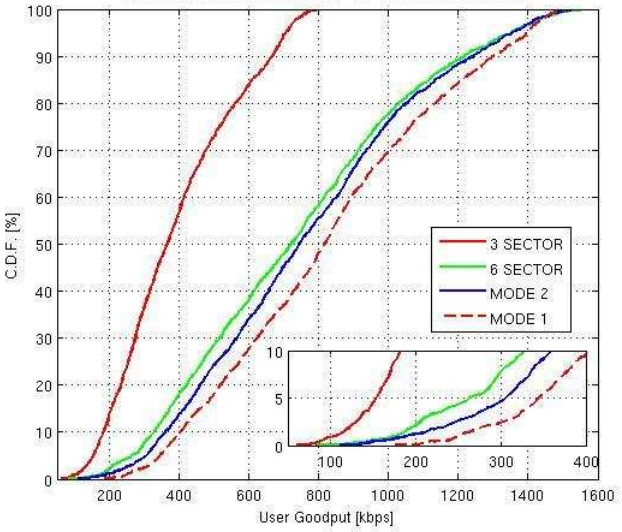

Figure 3.18: Comparison of user goodput distributions for homogeneous and proposed mixed network topologies

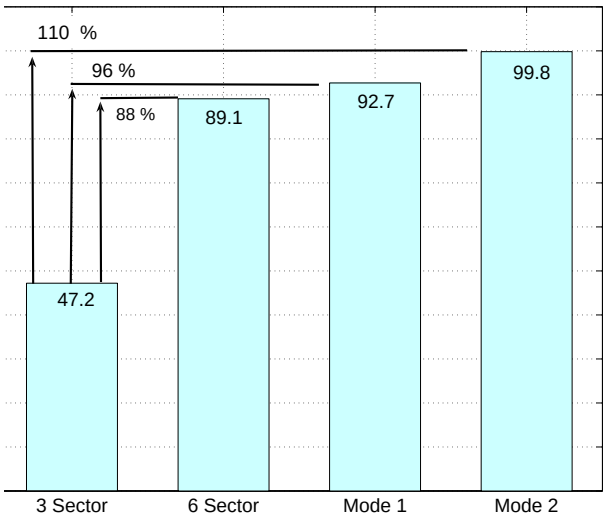

Figure 3.19: Comparison of site throughput performance for homogeneous and proposed mixed network topologies

3.6 Conclusions

In this 6 sector the performance of deployment is investigated in the LTE DL. The comparisons of the performance of 6 sector deployment against 3 sector are carried out. The main idea of this investigation was to increase capacity per unit area by increased spatial reuse of the spectrum. The geometry factor for 6 sector is found approximately 0.5 dB to 1 dB lower compared to 3 sector. A significant increase in the user goodput performance is realized by keeping the total number of UEs per site equal for both 3 and 6 sector deployment. The average cell throughput for 6 sectors is found 6 % lower, but per site average throughput is 88% higher compared to 3 sectors. This brings into light the potential gain in capacity per unit area from 6 sector deployment.

In addition, a detailed investigation on 6 sector performances was conducted under various assumptions such as finite and infinite buffer traffic models, different degrees of antenna azimuth spreads, ideal and non-ideal serving cell selection, macro cell case #1 and case #3 deployment scenarios. It was observed that as the cell size increases such as in macro case #3, a lower geometry is realized, specially at the cell edge, and therefore, as distance from cell centre increases the goodput distribution also becomes lower. The main observation is that varying the hand over window margin from 0 dB to 3 dB seems to impact relative 6 sector capacity gains only marginally. It was found that the relative 6 sector capacity gain decreases with increase in effective beam width. The average site throughput with 45 degrees is 4 % lower, reducing the effective site throughput gain from 88% to 84%. However, a gain in the order of 80% from 6 sectors could probably be a realistic estimate.

Finally, two mixed network topologies, namely $mode1$ and $mode2$, were proposed, and their potential benefits were investigated. It was found that the $mode1$ yields the highest overall geometry factor distribution, while 6 sector homogeneous deployment gives the lowest geometry distribution among the considered cases. For $mode1$ and $mode2$ the overall respective site capacity gain in the range of 110 % and 96 % higher than 3 sector was realized. The main observation is that the relative site capacity gain from upgrading existing 3 sector sites to 6 sector sites is comparatively larger for the single site upgrade ($mode1$), as compared to upgrading a cluster of sites ($mode2$). The $mode1$ could provide a viable option to meet high traffic demands in a localized area such as hot spots.

The relative gains in the mixed network and 6 sector site homogeneous deployments are at the cost of slightly increased handoffs between the sectors, due to the increased number of sectors, as well as slightly higher cost of installation due to extra cabling and antenna requirements.

Chapter 4

Inter-Cell Interference Avoidance in Fractional Load for LTE DL

4.1 Introduction

LTE employs OFDMA in downlink. Due to the property of OFDMA, the intra-cell interference is ideally avoided, but the cellular environment still remains interference limited due to the presence of inter-cell interference (ICI), which limits the system performance. An investigation on inter-cell interference avoidance (ICIA) techniques for LTE downlink under fractional load conditions are presented in this chapter.

The chapter is organized as follows. Section 4.2 briefly discusses the Inter-Cell Interference Coordination (ICIC) techniques for LTE downlink, whereas section 4.3 presents a concept of inter-cell interference avoidance under Fractional Load (FL)conditions. Section 4.4 describes the proposed inter-cell interference avoidance schemes. The modeling assumptions and related results are presented in sections 4.5 and 4.6. Finally, the conclusions are outlined in section 4.7.

4.2 Inter-Cell Interference Coordination in LTE DL

The ICIC techniques have been considered to control ICI in order to improve the system performance, especially the cell edge performance. The ICIC techniques primarily rely on frequency domain sharing and/or adjustment of transmission power in order to ensure effective sharing of the spectral resources between the adjacent eNode-Bs. The reactive and proactive ICIC schemes are discussed for LTE [46]. In reactive scheme the performance is monitored based on the measurements. If the performance drops below the desired level due to excessive interference, then appropriate actions are taken to reduce the interference. Whereas, in proactive scheme, an eNode-B informs its neighbors in advance about its scheduling plan so that the neighboring eNode-Bs can plan their own scheduling, min-

imizing the intercell interference. The proactive scheme in LTE downlink is facilitated by standardized Relative Narrow Band Transmit Power (RNTP) indicator, signaled over X2 interface. The RNTP provides an indication on downlink power restriction per PRB to neighboring eNode-Bs for interference aware scheduling [47].

A considerable amount of studies are available on ICIC for LTE downlink under full load conditions [48], [49], [50], [51], [52] and [53]. The main conclusion from these studies is that under full load conditions the ICIC techniques do not bring significant performance gains. The signaling involved for ICIC consumes a considerable amount of transmission bandwidth, but the achieved SINR improvement is not high enough to realize effective gain. As Shannon's capacity expression, $C = Wlog_2(1 + SINR)$ requires that the SINR improvement should be high enough to compensate for the reduced useful transmission bandwidth W.

A dynamic eNode-B packet scheduler using CQI information for packet scheduling can effectively control the trade-off between coverage and capacity at full load [49]. However, a mechanism to control ICI under FL is still a potential research area. We aim in this chapter to present our investigations on mechanisms to control ICI under FL conditions for LTE downlink.

4.3 Inter-cell Interference Avoidance in Fractional Load

The fractional load conditions arise when only a portion of the system bandwidth is required to be used due to lack of traffic in the cell. Therefore, a packet scheduler needs to employ only a subset of PRBs for transmission. This leads to a situation where a certain PRB in a cell becomes *active* if employed, otherwise remains *dormant*. This results in a PRB activity state in the cell. Under fractional load conditions, the PRB activity state will be different at each cell as well as it can vary from frame to frame, resulting in larger inter-cell interference dynamics compared to the full load conditions. In this situation a packet scheduler can play an important role to control the ICI by proper selection of PRB activity state at each enode-B. Under low fractional load conditions it could be possible to employ non-overlapping sets of active PRBs at a eNode-B with respect to neighboring enode-Bs. In fact, the inter-cell interference reduction under fractional load will largely depend on allocation of the non-overlapping set of active PRBs with respect to the neighboring eNode-Bs.

Therefore, under low fractional load conditions the ICI may automatically be minimized by use of CQI aware frequency domain packet scheduling, without any need of dedicated signaling [54]. A detailed study on the performance of Frequency Domain Packet Scheduler (FDPS) under fractional load can be found in [55], where the packet scheduler aims to optimize the throughput performance under given load conditions in time and frequency domain by avoiding transmissions on PRBs that are experiencing severe interference. This assumes no coordination between eNode-Bs to avoid ICI. However, the performance of such a packet scheduler is very sensitive to the inaccuracy and delay in CQI reporting [55].

A further study in [56] highlights that under low fractional load conditions, an opportunistic scheduling leads to fast 'on-off' transitions of PRB activity state, due to inaccuracy and delay in the CQI reporting. The CQI estimated at the receiver is not instantaneously available at the transmitter due to processing delay at both ends. Meanwhile, the interference condition may change and the Link Adaptation (LA), which is based on the CQI feedback, will not be able to accurately track those variations, amounting to high Block Error Rate (BLER), resulting in reduced capacity and coverage. Hence, FDPS alone cannot guarantee an optimal performance.

A suitable mechanism is needed to control the fast 'on-off' transitions and also to set the PRB activity state over the eNode-Bs effectively in order to reduce the intercell interference. The effective PRB activity state can be achieved by careful selection of active PRBs, whereas, the 'on-off' transitions can be controlled by introducing time correlation to the PRB activity states. Keeping these perspectives in view we propose several intercell interference avoidance schemes for fractional load conditions.

4.4 The Proposed Schemes

The proposed Intercell Interference Avoidance schemes are referred to as autonomous schemes because there is no need for dedicated signaling among eNode-Bs for intercell interference avoidance. The decision at each eNodeB is based on the information available within the cell itself. The proposed schemes are as follows:

- **R**esource **O**verlapping **A**voidance (ROA) Scheme
- **R**andom **S**election with **C**orrelation (RSC) Scheme
- **C**orrelation with **W**eight **C**oefficient (CWC) Scheme
- **Q**uality **E**stimation based **S**election (QES) Scheme

4.4.1 Resource Overlapping Avoidance (ROA) Scheme

In this scheme, total PRBs are partitioned in three non-overlapping sets, where one set is allocated to each adjacent sector (cell) in the considered 3 sector hexagonal cellular network deployment scenario. This is essentially similar to traditional fixed frequency reuse scheme. Figure 4.1 shows this arrangement, where numerals 1, 2, and 3 represent three non-overlapping sets of PRBs. We assume that the total system bandwidth is divided into 50 PRBs [11], then a total of 16 PRBs can be assigned to each adjacent cell, considering a simple case with an equal number of non overlapping active PRBs in each cell. This amounts to a Load Factor (LF) of 0.32, where the LF is defined as ratio of the number of assigned PRBs to be active (N_{active}) in a cell over the total number of available PRBs

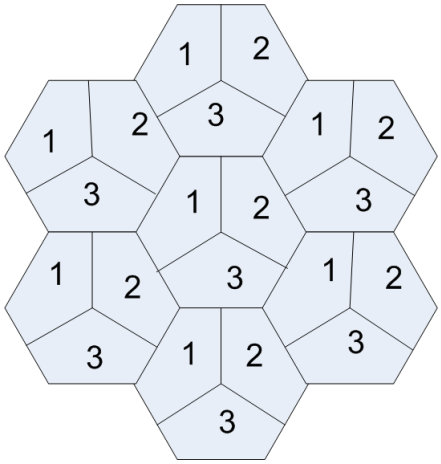

Figure 4.1: Resource partitioning and frequency planning for ROA scheme under low fractional load factor where complete overlapping avoidance of resources is possible

($N_{available}$), given as :

$$LF = \frac{N_{active}}{N_{available}} \tag{4.1}$$

We consider $LF = 0.32$ as low fractional load condition. It is obvious that, this scheme offers complete overlapping avoidance for $LF = 0.32$ or below. However, as the LF will increase over 0.32, the active PRBs in the neighboring cells will start to overlap, and therefore a fully orthogonal allocation will not be possible. In that situation it will be required to allow only those PRBs to overlap in the adjacent cells, which maximize the overall SINR condition. To deal with this situation the proposed ROA scheme selects the overlapping set of PRBs based on Quality Estimation Metric (QEM), where only PRBs with the best SINR conditions are selected (QEM is explained in section 4.5).

The ROA scheme requires a simple frequency planning. This is a simple, and a kind of static scheme aiming to ensure inter-cell interference avoidance. The complexity in this scheme increases only when the load factor goes above 0.32. The complexity under such condition increases due to QEM based PRB selection. This scheme also serves as a good reference to compare the performance of other proposed schemes.

4.4.2 Random Selection with Correlation (RSC) Scheme

In this scheme, the selection of active set of PRBs is performed randomly and independently in each cell. This scheme does not assume any time synchronization among eNode-Bs for PRB selection. After a set of PRB is selected, the selection is maintained for a specific duration of time by introducing time correlation. The duration for which the selection is maintained is called time correlation length T_{corr}, expressed in terms of number of Transmission Time Intervals (TTIs). The time correlation is achieved by setting a counter when PRBs become active. The counter is initialized with $T(k) = T_{corr}$, where T_{corr} corresponds to the maximum number of TTIs the PRBs can be active. In each TTI

the counter steps down by one unit step and when $T(k) = 0$, a new set of PRBs is selected. The required number of active PRBs for a particular LF is calculated as:

$$N_{LF} = N_{available} \times LF \tag{4.2}$$

Since the number of active PRBs may be time variant therefore it may be required to be increased or decreased.

- The N_{active} PRBs in a cell should be equal to N_{LF}.
- In case $N_{active} > N_{LF}$, then randomly $N_{active} - N_{LF}$ PRBs are set to dormant state from the set of N_{active} PRBs.
- In case, $N_{active} < N_{LF}$, then randomly $N_{LF} - N_{active}$ PRBs are set to active state from the set of $N_{dormant}$ PRBs.

The steadiness in PRB activity state is achieved by introducing time correlation. The time correlation should be kept long enough to control frequent 'on-off' transitions, and at the same time short enough to provide frequency diversity and interference averaging. This scheme does not ensure allocation of non overlapping set of PRBs with respect to adjacent eNode-Bs even under low fractional load conditions. It is a simple scheme due to random PRB allocation. It requires no frequency planing.

4.4.3 Correlation with Weighting Coefficient (CWC) Scheme

CWC is a channel aware scheme in contrast to RSC. The CWC selects PRBs based on the packet scheduler metric. A concept of weighting coefficient W_{TP} is introduced in this algorithm. The W_{TP} is determined by using the results of proportional fair (PF) packet scheduler metric [57]. We define W_{TP} as ratio between the PF metric of the dormant and the active PRBs, expressed in (4.3) and (4.4), W_{TP} is given in (4.5). If the instantaneous throughput of a dormant PRB is at least W_{TP} times higher than the one of an active PRB then the currently dormant PRB will be prioritized for scheduling. otherwise the previously scheduled PRB will be rescheduled.

$$M_{dormant} = \frac{TP_i(CQI_{dormant})}{\overline{TP}_i} \tag{4.3}$$

$$M_{active} = \frac{TP_i(CQI_{active})}{\overline{TP}_i} \tag{4.4}$$

$$W_{TP} = \frac{M_{dormant}}{M_{active}} = \frac{TP_i(CQI_{dormant})}{TP_i(CQI_{active})} \tag{4.5}$$

In (4.3) and (4.4) $\overline{TP}_i$ represents the average delivered throughput to user i. The instantaneous supported throughputs of user i over the dormant and active PRBs are represented by $TP_i(CQI_{dormant})$ and $TP_i(CQI_{active})$ respectively. The difference in the supported throughput is realized due to the difference in the number of data bits carried by employing different modulation and coding schemes (MCS), expressed as:

$$TP_i = log_2 N_{symbols} \cdot \frac{k}{n} \tag{4.6}$$

where $N_{symbols}$ represents the number of symbols in the constellation and $\frac{k}{n}$ represents the coding rate. Table 2 shows the relative throughput gain for a range of commonly used MCS as an example [58].

Table 4.1: Relative Throughput Gain for a Range of Commonly used MCS

	$64QAM\frac{4}{5}$	$64QAM\frac{2}{3}$	$64QAM\ \frac{1}{2}$	$16QAM\ \frac{4}{5}$	$16QAM\ \frac{2}{3}$	$16QAM\ \frac{1}{2}$	$QPSK\ \frac{2}{3}$	$QPSK\ \frac{1}{2}$
$64QAM\frac{4}{5}$	1.00	1.20	1.60	1.50	1.80	2.40	3.60	4.80
$64QAM\frac{2}{3}$		1.00	1.33	1.25	1.50	2.00	3.00	4.00
$64QAM\ \frac{1}{2}$			1.00	0.94	1.12	1.50	2.25	3.00
$16QAM\ \frac{4}{5}$				1.00	1.20	1.60	2.41	3.20
$16QAM\ \frac{2}{3}$					1.00	1.33	2.00	2.67
$16QAM\ \frac{1}{2}$						1.00	1.50	2.00
$QPSK\ \frac{2}{3}$							1.00	1.33
$QPSK\ \frac{1}{2}$								

A dormant PRB will be prioritized over an active PRB as long as a throughput upgrading equivalent to at least W_{TP} is realized, otherwise the previously scheduled PRB will be rescheduled. However, in order to limit the number of times a PRB being scheduled a concept of time correlation T_{corr} function, similar to RCS is also introduced. The time correlation function depends on the number of consecutive schedules which determines the maximum number of times the same PRB can be scheduled.

4.4.4 Quality Estimation based Selection (QES)

QES scheme selects the set of active PRBs based on Quality Estimation Metric (QEM). The QEM is generated based on the estimated quality over the PRBs. The estimated quality over the PRBs in downlink is based on the SINR estimates over the PRBs reported by the users, whereas, in uplink this is based on the e-NodeB's own estimates over the PRBs towards the users.

The Quality of the PRBs is estimated in the following steps.

1. The e-NodeB collects the SINR estimates over all the PRBs for each user at each time instant, represented as :
$$\overline{SINR}(t,i,k) \tag{4.7}$$
where, $i = 1, 2...N$ and $k = 1, 2...K$ represents the users and the PRB indices, and t represents the time instants.

2. The above SINR estimates are averaged over all the users:
$$\widehat{SINR}(t,k) = \frac{1}{N}\sum_{i}^{N}\overline{SINR}(t,i,k) \tag{4.8}$$

3. And finally the quality of a k^{th} PRB, denoted as $Q(k)$ is obtained by averaging the above expression over the time interval:
$$Q(k) = \frac{1}{T_{avg}}\sum_{t=1}^{T_{avg}}\widehat{SINR}(t,k) \tag{4.9}$$

The PRBs are sorted based on their estimated quality $Q(k)$ to form the QEM, and the quality estimation based selection scheme, i.e. QES selects the required number of active PRBs based on the QEM. This scheme helps to achieve an adaptive behavior because it takes the interference environmental variations in to account, besides ensuring full frequency diversity.

4.4.5 Integration of Proposed ICIA Schemes with Packet Scheduler

For packet scheduling functionality, the decoupled time and frequency domain packet scheduler is used [59] and [60]. In every subframe the Time Domain Packet Scheduler (TDPS) part firstly selects a set of N UEs based on the priority policy, and then the Frequency Domain Packet Scheduler (FDPS) performs the mapping of PRBs towards the users. The proposed intercell interference avoidance schemes are integrated with the FDPS part of the packet scheduler (as shown in figure 4.2) in order to impact its decision in the selection of the set of active PRBs.

4.5 Modeling Assumptions

The performance of the proposed schemes is evaluated in a quasi-dynamic DL multicell system level simulator, which is also employed in chapter 3. The macro cell case #1 defined in [11] is chosen as the simulation scenario. Link to system level mapping is based on exponential effective SINR model [43]. The layout is assumed to be of 19 sites with 3 sector antennas. However, only 7 sites are explicitly simulated (to avoid excessive simulation time), where users are dropped in all the cells with uniform random probability.

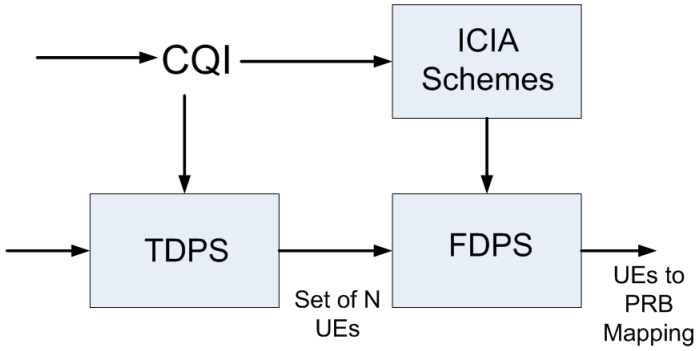

Figure 4.2: The proposed Intercell Interference Avoidance schemes are integrated with FDPS part of the employed packet scheduler

In order to obtain a fair interference pattern, wrap around is employed. The decoupled time and frequency domain proportional fair packet scheduler is used. A summary of main parameters and simulation assumptions is given in table 4.2.

Table 4.2: Main Parameters and Simulation Assumptions

Parameter	Settings
Cellular Layout	Hexagonal Grid 19 Sites
Inter Site Distance	500 m (Macro Case #1)
Carrier Frequency	2 GHz
System Bandwidth	10 MHz
Number of Subcarriers	600
Number of PRBs	50 (12 Subcarriers/PRB)
Sub Frame Duration	1ms (14 OFDM Symbols)
Total eNode-B Transmit Power	46 dBm (1 Tx Antenna)
UE Receivers	2-Rx Interference Ratio Combining
Antenna Height	15 m
Antenna Gain	14 dBi
Shadowing Standard Deviation	8 dB
HARQ Model	Ideal Chase Combining
Ack/Nack Delay	2 ms
CQI Log Normal Std. Error	1 dB
CQI Reporting Resolution	1 dB
CQI Reporting Delay	2 ms
BLER Target	20 %
Power Delay Profile	ITU 20-Paths Typical Urban
UE Speed	3 kmph
Min. UE to eNB Distance	35 m
AMC	QPSK (1/3, 1/2, 2/3)
	16-QAM (1/2, 2/3, 4/5)
	64-QAM (1/2, 2/3, 4/5)

The Best Effort (BE) and the Constant Bit Rate (CBR) traffic models are employed for the simulation. The BE traffic model does not guarantee any specific data rate. It rather allows the use of as many resources as possible to complete the transmission based on the channel conditions, and therefore the users with good channel conditions achieve higher data rates compared to the users with poor channel conditions. Under BE traffic model low and medium LF are simulated. Where low corresponds to $LF = 0.32$, and medium corresponds to $LF = 0.50$. With low load factor a fixed load model is used, where $LF = 0.32$ is simply fixed for each cell. The simulation with medium load factor uses stationary stochastic process with a average value of 0.50, which is determined by two states Markov chain of 50 PRBs, where one state corresponds to the active, and the other state corresponds to the dormant state of the PRBs [55]. The LF is determined by the number of states representing the active PRBs. Under CBR traffic model, a constant bit rate of 512 kbps is assumed with 2 seconds session time. The Poisson call arrival model is employed with 5 calls per second. Table 4.3 summarizes the considered traffic scenarios.

The CBR model provides an adaptive traffic load model and represents close to the actual traffic conditions. However, in this model the estimation of LF is required to be performed before the PRB allocation. Two approaches are used for estimation of the LF.

- **C**hannel **B**lind **E**stimation (CBE) or Channel Agnostic Estimation
- **T**hrough**P**ut based **E**stimation (TPE).

Under CBE approach, the LF is determined as a function of the number of users (N_{users}) only, with no consideration of their distribution within the cell:

$$LF_{CBE} = \frac{N_{users} \cdot TP_{CBR}}{\overline{TP_{cell}}} \tag{4.10}$$

where, $\overline{TP_{cell}}$ represents an estimate of the cell capacity. We choose $\overline{TP_{cell}}$ = $12Mbps$, based on the previous LTE studies [60].

The throughput based estimation approach determines LF as:

$$LF_{TPE} = \frac{TP_i}{\overbrace{TP_{cell}}} \tag{4.11}$$

where TP_i is the required throughput of user i, and $\overbrace{TP_{cell}}$ is the maximum estimated cell throughput. However, this is heavily related to the user conditions, and therefore every user experiences a different value. Hence, user,s estimate of TP_{cell} is used denoted as $\widehat{TP_i, cell}$ and then the LF is expressed as:

$$LF_{TPE} = \sum_{i=1}^{N_{users}} \frac{TP_i}{\widehat{TP_i, cell}} \tag{4.12}$$

where,

$$\widehat{TP}_i, cell = \sum_{k}^{N_{PRB}} TP_k(CQI_{i,k}) \tag{4.13}$$

Table 4.3: Considered Traffic Scenarios

Type of Traffic	Average FLF	Traffic Model
BE with Finite Buffer	0.32	Fixed Load Model
	0.50	Markov Model
CBR	Variable	Poisson Call Arrival

Key Performance Indicators (KPIs) and Reference Schemes

Geometry Factor, Coverage, Throughput per PRB, Effective SINR and Number of Collisions are taken as KPIs. Geometry Factor and Coverage are described in section 3.4.2, whereas Effective SINR is explained in section 2.5.

Throughput per PRB: The average cell throughput is the amount of bits delivered successfully in a unit time (see section 3.4). In fact, with different amount of traffic loads, the number of PRBs employed in different cells will be different, resulting in different average cell throughput. In such condition, the average cell throughput does not provide a uniform measure of performance. Therefore the *throughput per PRB* is chosen as a KPI, which is defined as the average cell throughput over the mean number of active PRBs, expressed as :

$$TP_{PRB} = \frac{\overline{TP}_{cell}}{\overline{N}_{active}} \tag{4.14}$$

where $\overline{TP}_{cell}$ represents the average cell throughput, and $\overline{N}_{active}$ represents the mean number of active PRBs employed in the cell. TP_{PRB} provides a throughput performance independent of the amount of load in the cell besides providing an indication on how effectively the PRBs are utilized.

Number of Collisions : A collision takes place when the same PRB becomes active in two adjacent cells at the same time. The magnitude of interference between the adjacent cells is directly related to the number of PRBs in collision. The higher the number of PRBs in collision, the higher the ICI. The number of collision N_{col} is taken as an indicator of the interference environment within the cell. N_{col} indicates how many collisions are taking place on an average over any PRB at any time. This is obtained by averaging the collision time and frequency and is defined as the mean number of collisions per PRB per TTI.

Reference Scheme.

In order to evaluate the performance of the proposed schemes under fractional load, the performance under full load scenario can be taken as a reference scheme. However, the performance at full and fractional load scenarios cannot be compared directly due to the difference in the number of PRBs in use. Therefore, a reference scheme with equivalent amount of fractional load with full resource overlapping is considered. In this reference scheme, the number of PRBs are taken as equal to the considered fractional load, with all the PRBs forced to overlap in adjacent cells to represent the full load condition. Although it represents a pessimistic condition, yet it provides a means to evaluate the comparative performance of the proposed schemes. The proposed schemes are also compared with full load, whenever needed.

4.6 Performance Evaluations

The performance results under Best Effort traffic with low and medium load factors are shown in subsections 4.6.1 and 4.6.2 respectively. The results with Constant Bit Rate traffic are given in Subsection 4.6.3.

4.6.1 Performance in Best Effort Traffic with Low Load Factor

Under low fractional load conditions, i.e. $LF = 0.32$, the effective SINR ($SINR_{eff}$ will be high enough because of fewer collisions, and therefore it provides a good setup to analyze the behavior of the schemes under favorable conditions. Table 4.4 shows the parameter settings of different schemes for simulation under low fractional load condition. Extensive simulations were performed to decide the most suitable numerical values for these parameters [58].

Table 4.4: Main Parameters for Different Schemes

RSC	CWC		QES
T_{corr}	T_{corr}	W_{TP}	T_{Avg}
$130TTIs$	$130TTIs$	1.75	$325TTIs$

The performance in terms of number of collisions(N_{col})for different schemes, along with the reference case is given in Figure 4.3. With low load factor, there is absolutely no collision for resource overlapping avoidance(ROA)scheme, the allocation of PRBs are planned to be fully orthogonal in adjacent cells. Therefore, this scheme naturally achieves the best ICI avoidance. On the other hand, the reference case gives the most pessimistic results, where the number of collisions is the highest; in fact the maximum possible, since all the resources are in collision.

Contrary to the above two cases, the random selection based scheme, i.e. RSC selects the PRBs randomly, with equal probability of selection for all the PRBs. The probability

for a PRB being selected is in agreement with the definition of LF, which is defined as the number of active PRBs in the cell over the total number of available PRBs. Therefore, the number of collisions for RSC with 6 interfering neighboring eNode-Bs will be:

$$N_{col} = LF \cdot \text{Number of interferers} = (0.32) \cdot (6) = 1.92 \tag{4.15}$$

This is shown in the figure as well.

The number of collisions experienced by the quality estimation based selection scheme, i.e, QES is lower than random selection scheme. Moreover, it does not guarantee fully orthogonal selection of PRBs, therefore the number of collisions in this scheme is higher than the resource overlapping avoidance scheme.

The correlation with weight coefficient scheme i.e. CWC, experiences the highest number of collisions amongst all the proposed schemes. CWC combines the features of time correlation and weight coefficient, where the weight coefficient prioritizes PRBs with considerably low interference, based on the latest CQI report. Between two subsequent reports, different cells may decide to allocate the same PRB, leading to concurrent allocation. In addition, the rescheduling of the same PRBs is further encouraged by feature of time correlation, which prolongs this condition, and hence higher number of collisions.

The results on throughput per PRB and coverage are presented in figure 4.4. In general the schemes with lower number of collision yield higher throughput per PRB and coverage. However, some variations from this general trend could be observed. For instance, between RSC and CWC the difference in their throughput and coverage performance is smaller compared to the difference in their number of collisions. This variation could be understood by interpretation of the MCS used by these two schemes, shown in figure 4.5. The CWC provides higher MCS usage than RSC and therefore achieves higher coverage. The poor ICI condition due to higher number of collisions is also compensated to some extent, and therefore throughput per PRB becomes closer to the performance of RSC.

Another noticeable example is the quality estimation based selection scheme i.e.QES which gives higher throughput per PRB and coverage compared to the overlapping avoidance scheme, ROA, even if the number of collisions for QES is higher compared to ROA. This is due to the fact that the QES selects PRBs based on overall channel quality, whereas in case of ROA only the interference avoidance is considered by orthogonal allocation. This highlights the ability of the QES scheme regarding selection of the best available PRBs.

The performance in terms of effective SINR is shown in figure 4.6. It is clearly visible that the QES provides the highest effective SINR, even though it has a higher number of collisions compared to ROA. The effective SINR gains over the reference case lie between $7.8dB$ to $8.5dB$, leading to cell throughput per PRB gain in the order of 70% to 95% for different schemes. It is worth noticing that a significant effective SINR gain is realized even with the simplest scheme proposed, which is based on the random selection of PRBs.

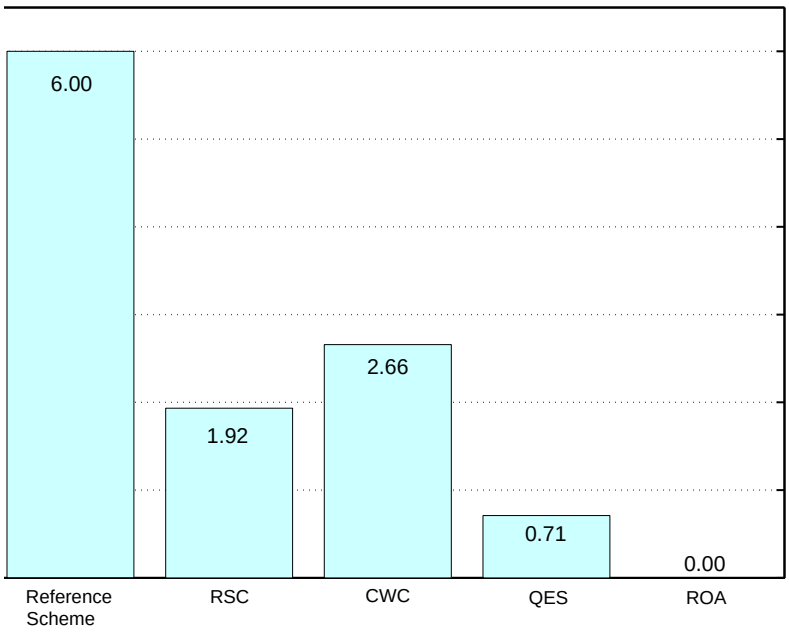

Figure 4.3: The number of collisions for different schemes under low fractional load factor compared with reference scheme

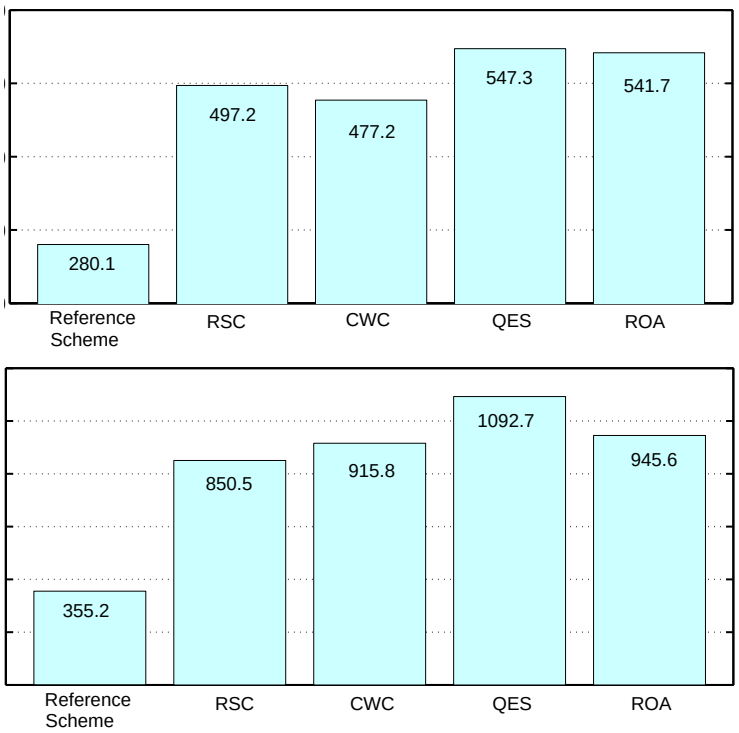

Figure 4.4: Throughput per PRB and coverage for the proposed schemes under low fractional load factor compared with reference scheme

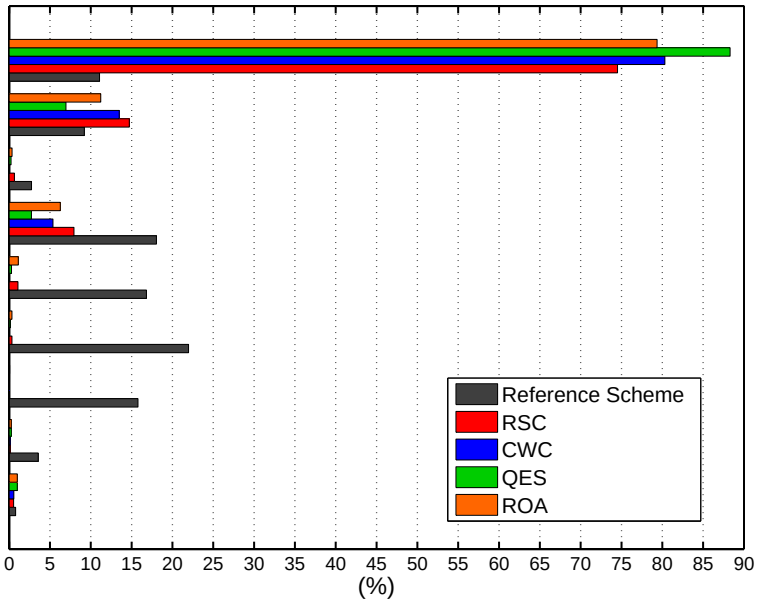

Figure 4.5: MCS distribution for different schemes under low fractional load factor.

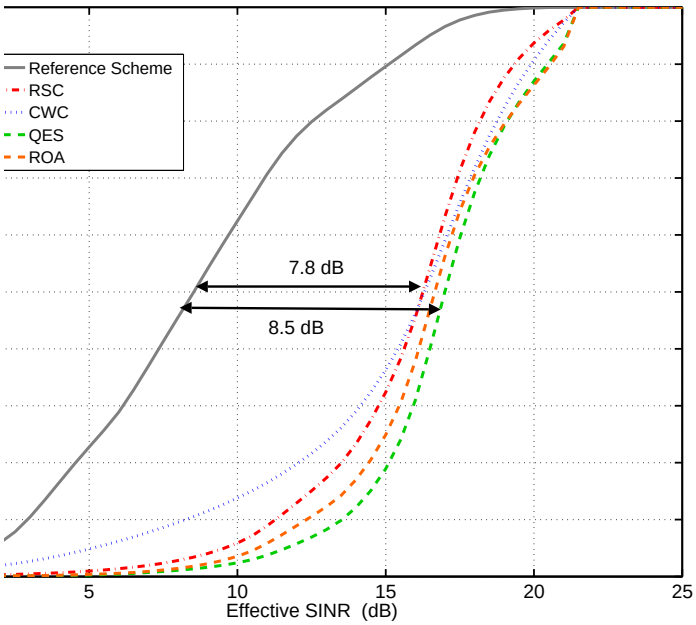

Figure 4.6: Effective SINR for different schemes under low fractional load factor compared with the reference scheme.

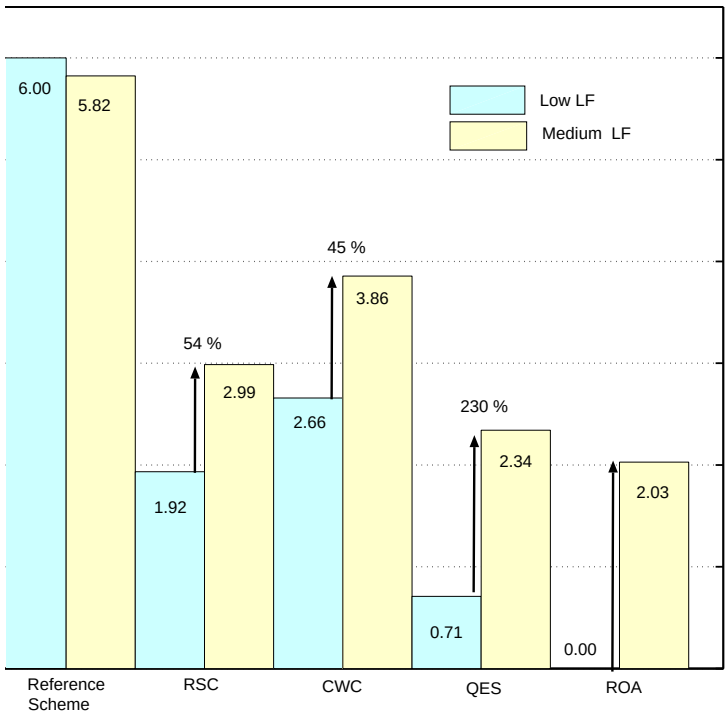

Figure 4.7: Comparison of the number of collisions for different schemes in low and medium fractional load factor.

4.6.2 Performance in Best Effort Traffic with Medium Load Factor

In case of medium load, i.e. $LF = 0.50$, an average of 25 PRBs will be active in each cell. Therefore, $25 - 16 = 9$ PRBs will be overlapping. Thus, a general increase in number of collisions, compared to low load should be observed, which is seen in figure 4.7. Considering equal usage of all the PRBs the minimum number of collisions can be found as :

$$N_{col} = (1/25).(9).(6) = 2.16 \tag{4.16}$$

In the figure it can be observed that the overlapping avoidance scheme ROA, shows the number of collisions below the minimum expected, because it selects the overlapping set of PRBs based on quality estimation metric, QEM. The random selection scheme, RSC, shows the number of collisions as expected, i.e.$N_{col} = (0.5).(6) = 3$. It is interesting to note that the reference scheme behaves contrary to the general trend, where the lower number of collisions is reported with medium load compared to low load. The reason is that in medium the markov model is used, which introduces time variation in PRB selection. Therefore, all the PRBs may not be in collision all the time, as was the case in low load condition, where the load factor was simply fixed.

The throughput per PRB and coverage performance are presented in figure 4.8, showing a general decrease in medium load compared to low load. The QES undergoes a

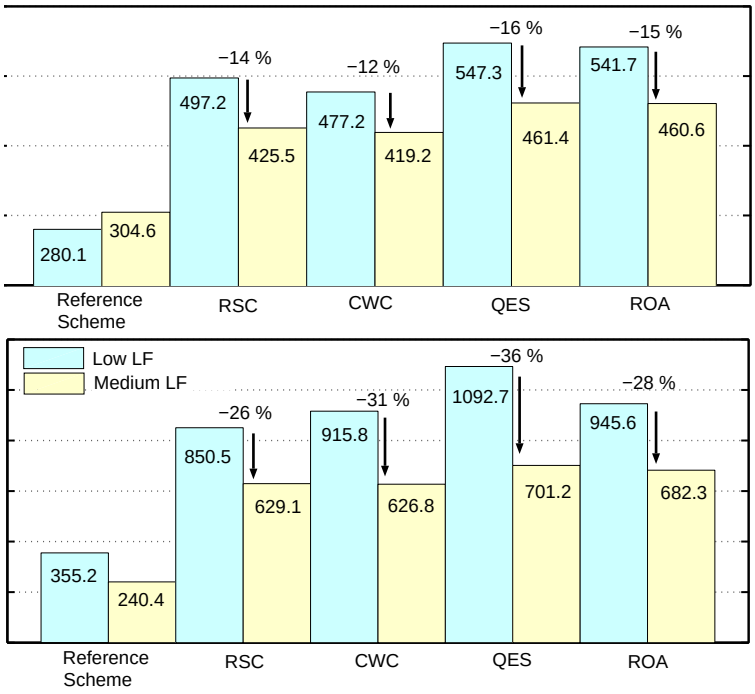

Figure 4.8: Comparison of throughput per PRB and coverage under low and medium fractional load factor for the proposed schemes.

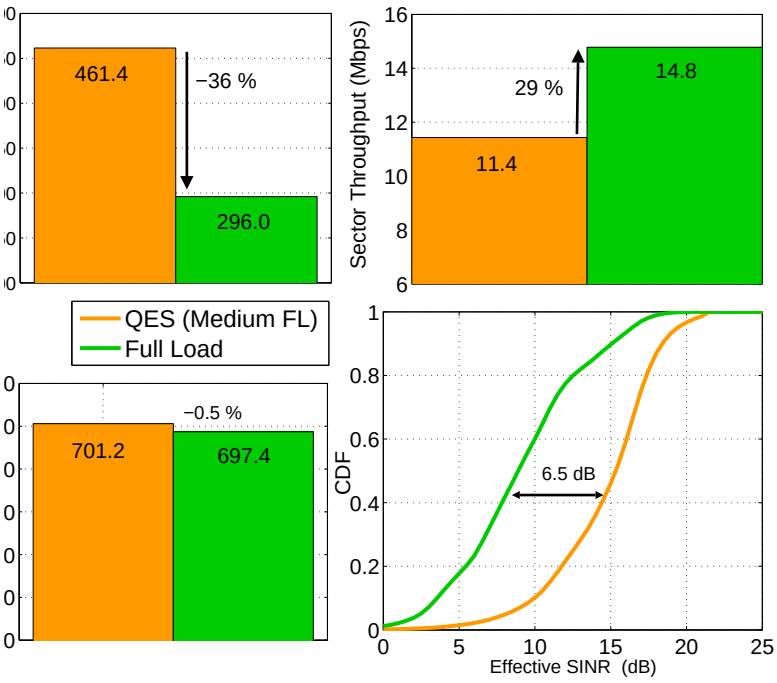

Figure 4.9: The performance of quality estimation based scheme (QES) at medium fractional load factor compared with full load.

high throughput and coverage penalties, due to significantly increased number of collisions. The ROA exhibited an increase in number of collisions lower than expected as a minimum, therefore it undergoes comparatively lower losses in throughput per PRB and coverage. The performance of CWC is less affected in terms of throughput per PRB, because it records the minimum increase in number of collisions amongst the proposed schemes.

It is noticeable that QES results in the highest throughput per PRB and coverage performance compared to all the other schemes. This is further compared with full load scenario with the same number of users and shown in figure 4.9, where it is worth noticing that even though full load employs twice the bandwidth, it offers only 29 % increase in the sector (cell) throughput. Also, the effective SINR for full load is 6.5 dB lower, i.e. more than 4 times. This clearly indicates the SINR improvement achieved by QES used under FL conditions. This allows higher MCS to be employed, resulting in significantly higher throughput per PRB.

4.6.3 Performance in Constant Bit Rate Traffic

To evaluate the performance under constant bit rate, the quality estimation based resource selection scheme (QES) is employed with channel blind estimation (CBE) as well as throughput based estimation(TPE) methods. The results are compared with the full load results. The user throughput versus G factor, and the user outage throughput are taken as measures to evaluate if the guaranteed bit rate is achieved.

From figure 4.10 it can be observed that, when channel blind estimation is used, then almost all the users are below the guaranteed bit rate. At the same time average delay experienced is also significantly higher compared to full load condition. Whereas this is not true when throughput based estimation is employed. This can be understood as : the estimation of load factor in case of channel blind estimation method starts with a homogeneous number of users in all the cells. But subsequently the number of users in each cell varies dynamically with respect to time due to the dynamic load model employed using Poisson call arrival. Due to the variation and uneven distribution of the LF throughout the layout a mismatch is created between the expected and actual interference level, when using CBE method. The LF is often under or over estimated. When under estimated, throughput produced will be lower than expected. When over estimated, the throughput is limited by the CBR requirement. Hence, the throughput loss occurred, while under estimated, is not compensated while it is overestimated. Thus, the performance using channel blind estimation is adversely affected.

In fact,a tight relationship between number of users and load factor cannot be established. Even with the same number of users two cells may present different magnitudes of load factors due to difference in spatial distribution of users. In addition to this, when one users leaves, the new one arrives at random location, and this new distribution also impacts load factor variation. The time variant nature of the radio channel also contributes to this variation. Since channel blind estimation method does not account for these variations,

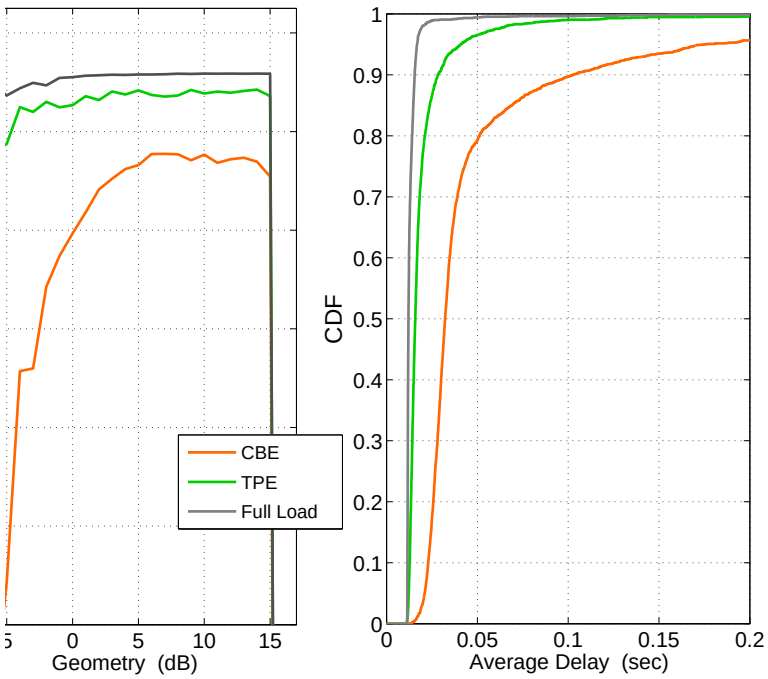

Figure 4.10: User throughput vs geometry factor and delay for QES with constant bit rate traffic compared with full load.

thus results in lower performance.

The throughput based estimation method aims to account for these variations and therefore reduces the mismatch between the expected and actual load factor estimation to a great extent. Thus, user throughput and delay performance of QES scheme with throughput based estimation is significantly higher than using the channel blind method, and is very close to the full load scenario (4.10). It gives a moderate user outage performance, with about 10 % users in outage. It is important to notice, this is achieved by using an average LF as low as 0.17 (see figure 4.11). The usage of such low LF leads to an effective SINR as much as 13.76 dB higher compared to full load (figure 4.13). Figure 4.12 shows that a significantly higher throughput per PRB is realized.

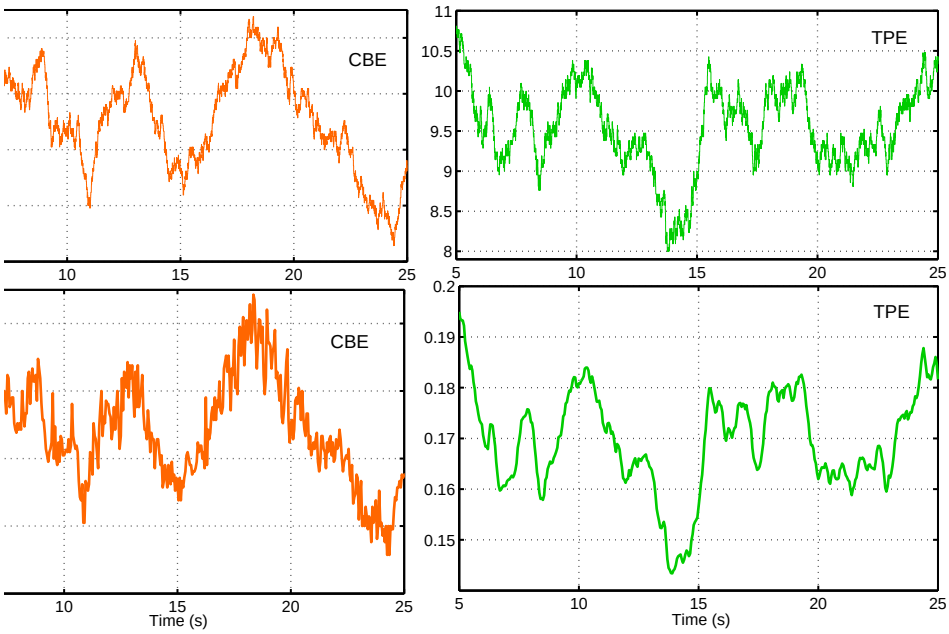

Figure 4.11: The variation in load factor with number of users.

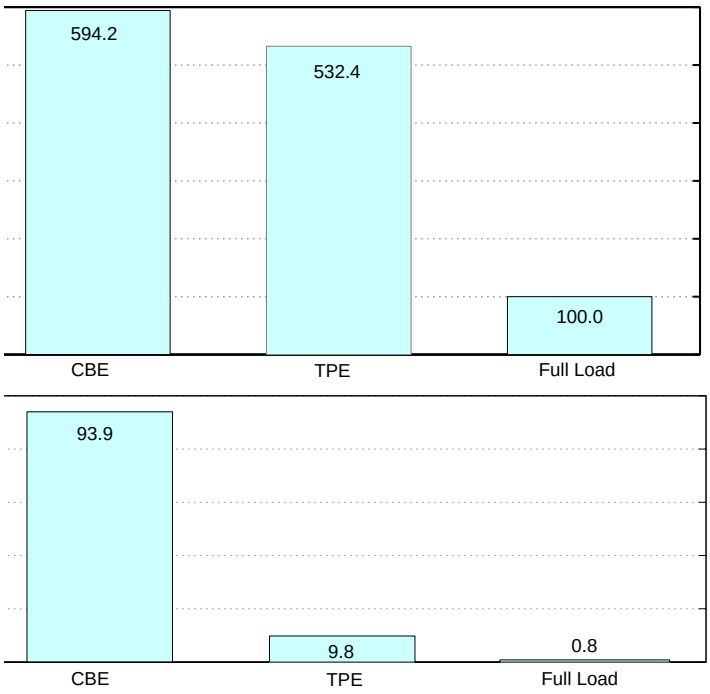

Figure 4.12: The throughput per PRB and coverage for QES with constant bit rate traffic compared with full load.

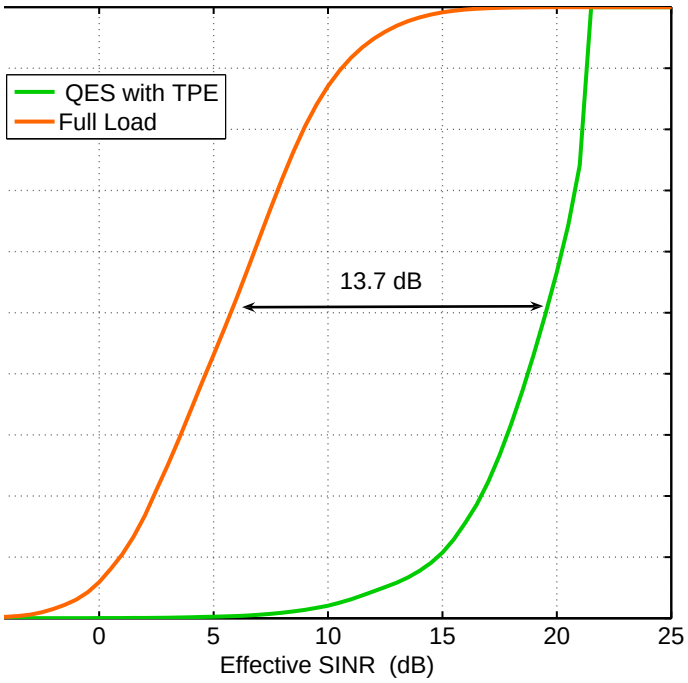

Figure 4.13: Effective SINR for QES with throughput based traffic load estimation compared with full load.

4.7 Conclusions

This chapter investigates schemes to avoid inter-cell interference in fractional load conditions. It was discussed that under fractional load condition, a CQI aware frequency domain packet scheduling can avoid inter-cell interference by avoiding scheduling of PRBs with high interference. But the performance of such scheduling is highly sensitive to inaccuracy and delay in CQI reports, leading to fast on-off transition of PRBs and high BLER. Therefore, the need for a mechanism was realized for : i) proper selection of PRBs with respect to adjacent cells in order to avoid/minimize ICI and ii) controlling the fast on-off transitions to control the high BLER.

Several autonomous intercell interference avoidance schemes are proposed for fractional load conditions in this chapter. The proposed schemes require no dedicated inter-cell signaling for controlling the ICI. The simplest proposed scheme that is based on random selection of PRBs combined with time correlation, also gives significant SINR improvement, resulting in throughput per PRB and coverage enhancements over the reference scheme. Moreover, the proposed Quality Estimation based PRB selection Scheme (QES) further improves the performance.

When QES with medium load factor (i.e. 50% fractional load) is compared with full load under best effort traffic, it was found that QES gives 6.5 dB higher effective SINR. Besides, even though full load employs twice the bandwidth, it offers only 29% increase in the sector (cell) throughput. The QES achieves significantly higher throughput per PRB compared to full load. However, the coverage gain is only slightly higher in QES compared to full load.

Further, the comparison of QES was performed with full load under constant bit rate (CBR) traffic with throughput based traffic load estimation method. A much higher effective SINR (in the order of 13 dB) compared to full load is realized, resulting in significantly higher throughput per PRB (in the order of 5 times). This performance is achieved with only about 10 % users in outage.

Chapter 5

Flexible Spectrum Usage for Local Area Deployment

5.1 Introduction

IMT-A has increased focus on nomadic / local area network solution [24], [7], which is envisioned to be the only way to significantly boost the increasing demand for high network capacity and high user data rates. 80 to 90% of traffic volume is estimated to be generated in the indoor and hot spot nomadic scenarios [61]. Currently, Home eNode-B (HeNB) is emerging as a potential solution for high data rate and high quality services in indoor local area [62]. It is considered as an alternative way of delivering the benefits of fixed-mobile convergence [62].

5.1.1 Home eNode-B

A HeNB is a small cellular base station, typically designed to be used in indoor environment. It incorporates the functionality of a typical base station and uses a simple plug and play device. HeNB will likely be deployed by the subscribers to support an individual coverage in a small area. A large scale deployment of HeNBs is expected, potentially in an uncoordinated manner, and therefore a rigorous planning is not necessarily feasible, which gives rise to several deployment issues.

5.1.2 Key Issues for HeNB Deployment in Local Area

- A conventional cellular network is designed to support a relatively small number of base stations in a given area, whereas HeNBs will be deployed in large numbers. As a consequence, a different architectural approach will be required [62].
- Due to the fact that the HeNBs are likely to be deployed by the subscribers, it

seems difficult for the operator to pre-configure and coordinate the deployment in order to minimize mutual interference. Under such deployment conditions it will be difficult to estimate the level of interference beforehand, that one HeNB could practically cause towards the coverage area of the other HeNBs. Hence, a key issue will be to address the question, how the HeNBs will coexist in the given area with desired performance?

- The HeNB should provide reasonable performance whether it is deployed in isolation or in the vicinity of multiple HeNBs. In the later case, the level of interference could be very high, and therefore, requires an effective interference management mechanism to provide reasonable performance. The interference management mechanism may pose challenges to HeNBs in managing their radio resources. The maximum power output of a HeNB should be able to provide adequate coverage, while not exceeding the HeNB interference limits [62].

- Therefore, an efficient technique will be essential to support HeNBs to self-configure, use spectrum in a flexible manner, minimize interference and to ensure coexistence with other HeNBs in the given area [9],[63].

The above mentioned issues are important to be considered in order to provide an efficient local area solution. The concept of Flexible Spectrum Usage (FSU) is widely seen as an important component to facilitate such solution.

5.1.3 Flexible Spectrum Usage (FSU)

The increasing demand of spectrum for wireless applications makes it necessary to improve efficiency of spectrum utilization by spectrum sharing techniques [64]. A large number of wireless systems and services under development will make it difficult to identify exclusive spectrum for all wireless systems and services [65]. In face of the above scenario, the Federal Communication Commission (FCC)'s Spectrum Policy Task Force (SPTF) has made recommendations to develop a spectrum policy that maximizes the flexibility of spectrum use [9]. Therefore, the framework of radio spectrum regulation is undergoing a vital change towards flexible and open access to the spectrum[63].

The commercial success of flexible and open access to spectrum for wireless applications such as WLAN in the unlicensed bands is one example, to believe that it will be useful to move towards a more flexible spectrum access [66].

Recently, the flexible sharing of spectrum is extensively addressed by the research community. The underlying concept considers two mechanisms in order to share the spectrum: (i) Spectrum Sharing (SS) and (ii) Flexible Spectrum Usage (FSU) [65]. The spectrum sharing is the notion that considers sharing of spectrum between different radio access technologies (RATs). This can be regarded as a form of inter-system spectrum sharing. Whereas, sharing of spectrum between different radio access networks (RANs) using the same RAT is defined as FSU. Wireless World Initiative New Radio (WINNER)

has developed a flexible and scalable radio interface, which covers different domains (local area, metropolitan area, and wide area) with the same radio interface [67].

The FSU is mainly viewed in the context of multi-operator scenario providing services over the same RAT. It is based on the concept that, when one network operator is in demand of additional spectrum, the other operator might have an excess of it. If a means can be provided to dynamically access spectrum on spatio-temporal basis in the situation described above, rapid traffic fluctuations can be met efficiently, and the capacity-on-demand capabilities can be achieved [9]. FSU can inherently enable such dynamic access and help to expand network capacity at peak traffic times. However, FSU is not limited to the multi-operator domain only. It can be employed within a single operator's network as well. While the multi-operator FSU allows different operators to access the common spectrum pool in a flexible manner based on their individual requirements, the single operator FSU aims to achieve high performance in uncoordinated and random network deployment. In this chapter we focus on a single operator FSU in local area indoor deployment.

A somewhat similar scenario is introduced in [68], [63] and [69], where an algorithm is provided to smooth out the allocation of the available transmission time among the devices in a WLAN scenario. The algorithm uses the concept of water filling. The water filling in time domain enables a decentralized, coordinated and opportunistic use of spectrum [66]. The algorithm is referred to as spectrum load smoothing (SLS). With SLS the competing radio systems aim simultaneously at an equal utilization of the spectrum. Based on the observation of the past usage of the radio resource, the radio systems interact and redistribute their allocations of the spectrum under the consideration of the QoS requirements. In these references, only time domain and fully orthogonal redistribution of the spectrum is shown. However, we aim to provide a mechanism for sharing in frequency domain with some degree of spectrum overlap, with an objective to enhance spectrum usage.

5.1.4 Aim of this Chapter

We aim to provide non-contention based algorithms to enable FSU among HeNBs, and ensure their co-existence in local area deployment by partially or completely preventing mutual interference on the shared spectrum. We assume an uncoordinated deployment of HeNBs by a single operator. The proposed algorithms work on the principle of self assessment of surrounding radio environment and aim to provide self-configurable, decentralized and scalable solution. The following two algorithms are proposed in this chapter:

1. Fixed SINR threshold based **S**pectrum **L**oad **B**alancing (**SLB**) algorithm.

2. Comparative interference threshold based **R**esource **C**hunk **S**election (**RCS**) algorithm.

This chapter is organized as follows. Section 5.2 presents the description of the spectrum load balancing algorithm proposed for flexible spectrum usage. Section 5.3 gives an account of the simulation environment. The main parameter settings and simulation assumptions, key performance indicators and the reference schemes are described in this section. In section 5.4 main results on the performance of the SLB algorithm are presented, and their pros and cons are discussed. Section 5.5 describes comparative interference threshold based RCS algorithm, which has been proposed as an improvement over the SLB algorithm, and the performance results of this algorithm are also presented in this section. Finally in section 5.6 the main findings are summarized.

5.2 SLB Algorithm for Flexible Spectrum Usage

Our assumption is that several HeNBs access the common pool of spectrum in order to meet individual traffic requirements. These HeNBs potentially interfere with each other due to their vicinity in the given geographical area. We assume that there is no dedicated communication link between HeNBs. However, a limited information exchange is assumed via over-the-air-communication [70].

The SLB algorithm aims to ensure co-existence of mutually interfering HeNBs by spectrum allocation based on SINR threshold ($SINR_{th}$). The spectral resources with SINR below the $SINR_{th}$ are not selected by HeNBs. The SINR threshold plays an important role in setting the level of tolerable mutual interference as well as it ensures a desirable throughput performance. The degree of spectrum overlap is controlled by the level of SINR threshold. The higher the SINR threshold the lower the spectrum overlap and vice-versa. Therefore the selection of $SINR_{th}$ depends on the trade-off between the allowed mutual interference and spectrum utilization. The underlaying concept of SLB algorithm is explained below.

The cell capacity in terms of SINR for an individual HeNB in the network can be represented by using Shannon's expression as:

$$C = \rho \cdot B \log_2 \left(1 + \frac{S}{I+N}\right) \tag{5.1}$$

where, B, S, I and N represent respectively the system bandwidth, signal power, amount of interference and noise power over the system bandwidth respectively, and ρ represents the fraction of the bandwidth utilization. The total system capacity $\mathcal{C}$ for a multicellular network can be expressed as:

$$\mathcal{C} = \sum_{i=1}^{N_{cells}} \sum_{k=1}^{K} C_i^k \tag{5.2}$$

where,

$$C_i^k = \rho_i^k \frac{B}{K} \cdot \log_2 \left[1 + \frac{\frac{P}{\sum_{k=1}^{K} \rho_i^k} g_{ii}^k}{\sum_{j \neq i, j=1}^{N_{cells}} \frac{P}{\sum_{k=1}^{K} \rho_j^k} g_{ij}^k \rho_j^k + N_0 \frac{B}{K}} \right] \tag{5.3}$$

where, $i = 1, 2, ..., N_{cells}$ and $k = 1, 2, ..., K$ represent the number of considered cells in the network and total number of available Resource Blocks (RBs) over the total system bandwidth, where a RB is defined as a unit of spectrum allocation in time and frequency domain. P represents the total transmit power, and C_i^k represents capacity of cell i over the k^{th} RB. The channel gain between the cell i and its own user within the cell is represented by g_{ii}^k whereas, g_{ij}^k is channel gain from the interferers over RB k from cell j. N_0 represents noise spectral density.

The consideration of ρ_i^k in the expression (5.3) is crucial for FSU algorithms, which significantly impacts SINR conditions and therefore the overall network performance in a multicellular environment. The FSU algorithm at HeNB aims to suitably determine ρ_i^k by selecting a subset of resource blocks such that it avoids the mutual interference as much as possible. If the k^{th} RB is selected for the i^{th} HeNB then $\rho_i^k = 1$, otherwise $\rho_i^k = 0$. Where, the expression $\sum_{k=1}^{K} \rho_i^k$ gives the fraction of total spectrum allocated by i^{th} HeNB.

In the proposed SLB algorithm the SINR threshold ($SINR_{th}$) is used as a decision criterion to select $\rho_i^k = 0$ or $\rho_i^k = 1$ for a HeNB over set of all the resource blocks. The detailed explanation of the algorithm is given below.

Description of SLB Algorithm

The SLB algorithm is performed in two phases, A) initialization phase and B) spectrum allocation phase.

A. Initialization Phase

The initialization phase starts as soon as the HeNB is powered on. At this moment there is no information on which PRBs to use, therefore the HeNB allocates PRBs randomly in order to start carrying traffic. In this phase, $\rho_i^k = 1$, if $k \in N_i^{load}$, otherwise $\rho_i^k = 0$, where N_i^{load} is the set of PRBs selected randomly to meet the requirements of the traffic load by i^{th} HeNB. Once the communication is established between UE (s) and HeNB, the SINR estimates over the PRBs become available. The SINR estimates are used for allocation of the PRBs in the next phase of the algorithm.

B. Spectrum Allocation Phase

This is performed in two steps, i) Allocation of free PRBs using Water Filling (WF) and ii) Allocation of PRBs based on SINR threshold.

Step 1: Allocation of Free Spectrum using WF

The aim of the algorithm in this step is to identify free PRBs and enable HeNB to select the free PRBs using WF in the following manner. Here the term WF has not been used in the information theoretic sense, which is generally meant by the term WF. However here we use the term WF which aims to average out the PRBs allocation among HeNBs as far as possible.

- **Identification of Free PRBs**

  At first, the free PRBs are identified. Free PRBs are those which are not allocated by any HeNB. Free PRBs are identified as PRBs with no interference, i.e. if, $I_i^k = 0$ for all i, where $i = 1, 2...N_{cells}$, then the PRB k is identified as free PRB. No interference is experienced by any HeNB over this PRB. The set of free PRBs F can be obtained as below.

  $F = \emptyset \;\; for\; k = 1, 2...K$
  $if, I_i^k = 0$ for all $i = 1, 2...N_{cells}$
  $F = F \cup \{k\}$

  The total number of elements in F gives the number of free PRBs denoted by N_{free}.

- **Calculation of Mean Number of PRBs**

  After identification of free PRBs the mean number of PRBs (N_{mean}) is calculated, which gives the average of the number of PRBs to be allocated to each HeNB in order to have even PRB distribution. N_{mean} is defined as the aggregate of the free PRBs plus sum of individual allocations of each HeNB over the number of HeNBs in consideration, as expressed below:

  $$N_{mean} = \frac{N_{free} + \sum_{i=1, i\in M}^{nM} \sum_{k=1}^{K} \rho_i^k}{nM} \tag{5.4}$$

  where, M represents the set of HeNBs used for the calculation of N_{mean} and nM represents the number of elements in M.

- **Comparison of N_{mean} with Individual Allocations**

  The comparison of N_{mean} with individual allocation of each HeNB is carried out. If the allocation of any HeNB is found above N_{mean}, then this HeNB is excluded, and a new N_{mean} is calculated with the remaining HeNBs.

  $for\; m = 1, 2, ...N_{cells},\; m \in M$
  $if \sum_{k=1}^{K} \rho_m^k \geq N_{mean}$ then the m^{th} HeNB is excluded and M is updated

  In the first iteration $nM = N_{cells}$, but subsequently it decreases by excluding the HeNBs fulfilling the above condition.

- **Leveling of PRB Allocation**
  Finally, the free PRBs are allocated to HeNBs with the number of PRBs below N_{mean}. The number of free PRBs allocated to the j^{th} HeNB will be $N_{mean} - \sum_{k=1}^{K} \rho_j^k$. This brings the allocation of j^{th} HeNB at the level of N_{mean}. This step aims at distribution of free PRBs among HeNBs in order to bring them at the same average level of allocation as far as possible.

  Figure 5.1 shows an example of PRB allocation using above mentioned WF approach with 4 HeNBs. This figure is obtained after implementation of the WF step. The PRBs shown in blue indicate the allocation of HeNBs before the WF step, whereas the PRBs represented in red are allocated as a result of WF approach. It can be observed that the HeNB 1 selects a higher number of PRBs than HeNB 3 in order to have an equal share. No additional PRBs are allocated to HeNBs 2 and 4, indeed they are excluded since their allocations are already above N_{mean}.

We assume that the PRB allocations of neighboring HeNBs are known in order to perform such water filling. This information is available by limited signaling via over-the-air-communication.

Step 2: SINR Based Spectrum Allocation

Once the UEs are connected to HeNBs, the SINR estimates in the DL and UL are obtained over PRBs. In DL the SINR estimate is the SINR measured by UE on the scheduled PRBs and fed back to the connected HeNB. In UL the SINR estimate is the measured SINR at HeNB on the PRBs scheduled to UEs. We assume ideal SINR measurement without any SINR measurement errors and reporting delays.

In this step the required number of PRBs are selected based on desired SINR threshold ($SINR_{th}$). The SINR threshold allows opportunistic selection of PRBs with some degree of frequency-domain overlap, and ensures co-existence of mutually interfering HeNBs. The SINR threshold corresponds to the minimum desirable level of QoS and also defines the coverage of the cell. The PRBs with SINR above $SINR_{th}$ are selected, i.e. ρ_i^k is set to 1 if $SINR_i^k > SINR_{th}$, otherwise $\rho_i^k = 0$.

Out of all the PRBs above the threshold, only the required number of PRBs, i.e. those needed to meet the traffic requirements, are selected. Step 2 is finished when the required number of PRBs are selected or there are no more PRBs above the threshold. After that the algorithm moves to the next frame. The selected PRBs are mapped to UEs by packet scheduler. The SLB algorithm is equally suitable for DL and UL. The flow chart shown in figure 5.2 summarizes the steps of the SLB algorithm.

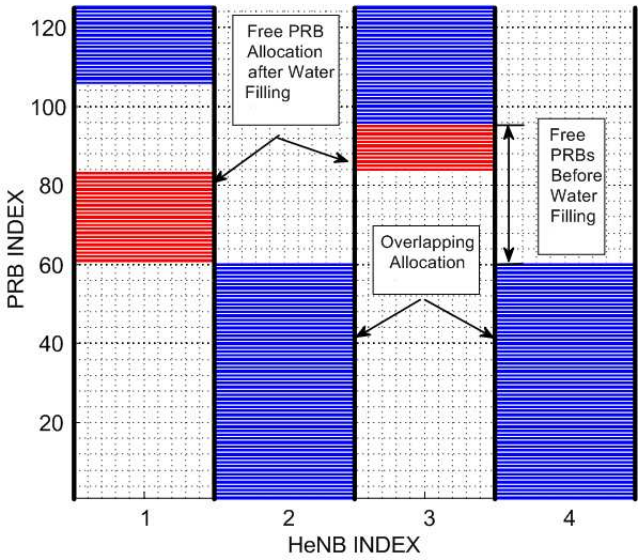

Figure 5.1: Free PRBs allocation using WF approach. The allocation of HeNB 1 and 3 are equalized in terms of number of PRBs. No additional PRBs are allocated to HeNB 2 and 4.

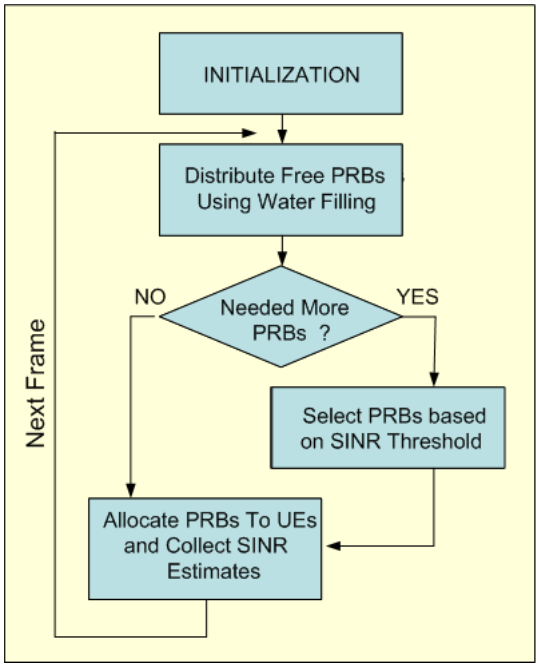

Figure 5.2: Flowchart describing the various phases of the SLB Algorithm

5.3 System Modeling

5.3.1 Assumptions and Main Parameters

The system model used for performance evaluation of the proposed algorithms follows the description given in section 2.6. A single operator indoor corporate deployment with 4 HeNBs, presented in chapter 2 Figure 2.8 is used. In order to evaluate the performance at different SINR thresholds, the $SINR_{th}$ is varied from -10 dB to 20 dB in steps of 5 dB. Power control is not used either in UL or DL. Minimum 5 and maximum 10 UEs are assumed for each HeNB. The number of PRBs per UE is varied from 2 to 14, in order to have different amount of traffic loads at HeNBs. The main parameters and the simulation assumptions are outlined in table 7.4.

Table 5.1: Main Parameters and Simulation Assumptions

Parameter	Settings
Deployment Scenario	Indoor Corporate
UE Mobility	Nomadic
Carrier Frequency	3.5 GHz
System Bandwidth	100 MHz
Access Scheme	DL : OFDMA; UL: SC-FDMA
Duplexing Scheme	TDD
Number of HeNBs	4
Number of UEs per HeNBs	Min. 5; Max. 10
HeNB Transmit Power	24 dBm
HeNB Antenna System	Omnidirectional, 3 dBi gain, SISO
HeNB Receiver Noise Figure	9 dB
UL Transmit power	24 dBm
UL Antenna System	Omnidirectional, 0 dBi gain, SISO
Serving Cell Selection	Geographical Location Based
Target SINR Thresholds	-10,-5,0,5,10,15 and 20 dB
Offered Cell Loads (%)	12,24,36,48,60,72,84 and 100

5.3.2 Key Performance Indicators (KPIs)

Average Carried Cell Load, Mean Cell Throughput and User Outage Throughput are taken as key performance indicators. Mean Cell Throughput and User Outage Throughput are described in section 3.4.

Average Carried Cell Load is defined as the percentage of the actual number of PRBs utilized by HeNB and is denoted by $N_{carried}$. This is compared against the average offered

cell load, which is denoted by $N_{offered}$, and expressed as:

$$N_{offered} = \frac{N_{UEs} \cdot N_{PRB}}{N_{total}} \tag{5.5}$$

where, N_{UEs} denotes average number of UEs per HeNB, N_{PRB} denotes Number of PRBs assigned to each UE, and N_{total} denotes the total number of PRBs available. Therefore $N_{offered}$ is the average fraction of the total number of PRBs offered at each HeNB, expressed in percentage.

5.3.3 Reference Schemes

In order to evaluate the performance of SLB algorithm, the fixed frequency reuse schemes with frequency reuse factors of 1, 2 and 4 are considered as the reference schemes. The fixed frequency reuse schemes are used for regular network deployment with frequency planning and coordination, hence are expected to give desired performance. However, reuse scheme with reuse factor 1 does not require frequency planning and is also called 'universal reuse scheme'.

The reference schemes are briefly described here. In case of reuse 1 scheme, all the spectral resources are available in all the cells. In terms of ρ i.e. the fractional bandwidth utilization, for this scheme $\rho_i^k = 1$ for all i and k.

The expression used for other fixed frequency reuse schemes is given as:

$$S(r) = \left[\frac{K}{R}(r-1)+1, ..., \frac{K}{R}(r-1)+\frac{K}{R}\right] \tag{5.6}$$

where, $S(r)$ represents the set of all the resource blocks within a resource chunk. $r = 1, 2.....R$ where, R represents the total number of resource chunks and also the index of the frequency reuse scheme. For example $R = 2$ and $R = 4$ represent frequency reuse 2 and frequency reuse 4 schemes respectively, considering that only one chunk is allocated to each cell. For a particular resource chunk r of cell i, if $k \in S(r)$, then $\rho_i^k = 1$, otherwise $\rho_i^k = 0$.

The mapping of resource chunks to the cells is an essential part of frequency planning for fixed frequency reuse schemes to ensure suitable allocation pattern of the resource chunks in order to achieve optimal performance by minimizing the co-channel interference.

5.4 Performance Evaluation

The performance of the SLB algorithm is evaluated under different amounts of offered loads and for different SINR thresholds. At first, the performance of the SLB algorithm is

compared with universal frequency reuse scheme in the DL and UL. Then the evaluation is performed in the DL with all the three considered reference schemes.

5.4.1 Comparison in DL and UL with Reuse 1 Scheme

Figure 5.3 compares DL and UL SINR distribution under full load condition. The UL SINR distribution shows higher variance in distribution compared to the DL distribution. The experienced SINR for almost all the users in DL is below $30dB$, whereas in UL about 6% users have SINR higher than $30dB$. At the lower end of the SINR distribution curve, only about 2% users are below $0dB$ in DL, whereas, in UL they are about 10%.The users appear randomly at random locations, therefore high variance in the UL is experienced. In DL SINR variance experienced by an user is comparatively lower due to relatively fixed HeNB positions. The impact of the difference in SINR distribution is visible in the performance in UL and DL. The SLB algorithm is seen to take advantage of the high variance in the UL, which can be observed subsequently in the mean cell throughput and user outage throughput performance results.

Figures 5.4 and 5.5 present carried average cell load ($N_{carried}$) in DL and UL respectively vs different offered cell loads $N_{offered}$, with different SINR thresholds ($SINR_{th}$). The carried cell load increases for a particular amount of offered load by selecting lower SINR threshold. At very low SINR threshold (i.e. -10 and -5 dB) the carried cell load becomes very close to the offered cell load, and it approaches that of frequency reuse 1 scheme. This is because by lowering the SINR threshold, a higher amount of overlapping frequency allocation is allowed, hence higher carried cell load is realized. At high SINR threshold (i.e. at 20 dB) the carried cell load is lowest and does not vary significantly at different amounts of offered loads. At very high SINR threshold, the HeNB tends to allocate the spectrum in a nearly orthogonal manner. DL and UL show the similar trends. However, at higher SINR threshold the carried cell load is slightly higher in UL compared to DL (2 % and 4% higher with 20 dB and 10 dB), and at lower threshold it is slightly lower (2% and 7 % lower at -10 and -5 dB). This difference is experienced because of the difference in the SINR distribution in UL and DL (see Figure 5.3).

The mean cell throughput performance of the SLB algorithm in DL and UL and that of frequency reuse 1 scheme are presented in figures 5.6 and 5.7. At lower offered cell load there is no significant difference in the mean cell throughput performance at different SINR thresholds. As the offered cell load increases the difference in performance becomes visible. Figures 5.8 and 5.9 show the comparative mean cell throughput gain of SLB algorithm with respect to frequency reuse 1 scheme. The maximum gains of 44% in DL and 54% in UL are observed at 24 % offered cell load. This gain is achieved due to SINR aware PRB allocation performed by SLB algorithm, which is not the case with frequency reuse 1 scheme.

In case of SLB, up to 24 % offered cell load, the mean cell throughput performance re-

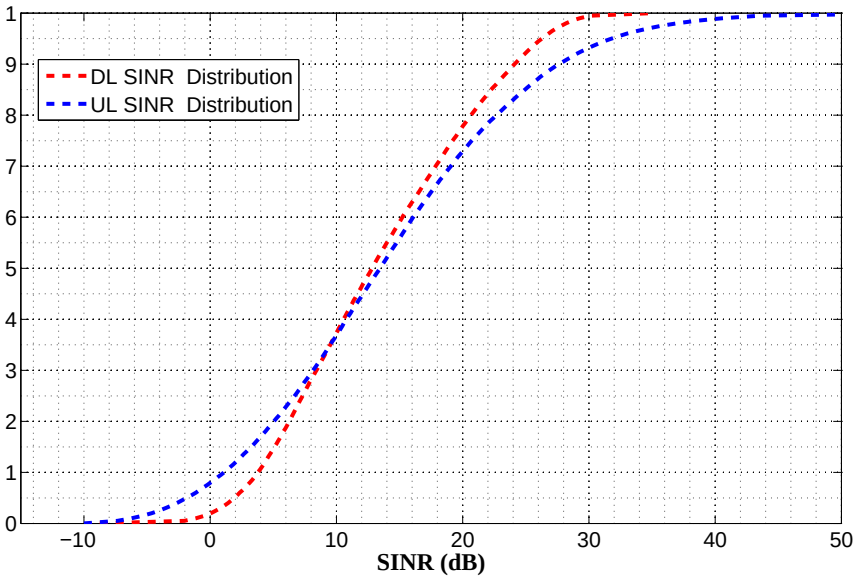

Figure 5.3: Comparison of DL and UL SINR distribution. UL shows higher variance in SINR distribution compared to DL.

mains bandwidth limited. Therefore SINR threshold has negligible impact in this region, and different SINR thresholds show almost no difference in mean cell throughput performance. Above 24 % offered load the performance no longer remains only bandwidth limited, but the interference also starts affecting the performance, since non-orthogonal allocation starts increasing after this point. Therefore, in this region the difference in the performance at different SINR thresholds becomes visible.

Slightly higher gain is realized in UL compared to DL. At full load SLB provides no gain over frequency reuse 1 in DL. However, in UL for $15dB$ and lower SINR thresholds, the gain is realized. At $20dB$ SINR threshold the DL results in 16 % lower mean cell throughput performance compared to reuse 1, whereas, in UL it is only 2 % lower. $5dB$ $SINR_{th}$ gives nearly the best overall performance in DL, while the same goes for $10dB$ SINR threshold in UL. The observed difference in DL and UL performance in this bandwidth-cum-interference limited region is due to difference in their SINR distribution. Higher gain in UL is achieved due to higher variance in SINR distribution.

Figures 5.10 and 5.11 show the user outage throughput in DL and UL respectively, whereas figures 5.12 and 5.13 show the gains compared to frequency reuse 1 scheme. The maximum gains of 190 % in DL and in the order of 310 % to 340 % in UL are realized. The SLB significantly improves the user outage performance at the cell edge compared to the frequency reuse 1. At the cell edge this gain is realized by ensuring cell edge users to be scheduled above the SINR threshold. At higher SINR threshold higher user outage gain is obtained. With respect to DL the gain is much higher in UL.

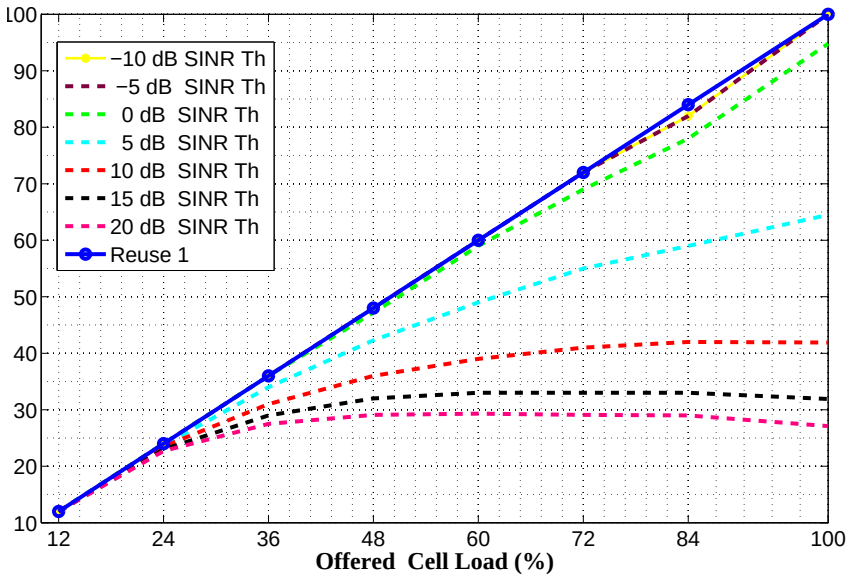

Figure 5.4: Average Carried Cell Load under different Offered Cell Loads with different SINR Thresholds in DL compared with Reuse 1

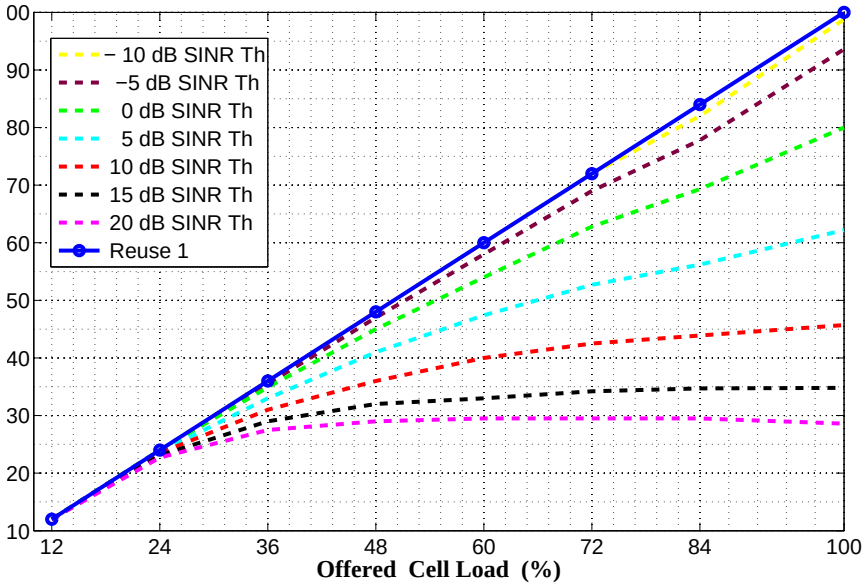

Figure 5.5: Average Carried Cell Load under different Offered Cell Loads and different SINR Thresholds in UL compared with Reuse 1.

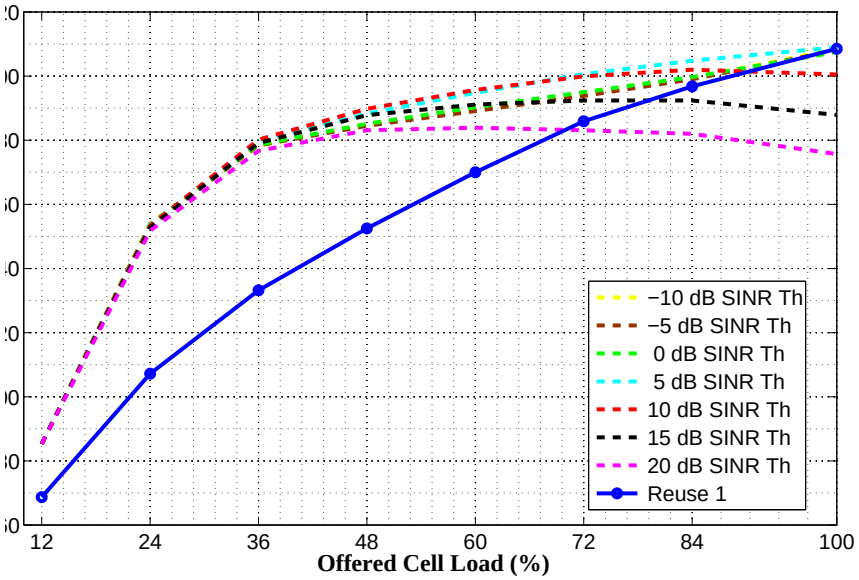

Figure 5.6: Mean Cell Throughput performance of SLB algorithm in DL along with reuse1

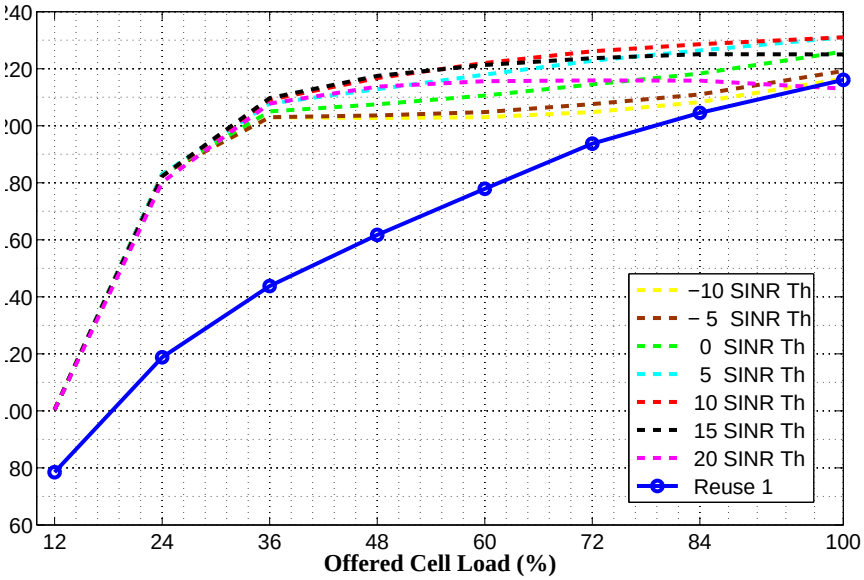

Figure 5.7: Mean Cell Throughput performance of SLB algorithm in UL along with reuse1

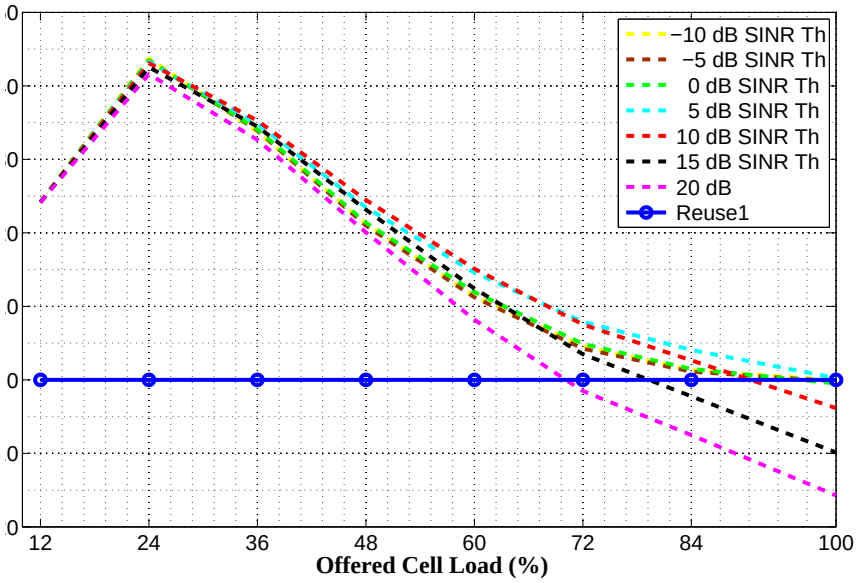

Figure 5.8: Mean Cell Throughput performance gain of SLB algorithm in DL compared with reuse 1

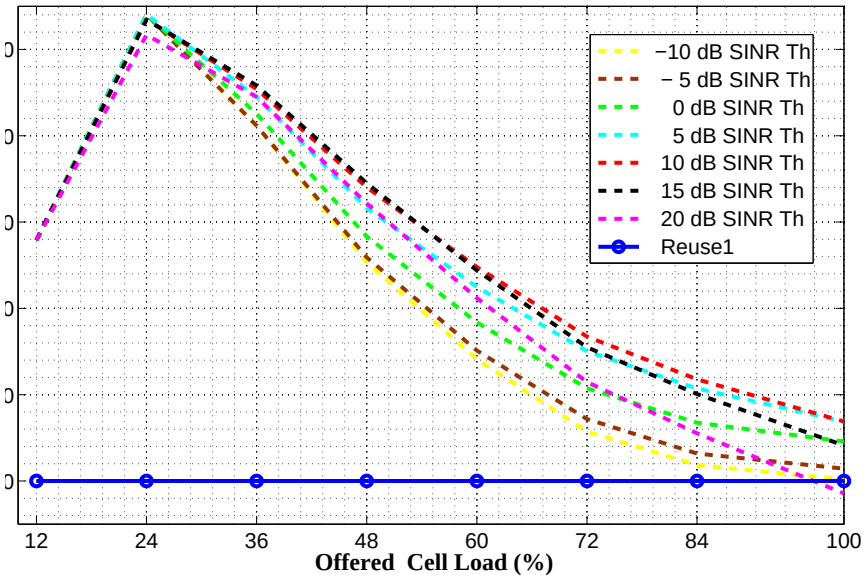

Figure 5.9: Mean Cell Throughput performance gain of SLB algorithm in UL compared with reuse 1. UL shows higher gain compared to DL.

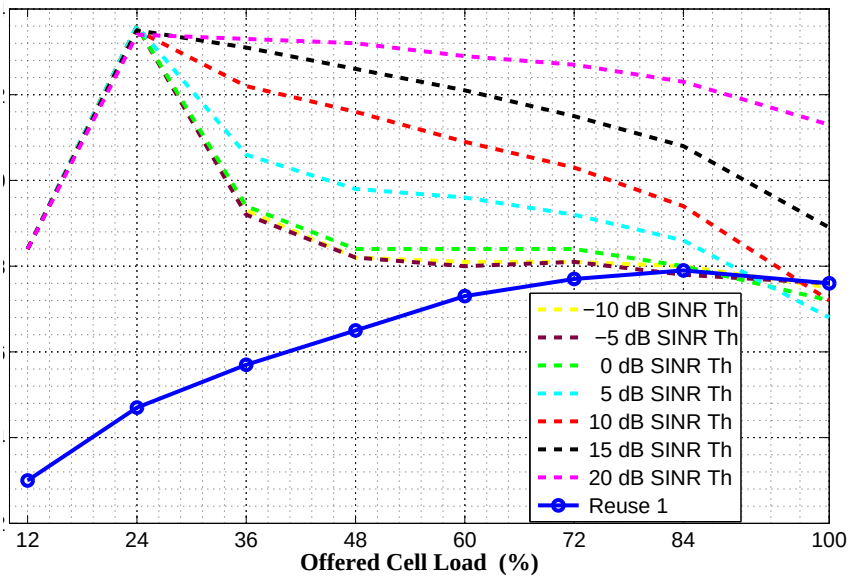

Figure 5.10: User Outage Throughput performance of SLB algorithm in DL

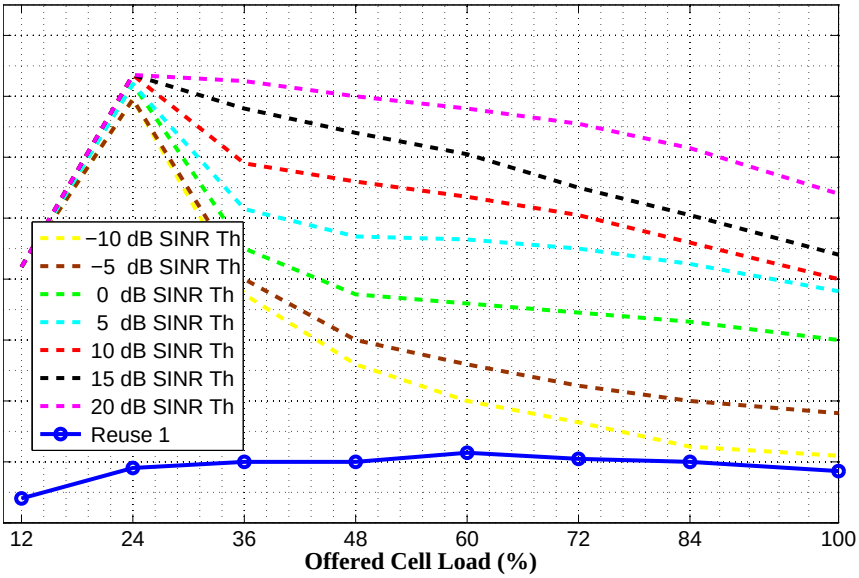

Figure 5.11: User Outage Throughput performance of SLB algorithm in UL

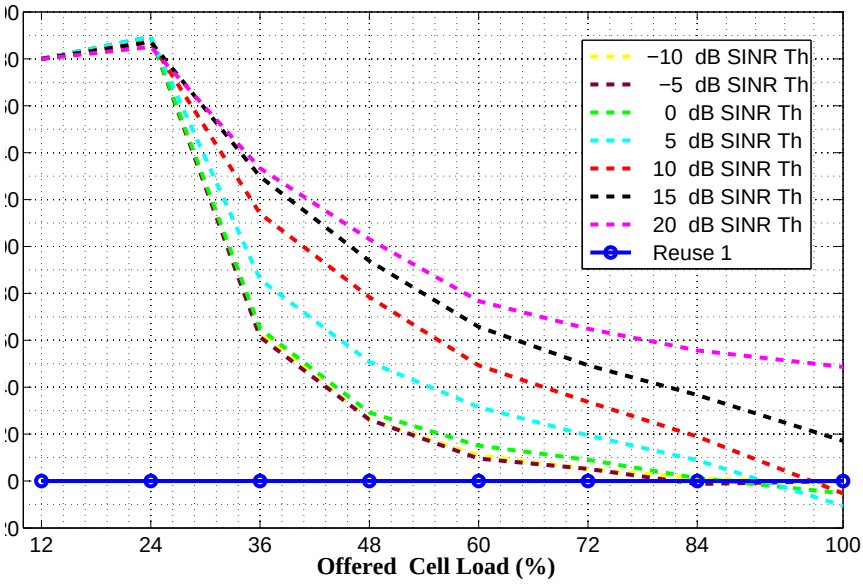

Figure 5.12: User Outage Throughput performance gain of SLB algorithm in DL compared with reuse 1

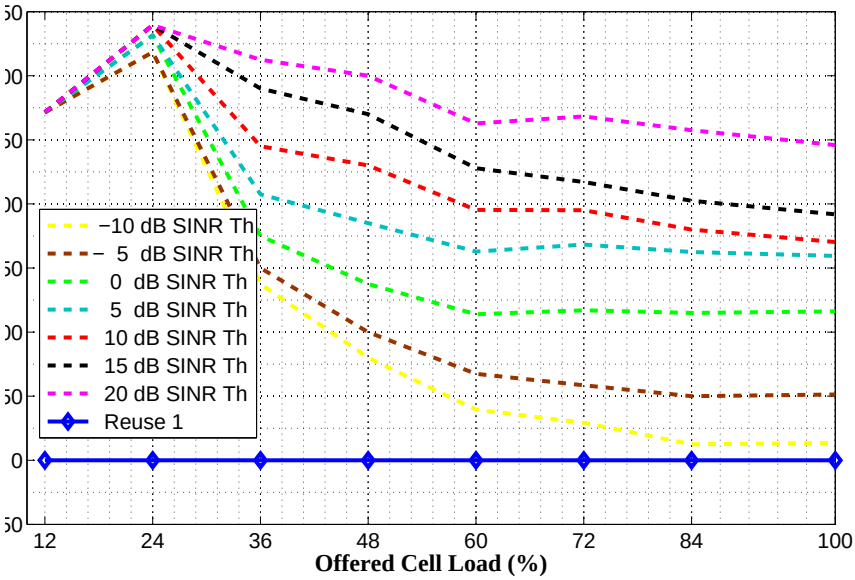

Figure 5.13: User Outage Throughput performance gain of SLB algorithm in UL compared with reuse1

5.4.2 Comparison with Reuse 1, 2 and 4 schemes in DL

Figure 5.14 shows carried cell loads in DL under different offered cell loads with different SINR thresholds compared with the reference schemes frequency reuse 1, 2 and 4 schemes. At very low SINR threshold the carried cell load is close to reuse 1, whereas at very high SINR threshold it is close to reuse 4. The carried cell load for reuse 2 lies between very low and very high SINR threshold cases. This shows that by proper selection of the SINR threshold the SLB algorithm can realize any given frequency reuse scheme in terms of carried cell loads. This inherent feature of the SLB algorithm shows its potential to support FSU.

Figure 5.15 compares mean cell throughput performance of SLB with the reference schemes in DL. For up to 24 % of the offered cell load there is no significant difference in the performance of SLB algorithm with the reference schemes of frequency reuse 2 and frequency reuse 4. At this point SLB is as good as the other two above mentioned schemes to ensure orthogonal allocation of PRBs. Thereafter until full load SLB provides higher mean cell throughput compared to reuse 4, since it makes more spectrum bandwidth available from the common pool. Up to 72 % of offered cell load SLB provides higher mean cell throughput over frequency reuse 1. But at offered cell load higher than 72 % , SLB achieves no significant gain over reuse 1. Further, at full load reuse 1 seems to be better than SLB. Reuse 1 allows transmission over full bandwidth, but this is not true in case of SLB algorithm where the amount of bandwidth is limited due to SINR threshold.

Reuse 2 provides the best overall performance. Reuse 2 allocates the spectrum in an orthogonal manner, like reuse 4, but it uses two times the bandwidth of the reuse 4. With respect to reuse 1, although reuse 2 uses only half of the transmission bandwidth, due to orthogonal allocation in the adjacent HeNBs, it minimizes the inter-cell interference and thereby achieves higher throughput and outage performance (figure 5.17). In case of SLB algorithm, with higher SINR threshold the carried cell load becomes lower, and therefore the transmission bandwidth is reduced considerably compared to reuse 2, whereas at low SINR threshold the majority of the PRBs are overlapped, causing inter-cell interference, resulting in reduced throughput and outage performance.

The comparison for user outage performance of SLB algorithm with the reference schemes is presented in figure 5.16. At 24 % offered load SLB has the same performance as reuse 4, which is higher than that of reuse 2 and reuse 1 schemes. As the offered cell load increases, the outage performance of SLB algorithm drops rapidly with lower SINR thresholds. The lower SINR thresholds result in higher number of PRBs to overlap, and therefore the user outage throughput is reduced. However, at higher SINR thresholds the user outage performance of SLB algorithm remains close to the reuse 2 and 4 schemes, which is significantly higher than that of reuse 1 scheme.

Based upon the investigations and results presented, it is understood that the proposed

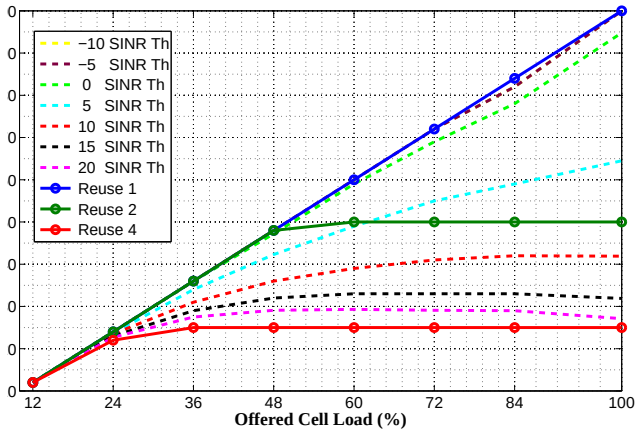

Figure 5.14: The comparison of DL carried cell load. By selection of appropriate SINR threshold the SLB algorithm achieves the frequency reuse patterns of all the reference schemes.

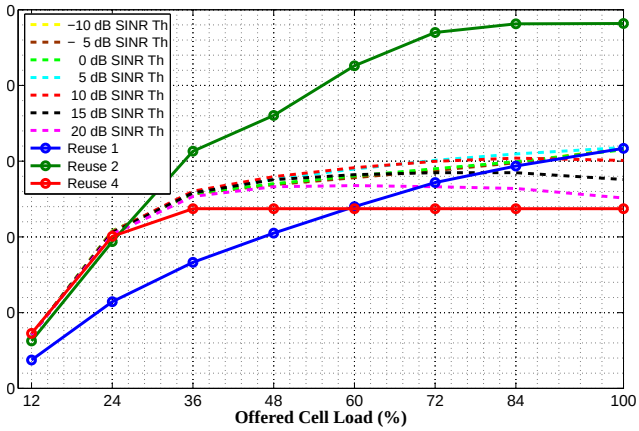

Figure 5.15: Comparison of DL mean cell throughput performance of SLB algorithm with the reference schemes.

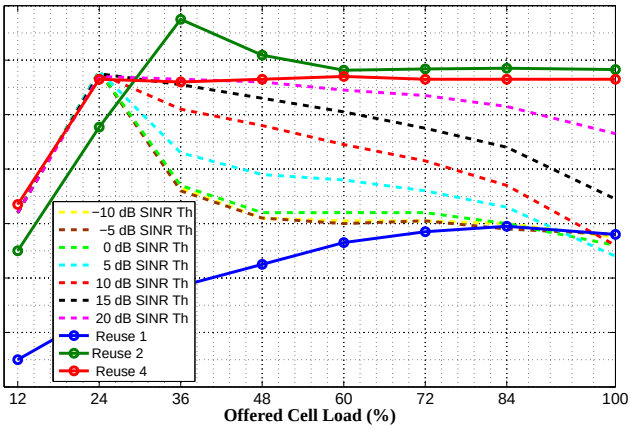

Figure 5.16: Comparison of DL user outage throughput performance of SLB algorithm with the reference schemes.

SLB algorithm provides a more efficient solution compared to frequency reuse 1 and 4 schemes over a wide range of offered cell loads. However, the SLB algorithm does not prove to be as efficient as the frequency reuse 2 scheme both in terms of mean cell throughput and user outage throughput. Then it could be argued, why an SLB algorithm ? In spite of being more efficient is there a reason why reuse 2 cannot replace the SLB algorithm?

- One of the main objectives of IMT-A in LA is deployment flexibility. It involves random, distributed and uncoordinated deployment. The self-organizing feature of HeNBs has a critical role in such deployment scenario. It is envisioned that the HeNBs shall probe the environment around them and adjust the spectrum allocation accordingly.
- The FSU and self-configuration of HeNBs are important requirements to achieve scalable and flexible deployment and also to ensure coexistence of randomly deployed HeNBs. These requirements cannot be achieved by the options that involve frequency planning and coordination. Therefore it is logical not to consider options that involve frequency planning [71]. The reuse 2 is a fixed frequency reuse scheme and involves frequency planning. Though it provides good performance in planned and regular network deployment, it cannot be considered as a viable option, for the above mentioned reasons.
- The usage of spectrum in flexible manner from a common pool is a key concept to meet dynamically varying traffic demand and also to provide a peak data rate of 1 Gbit/s in DL as envisioned for the IMT-A system. As discussed above, reuse 2 cannot be used in such a scenario.
- In this regard, the SLB algorithm presented in this chapter provides the initial results and the potential direction towards flexible spectrum utilization, random deployment, self-configuration and scalable solution. It is finally emphasized that self-organization will play a critical role in the design of adaptive and reconfigurable operation in future wireless networks [71].

5.4.3 Limitations of SLB Algorithm

The presented SLB algorithm assumed the following in order to achieve simplicity.

- Homogeneous traffic load for all HeNBs with full buffer was assumed. The dynamically varying cell load is not considered, which is expected to result in higher variance in SINR distribution. In such conditions the SLB algorithm is expected to perform more efficiently. These investigations are left for future work.
- In the SLB algorithm, the selection of PRBs is limited within the scheduled PRBs only, which limits the range and the diversity gain with respect to the selection of

PRBs from the full range of PRBs. This assumption was made in order to avoid the complexity in SINR estimation over the full range of PRBs, and also to save the battery life of UEs. Estimation of pilots over the whole spectrum involves power consumption at the UE. It Also increases the signaling overhead. Therefore we consider that the UEs sense the pilots over the scheduled PRBs only.

5.5 Resource Chunk Selection (RCS) Algorithm

5.5.1 Motivation and Aim for the Algorithm

During the performance evaluation of the SLB algorithm it was found that the fixed frequency reuse 2 scheme achieves the highest mean cell throughput and user outage throughput performance compared to all the other schemes in consideration. Fixed frequency reuse 2 scheme requires that the assignment of spectrum chunks to the HeNBs must be pre-planned so that the strongest interference can be avoided for optimized performance. In a regular network deployment this configuration can easily be achieved, however, in the assumed LA scenarios no such planning is feasible, where the deployment is assumed to be random and uncoordinated. Therefore a mechanism is needed to result in frequency reuse 2-like configuration in a self-organized manner in the absence of any coordination and network planning.

Keeping the above mentioned points in view, a comparative interference threshold based Resource Chunk Selection (RCS) algorithm is proposed. The chunk refers to the part of the system bandwidth allocated to one HeNB. In case of frequency reuse 2 the whole system bandwidth is divided in two equal size chunks; one chunk is allocated to each HeNB keeping in view to avoid the allocation of the same chunk to adjacent HeNBs. Since we aim to achieve a comparable performance with frequency reuse 2 configuration, therefore, as a starting point we consider that the RCS algorithm also divides the total system bandwidth in two equal size chunks. However, the RCS algorithm is not limited to the frequency reuse 2 like configuration. This algorithm can easily be adopted to approach the configuration of any other frequency reuse scheme. The proposed RCS algorithm starts with random selection of a chunk at each HeNB and aims to achieve frequency reuse 2 like configuration in self organized manner. The main motivation for this algorithm is to provide a self-configurable and scalable solution for random and uncoordinated LA deployment scenario with improved performance over SLB algorithm and close to frequency reuse 2 scheme.

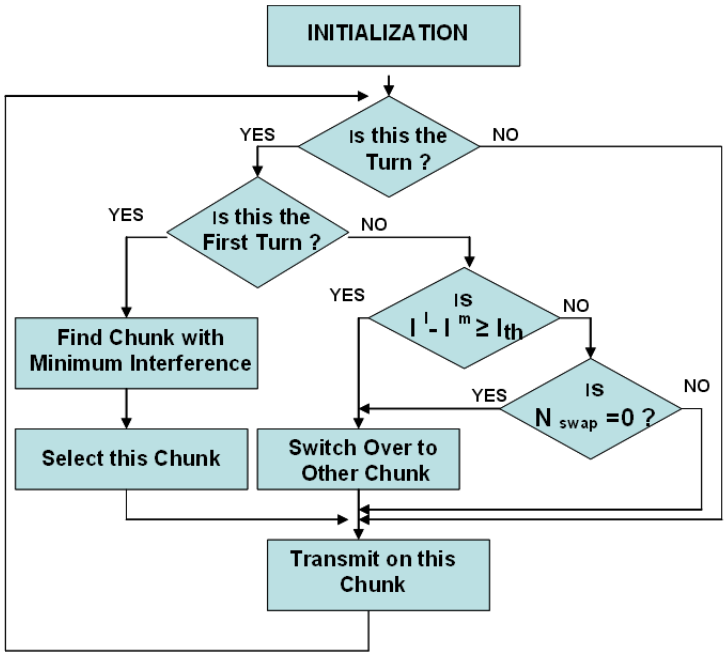

Figure 5.17: Flowchart of the Resource Chunk Selection (RCS) algorithm

5.5.2 Description of RCS Algorithm

This algorithm is based on the information of uplink Received Interference Power (RIP) over the resource chunks. The RIP is defined as uplink received interference power, including thermal noise, within one PRB bandwidth [18]. The RIP is averaged over the entire resource chunk, and is used to represent the interference power over the resource chunk. The algorithm selects the chunk with the minimum interference power and retains this selection until some specified condition appears. The full description of the different phases of the algorithm is presented below, and the flow chart of the algorithm is given in figure 5.17.

Step 1: Initialization Phase

As the HeNB is powered on, it randomly selects a chunk to connect to its UEs and to carry out the transmission. The HeNB is also initialized with the sequence number N_{seq} and swap number N_{swap} in the initialization phase.

The sequence number (N_{seq}) determines the position of a HeNB in the queue. It is assumed that in every frame all the HeNBs do not select their resource chunk simultaneously, instead the selection of resource chunk by a HeNB is performed only when a HeNB gets its turn in sequential order. Therefore, HeNBs have to wait for their turn to update the chunk selection. The sequence number indicates their turn. When waiting for its turn a HeNB retains the previously selected chunk for transmission. We assume a need for very

limited signaling via over-the-air-communication to set up the sequence number for each HeNB in the queue, as was required for SLB as well.

The swap number (N_{swap}) determines how many number of times a HeNB can retain the same resource chunk. The purpose of the swap number is to force a HeNB to switch over to another resource chunk to avoid the occurrence of dead lock situation. The dead lock situation occurs when all the HeNBs become stable over the condition of non optimal allocation. After the initialization phase the next step is to select the resource chunk with minimum interference, as explained below.

Step 2: Selection of Chunk with Minimum Interference

In this step the HeNB selects the resource chunk which has the minimum interference power as follows:

$for\ i = 1, 2, ...N_{cells}$
The i^{th} HeNB will select l^{th} chunk provided $l = argmin I_i^l$
where,

$$I_i^l = \sum_{j=1, j\neq i}^{N_{cells}} \frac{P}{\sum_{k=1}^{K} \rho_j^k} g_{ij}^l \tag{5.7}$$

After selection of the chunk in this step, the sequence number (N_{seq}) is reset to its original value, indicating that the HeNB has availed its turn. The sequence number is reduced by a unity at each update interval. N_{seq} =0 indicates the turn for HeNB to update its chunk selection.

Step 4: Switching Over to other Chunk

The selected resource chunk is retained until the condition appears for switch-over. There are two conditions for switch-over. The first one is based on the difference in the received interference power over the chunks, and the second is determined by the swap number, described below.

An interference threshold I_{th} is defined to compare the level of interference over the chunks. The chunk with lower interference is selected fulfilling the following conditions.

$$|I_i^l - I_i^m| > I_{th} \ \ for\ l, m = 1, 2, ...N_{chunks}, m \neq l$$

where I_i^l indicates the level of interference for chunk l of i^{th} HeNB, which is the chunk presently engaged, and I_i^m indicates the interference level experienced by the same

HeNB over the chunk m. If the difference between these two is higher than the interference threshold I_{th}, then the switch-over takes place, otherwise the same chunk is retained. The switching over to a chunk involves signaling and overhead for reconfiguration, which may cause disruption momentarily, and therefore the selection of the interference threshold needs a careful decision. The selection of interference threshold is based on a trade-off between how much the interference can be tolerated against the increased disruption and the signaling requirement in case of switching over to another chunk. By this it is ensured that the switch over is not undertaken unless there is a significant gain by doing so.

If the difference in the interference level of the two chunks is smaller than the interference threshold, the same chunk is retained, but for a specified number of times. The number of times is specified by the swap number N_{swap}. Every time the chunk is selected the N_{swap} is initialized with the original value, and in every update interval, when the same chunk is retained, the N_{swap} is reduced by a unity. N_{swap} =0 sets the condition to switch over to another chunk.

Changing to another chunk gives possibility to overcome the potential deadlock situation, by allowing other HeNBs to select a more suitable chunk. This may, however, result in slightly lower performance for the next update interval for the HeNB forced to change, but in the subsequent intervals it is expected to improve the overall condition for resource chunk selection. After the selection of the chunk the packet scheduler maps the PRBs of the chunk to UEs to carry out traffic.

The RCS algorithm is based on the UL RIP measurement for chunk selection. The selected chunk based on this measurement is used for the UL as well as DL traffic in our simulation. The algorithm works in an uncoordinated manner, with requirement of very little signaling via over-the-air-communication among the HeNBs. However, the performance of this algorithm is upper bounded by the performance of fixed frequency reuse with reuse factor equal to the number of chunks.

5.5.3 Performance Evaluation

The simulation parameters and the assumptions used to evaluate the performance of the RCS algorithm are the same as the ones used for the SLB algorithm, which is outlined in section 5.3. The mean cell throughput and the user outage throughput are taken as the key performance indicators. Apart from the previously used reference schemes, i.e. frequency reuse 1 , 2 and 4, the SLB algorithm with 20 dB and 5 dB SINR thresholds is also taken as the reference scheme. The 20 dB SINR threshold gives the best user outage throughput performance both in DL and UL, compared to all other SINR thresholds investigated. The 5 dB SINR threshold gives the highest mean cell throughput performance in DL (although 10 dB gives the best performance in UL, which is very close to the performance at

5 dB. In order to select one reference, 5 dB has been preferred). Therefore, at the selected thresholds, the best performance of SLB is considered as reference, both in user outage and average cell throughput.

Figure 5.18 compares the mean cell throughput performance of the RCS algorithm with all the considered reference schemes. The frequency reuse 2 gives the highest mean cell throughput and frequency reuse 4 the lowest. The mean cell throughput obtained by SLB with 20 dB SINR threshold is close to reuse 4, and with 5 dB SINR threshold is close to frequency reuse 1 scheme. (These observations are similar to the one previously obtained and documented in section 5.4.) The RCS algorithm brings significant improvement in the mean cell throughput performance compared to the SLB algorithm, i.e. 24% higher, and also close to reuse 2, i.e. 6% lower. Again, it is important to note that the performance achieved through RCS is in a self-organized manner, whereas reuse 2 requires frequency planning.

The comparison of mean cell throughput performance in UL is given in Figure 5.19. Similar trends as found in DL are observed in the UL as well. However, the gain of RCS compared to SLB with 5 dB SINR in UL is relatively lower than that of DL. The gain in UL is 20 % in comparison to the 24% gain in DL. The relatively lower gain in UL compared to DL can be explained with the previous results of the SLB algorithm presented in figures 5.8 and 5.9, where it is found that the performance of the SLB algorithm is higher in UL compared to DL, due to high variance in the SINR distribution in UL. Since SLB realizes a higher gain in UL compared to DL, the exhibited relative gain of RCS with respect to SLB in UL is lower compared to DL. The mean cell throughput of RCS is again close to reuse 2, i.e. only 7 % lower. Therefore, the RCS algorithm provides an improvement over SLB algorithm and becomes close to the mean cell throughput performance of reuse 2 scheme in DL as well as UL.

The user outage performance in DL and UL are shown in figures 5.20 and 5.21 respectively. The user outage throughput of RCS algorithm is below the frequency reuse 2 and 4 schemes, since these two frequency reuse schemes ensure fully orthogonal allocation in adjacent cells. However, frequency reuse 2 gives a higher user outage throughput compared to reuse 4, since apart from the orthogonal allocation in the adjacent cells it has twice the bandwidth available. It can be seen in Figure 5.20 for DL that the user outage throughput of the RCS algorithm is comparable to the best performance achievable by the SLB algorithm, which is at $20dB$ SINR threshold. The similar trend is observed in UL. An important observation that can be made here is that the RCS algorithm achieves the comparable user outage throughput with the maximum achievable by SLB algorithm, but at the same time it brings significant improvement in the mean cell throughput performance over SLB.

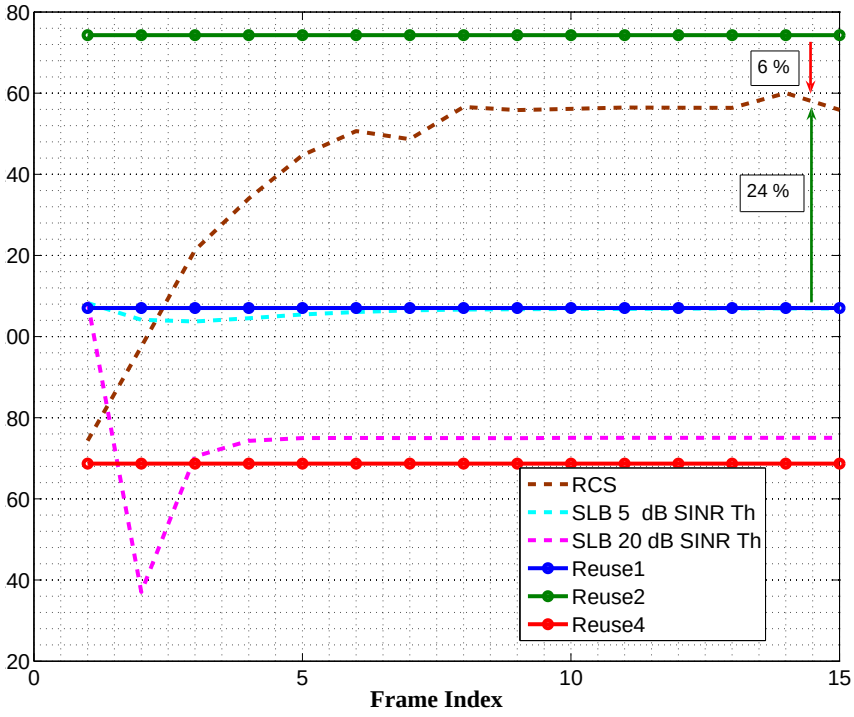

Figure 5.18: Comparison of mean cell throughput performance of the RCS algorithm with all the considered reference schemes in DL.

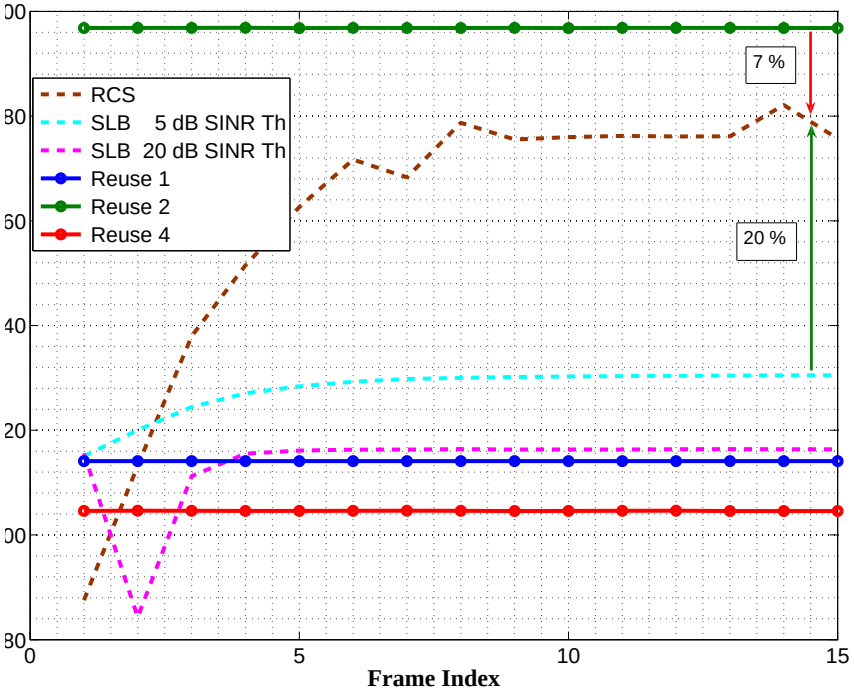

Figure 5.19: Comparison of mean cell throughput performance of the RCS algorithm with all the considered reference schemes in UL.

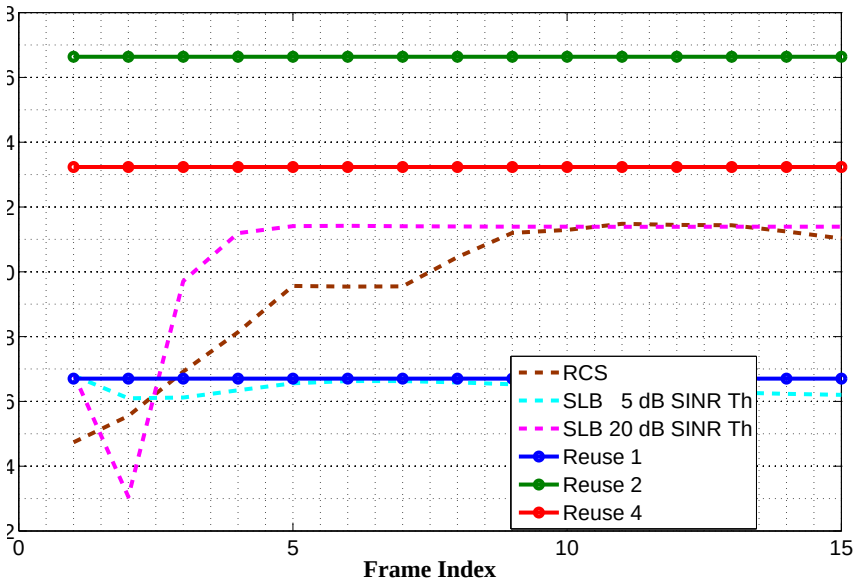

Figure 5.20: The user outage throughput of RCS algorithm compared with the reference schemes in DL

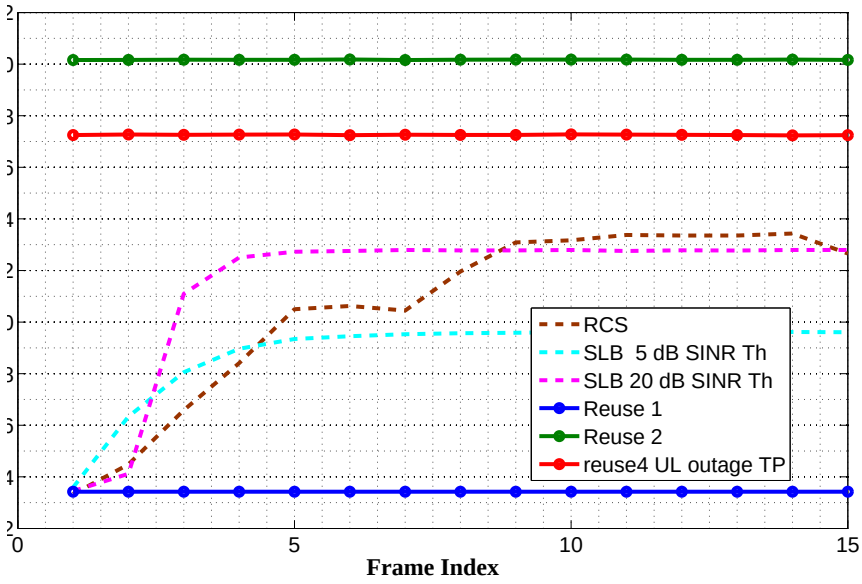

Figure 5.21: The user outage throughput of RCS algorithm compared with the reference schemes in UL

5.6 Conclusions

Currently HeNB is emerging as a potential solution for high quality and high data rate services in local area indoor environment. A large scale, random and uncoordinated deployment of HeNBs is envisioned in near future. This will require a mechanism to support self-configurable and scalable deployment. The Flexible Spectrum usage (FSU) is considered as key enabler for such deployment scenario.

This chapter proposes Spectrum Load Balancing (SLB) and Resource Chunk Selection (RCS) algorithms for FSU. The SLB is SINR threshold-based, whereas RCS is a comparative interference threshold-based algorithm. Both algorithms work on the principle of self assessment of surrounding radio environment and ensure coexistence of HeNBs by partially or completely preventing mutual interference on the shared spectrum. The algorithms support self configurable deployment of HeNBs.

The proposed algorithms are compared with fixed frequency reuse 1, 2 and 4 schemes. The SLB algorithm is found to provide higher average cell throughput and user outage throughput performance compared to reuse 1 and 4 schemes over a wide range of offered cell loads. However, the SLB is outperformed by reuse2 scheme. One important characteristic of SLB is that, it can resemble any given fixed frequency reuse pattern by proper selection of SINR threshold, therefore it supports FSU.

The RCS algorithm has been proposed to further improve the performance over SLB. The mean cell throughput and user outage throughput achieved by RCS is significantly higher compared to SLB. The throughput provided by RCS is close to reuse 2 scheme. However, in terms of outage, the reuse 2 still gives higher performance in the given scenario. The significance of the RCS algorithm is, it achieves the performance in self-organized manner in the uncoordinated and random deployment scenario. Whereas reuse 2 performs in regular deployment with frequency planning, which is potentially not feasible in the envisioned scenario.

The proposed algorithms support flexible spectrum usage, self configuration, flexible and scalable deployment. Therefore, the algorithms are suitable for implementation in the local area solution envisioned for IMT-A systems.

Chapter 6

Autonomous Component Carrier Selection for Local Area Deployment

6.1 Introduction

The LTE Release'8 standardization is coming to its completion and the focus is now gradually shifting towards its further evolution, referred to as LTE-A. One of the goals of this evolution is to reach and even surpass the requirements of IMT-A in terms of data rates and low cost deployment. This includes the possibility for peak data rates up to 1 Gbps in Downlink (DL) and 500 Mbps in Uplink (UL) [72],[7] and [6]. Such high data rate targets can only be fulfilled in a reasonable way with a further increase of the transmission bandwidth. A transmission bandwidth up to 100 MHz has been considered in the context of LTE-A [6]. Such a bandwidth extension should be done while preserving the backward spectrum compatibility, since LTE-A will be an evolution of LTE. A direct consequence of this requirement is that an LTE-A network should appear as an LTE network for a legacy terminal. Such compatibility is of critical importance for a smooth transition to LTE-A capabilities.

6.1.1 Carrier Aggregation

The bandwidth extension for LTE-A can be achieved by carrier aggregation [73] and [74]. The carrier aggregation can also fulfill the requirement of backward compatibility, where multiple LTE *component carriers* are aggregated to provide the desired LTE-A system bandwidth [72], [75] and [76]. Further, it is expressed that operation of LTE and LTE-A should be possible over the same radio spectrum [6]. In this context, a LTE terminal can receive one of these *component carriers* while an an LTE-A terminal can simultaneously access multiple *component carriers*.

In principle, the aggregation of *component carriers* could be either contiguous or non

contiguous over the spectrum. Typically, contiguous aggregation is assumed, but this is not essential. Access to large amount of contiguous spectrum, in the order of 100 MHz, may not always be possible. Therefore, aggregation over the non-contiguous spectrum is also supported considering reasonable UE complexity [6], even though it is more challenging from an implementation perspective [72]. One important merit of carrier aggregation is that it does not require extensive changes to the existing LTE physical layer structure and therefore simplifies the implementation [75].

An aggregation of 5 *component carriers* with 20 MHz bandwidth is generally assumed in order to obtain 100 MHz system bandwidth for LTE-A, illustrated in figure 6.1. However, this is not the prerequisite. Other configurations such as 4 component carriers of 10 MHz to obtain 40 MHz system bandwidth or any other configuration could potentially be used [77].

6.1.2 Concept of Primary and Secondary Component Carriers

Further, we assume that each cell selects one of the *component carriers* as its Primary Component Carrier (PCC). The PCC is assumed to be used for initial connection of terminals in the cell. Later on, a cell may dynamically select additional *component carrier(s)* depending on the offered traffic in the cell and the mutual interference coupling with the surrounding cells. The additional *component carrier* is referred to as Secondary Component Carrier (SCC). The SCC will be selected when required. This concept is motivated by the fact that transmission/reception on all the *component carriers* may not always provide an efficient solution. It is also assumed that all the *component carriers* not selected for primary or secondary are fully muted within the cell [77].

It is assumed that the PCC should be accessible by all the terminals within the coverage area of the cell, whether it is LTE or LTE-Advanced (LTE-A) terminal. Therefore, PCC should have sufficiently good channel quality. In our concept it is mandatory that each cell has one PCC. The synchronization signals and broadcast channels should be present in PCC in order to be accessible by LTE terminals. An analogous concept in the form of anchor and non anchor carriers is also proposed in [76].

6.1.3 HeNB Deployment in Local Area

Currently, Home eNode-Bs (HeNBs) are emerging as a potential solution for high data rate access in the indoor local area deployment scenario. The HeNBs are expected to be deployed at large scale in the future, hence it will be necessary for LTE-A to support such deployment cases. The deployment of HeNBs will be potentially uncoordinated, where they are expected to self-configure in a distributed manner. The autonomous selection of component carriers will be beneficial for such deployment scenarios [73] and [74].

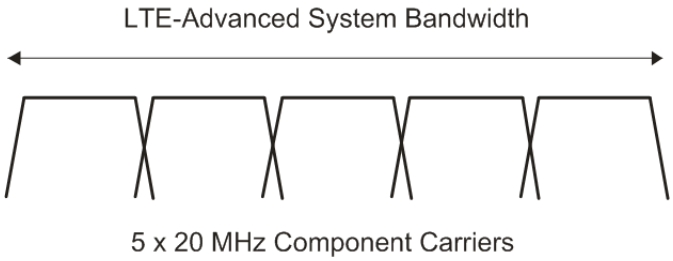

Figure 6.1: Basic illustration of component carriers to form LTE-A system bandwidth using carrier aggregation [77].

6.1.4 Aim of this Chapter

With above considerations, our aim in this chapter is to develop a mechanism to enable HeNBs for autonomous selection of component carriers under uncoordinated and distributed deployment in local area for the LTE-A. The whole mechanism for component carrier selection involves the selection of primary as well as secondary component carriers. However, our focus will be limited within the domain of primary component carrier, where its selection, quality monitoring and recovery actions will be outlined. Our focus will primarily be on single operator case. We assume the absence of X2 interface, and therefore the inter HeNBs exchange of information is considered to take place via over-the-air-communication. We focus on synchronous Time Division Duplex (TDD) case with all HeNBs having the same uplink/downlink ratio.

6.2 The Proposed Concept

The proposed concept relates to the possible mandatory mechanism that HeNB should follow for selection of a primary component carrier. It relies on the basic assumption of always having one, and only one, primary component carrier for each HeNB. We assume that there is no prior negotiation between HeNBs before selection of a primary component carrier. However, some information exchange is needed between neighboring HeNBs. The concept uses a distributed and a fully scalable approach, i.e. selection of primary carrier is done locally by each cell. Hence, in the proposed scheme there is no need for a central network coordinating component.

6.2.1 Description of Overall Primary States

Figure 6.2 presents the three main associated states related to the primary component carrier selection. The states are initial selection, monitoring and recovery action [78].

- State #1 is the initialization state, which starts immediately after the HeNB is powered on. In this state there is no traffic in the cell, so the HeNB does not have reports

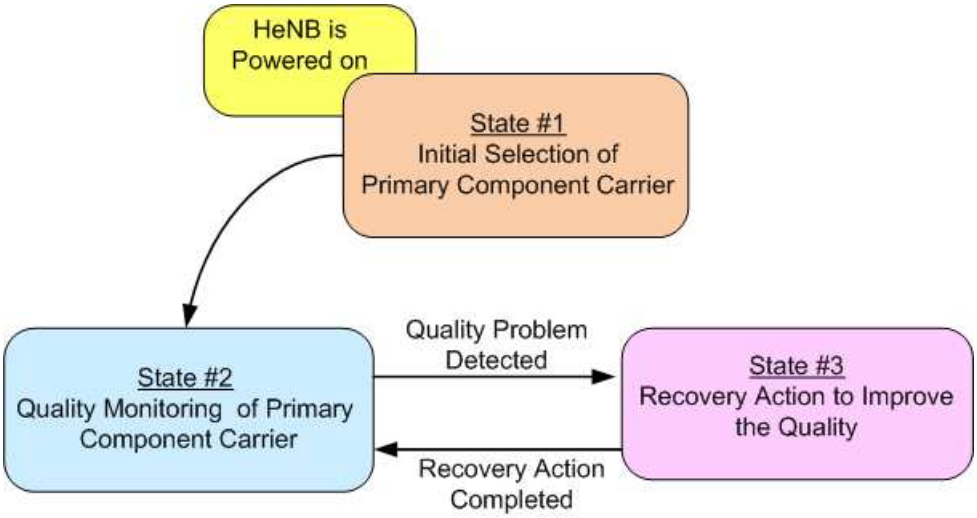

Figure 6.2: Overview of the three main states associated with the primary component carrier selection [78].

based on UE measurements. The information available in state #1 is local HeNB measurements and also the information via over the air communication [70] from neighboring HeNB. Based on this information the HeNB selects one PCC.

- Once a PCC has been selected, a transition is made to State #2, where the HeNB monitors the quality of the selected PCC . The quality of primary carrier is required to be fairly good, as it should be accessible by all the terminals whether they are LTE or LTE-A, within the coverage area of the cell. The quality monitoring is based on both local HeNB measurements, and the reports on UEs measurements. The UEs measurements mainly include reference symbol received power (RSRP) and reference symbol received quality (RSRQ). In this state each HeNB also starts to build local knowledge of background interference matrix (BIM) based on the UEs measurements, such as RSRP, which is later used for the selection of secondary component carrier.

- During the monitoring state, if the quality of the primary carrier is detected to be low, a transition is made to state #3 (recovery state), where appropriate actions are taken to recover the quality of the primary carrier. All the state transitions are assumed to be event triggered.

6.2.2 Proposed Measurements Required at Different Primary States

In this section we discuss measurements required for different primary states. They are grouped in UE and eNode-B measurements, and where required a relevance is given also with the well known WCDMA measurements. We propose to use the LTE Release 8 measurements, since it is desirable also to reuse Release'8 solutions for LTE-A as much as

possible [24].

UE Measurements

Reference signal received power (RSRP), is determined for a considered cell as the linear average over the power contributions (in[W])of the resource elements that carry cell-specific reference signals within the considered measurement frequency bandwidth [79]. This provides measurement on DL signal strength and is reported by UEs to the serving eNode-B.

Received Signal Strength Indicator (RSSI), is comprised of the total received wide-band power observed by the UE from all sources, including co-channel serving and non serving cells, adjacent channel interference and thermal noise etc. The measurement is performed over the bandwidth defined by the receiver pulse shaping filter [79].

Reference Signal Received Quality (RSRQ) is defined as the ratio $N * \frac{RSRP}{RSSI}$, where N is the number of resource blocks of the RSSI measurement bandwidth. The measurements in the numerator and denominator shall be made over the same set of resource blocks [79].

HeNB Measurements

Downlink Reference Signal Transmit (DL RS TX) power is determined for a considered cell as the linear average over the power contributions (in [W])of the resource elements that carry cell-specific reference signals which are transmitted by the eNode-B within its operating system bandwidth. This represents the measurement of eNode-B DL transmit power over reference symbols. Our assumption is that this measurement can be exchanged between HeNBs via over-the-air-communication, so one HeNB knows the DL RS Tx power of the neighboring HeNBs.

The Uplink Received Interference Power (RIP)is defined as uplink received interference power, including thermal noise, within one PRB bandwidth. The RIP measurement is in a certain manner similar to WCDMA RTWP (Received Total Wideband Power) measurement. Where it can be understood as RTWP = RIP + wanted signal.

Path Loss Estimates towards Neighboring HeNBs: The eNode-B to eNode-B path loss measurements could in principle be measured by the RSRP from other eNode-Bs during time periods where those are transmitting in the DL. Such measurements, combined with knowledge of the corresponding DL RS Tx power, can be used to get the knowledge of path loss towards the neighboring eNode-Bs. A eNode-B measuring the RSRP from

another eNode-B will have to be completely muted with no transmission, in this regard similar to the UE RSRP measurement. We assume that the HeNB measures the RSRP on PCC of the surrounding cells.

UL SINR is defined as the ratio of the received power of the reference signal transmitted by the UE to the total interference and noise power received by the eNode-B over the UE occupied bandwidth.

6.2.3 Algorithm for Initial Selection of Primary Component Carrier

The proposed algorithm provides a simple and fully distributed approach for the initial selection of PCC after the HeNB is powered on. The initial selection of PCC is mainly based on the local HeNB measurements and the information from neighboring HeNBs about the carriers they use as their primary and secondary. At this moment no UE measurements are available since there are no UEs attached to the HeNB. The proposed algorithm gives strong emphasis on assuring the quality of a primary carrier as it attempts to avoid its reuse by nearby HeNBs as much as possible. The goal is to make reconfiguration of these component carriers as slow as possible as opposed to secondary component carrier which can be reselected on a somewhat faster basis.

The process of initial selection of primary carrier involves three stages, shown in figure 6.3 [78], where information is gathered, aggregated and processed leading to the selection of the PCC. During the sensing and decoding step the newly entered HeNB gathers knowledge about surrounding cells. We assume that the limited inter-HeNB information exchange takes place via over-the-air-communication [70]. From this the neighbors' information on selection of primary and secondary carrier is obtained. In this stage the path loss to the neighboring HeNBs is estimated, and the uplink received interference power is measured. After the sensing and decoding stage, we assume that the following information becomes locally available [78]:

1. Neighboring cell indexes (cell IDs).
2. Component carrier occupancy of each detectable neighbor as well as information on whether a component carrier is used as either primary or secondary.
3. Path loss estimates towards each neighboring HeNBs.
4. Uplink RIP for each component carrier.

The first three pieces of information are then used to create a N x M matrix similar to the one depicted in figure 6.4, where N corresponds to the number of component carriers

into which the total bandwidth is divided. The number of columns M is not fixed and depends on the number of neighbors that can be detected. The fourth piece of information, i.e. Uplink RIP, reflects current traffic load conditions and is used as a last decision level as it will soon be explained.

All detected neighbors are listed in ascending order of estimated path loss. Component carrier usage as either a primary (P) or secondary (S) is also listed. Therefore, in figure 6.4 the left-most neighbors such as $N1$ and $N2$ are the most relevant sources/victims of interference. To account for estimation errors, neighbors with similar estimated path losses (e.g 1.5 dB) are later grouped as one entry. As a graphical example, columns corresponding to neighbors $N1$ and $N2$ in figure 6.4 could be grouped if their estimated path losses are very similar.

We also propose that whenever a grouping of two detected neighbors sharing the same primary chunk takes place, the lowest estimated path loss of these two neighbors is decreased by $3\ dB$, and the column ordering is reevaluated. For simplicity changes are made in steps of $3\ dB$. This is done to reflect the fact that two sources of interference can be as detrimental as one single $3\ dB$ stronger interferer.

Graphically, this means that columns corresponding to neighbors $N3$ and $N4$ in Figure 6.4 would be grouped because they both utilize the component carrier labeled as 3, and in our example they have similar path losses. In this case, after the $3\ dB$ reduction in estimated path loss it may occur that their estimated combined path loss is lower than that of $N2$, thus shifting their now merged column to the left (not shown).

The dotted red line in figure 6.4 corresponds to an absolute path loss value (a configurable parameter) beyond which a neighbor is no longer considered as a relevant source/victim of interference even if it can be detected. This implies that any selection will have little or no impact on those neighbors. Alternatively, there may be no explicit limit to the number of neighbors considered; this means that if no information can be decoded for a particular cell, then that cell is not relevant.

Finally, after the matrix is created the selection algorithm progressively restricts the solution space, until a single component carrier emerges as a clear winner.

1. If a fully idle component carrier is available, it will be selected. A fully idle component carrier means that a given row has neither P nor S entries.

2. If a component carrier without any prior P entries is available, it will be selected. This means that there are one or more rows with only S entries. If needed, a decision can be made according to criteria number 5 and 6.

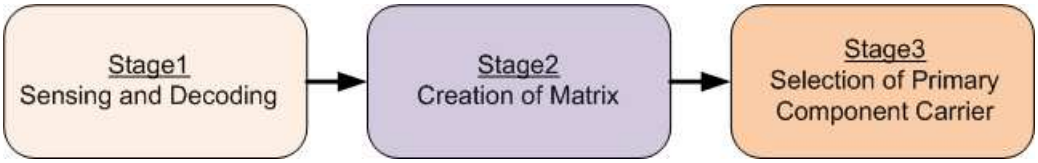

Figure 6.3: Outline of the three-stage process leading to the initial selection of primary component carrier [78].

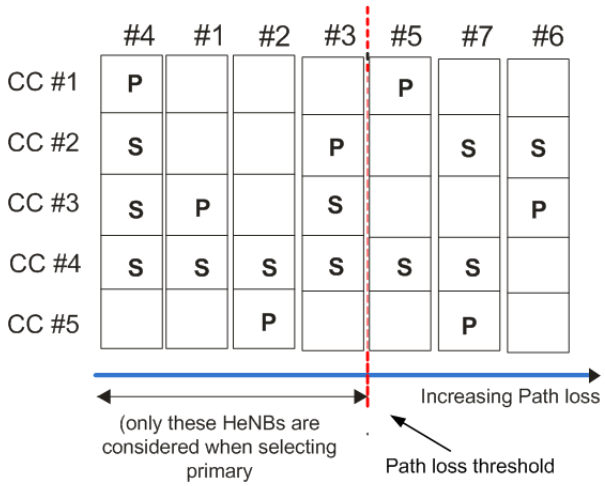

Figure 6.4: Matrix for initial selection of primary component carrier [80].

3. Max (Min (P index)): As it is the component carrier where the first occurrence of a P entry (Min (P index)) has the highest column index, (Max (.)).
4. Min(# P entries): Favor the component carrier having the smallest number of P entries in case a decision could not be made after the previous step.
5. Max (Min (S index)): Identical to criterion 3, except that we now consider S entries.
6. Min(# S entries): Favor the component carrier having the smallest number of S entries in case a decision could still not be made after the previous step.

Yet, if no selection was possible after stepping through all possibilities, the selection algorithm then relies on UL RIP measurements which reflect instantaneous traffic load conditions over the component carriers.

An Example Scenario

Figure 6.5 illustrates a simple scenario for initial selection of a primary component carrier using the above mentioned algorithm. An example scenario is assumed with four

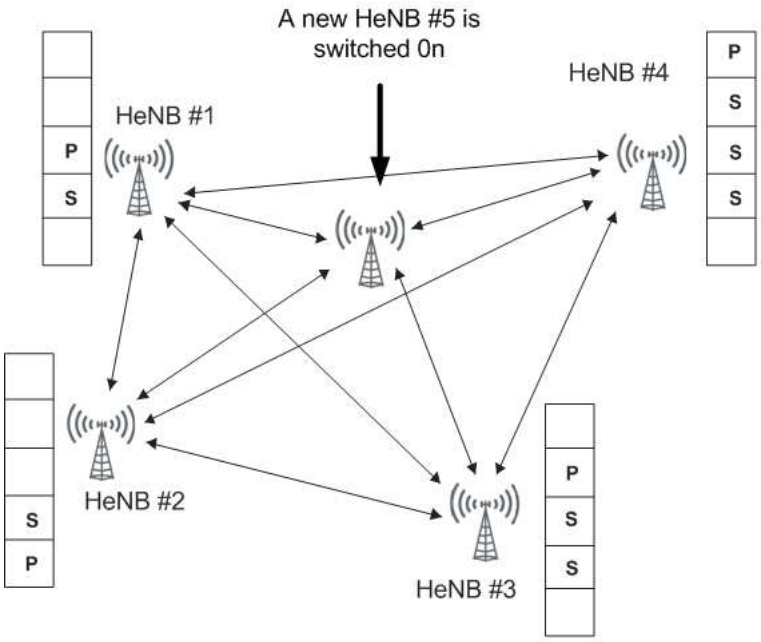

Figure 6.5: Sketch of a scenario with 4 existing HeNBs with selected primary (P) and secondary (S) component carriers. Subsequently the HeNB # 5 is switched on and therefore does not have any component carrier at this moment [80].

existing HeNBs (HeNB #1 to #4), where a new HeNB (eNB #5) is switched on. The first task of the new HeNB is to select one component carrier as its primary. We assume a configuration with 5 component carriers. Here, P and S denote the primary and secondary component carriers currently selected by the existing HeNBs. This information is available to the new HeNB from the surrounding HeNBs via over-the-air-communication. In addition to having this information the new HeNB performs path loss measurements of the surrounding cells locally. For this purpose inter HeNB RSRP measurements are used, where it is proposed that an HeNB measures the RSRP from its neighboring HeNBs. These measurements, combined with knowledge of the corresponding DL RS Tx power, are used to estimate the path loss towards the neighboring HeNBs. Using this information the new HeNB will select a primary component carrier. In this example the new HeNB will most likely select the #4 CC as its primary.

6.2.4 Quality Monitoring of Primary Component Carrier

After the HeNB selects a primary component carrier, it may start to carry traffic and also to monitor the quality of the PCC. Now the UEs gets connected, hence, apart from initial HeNB measurements, the other measurements such as UL SINR, throughput, RSRP, RSRQ etc. also become available. Some of these measurements are used for quality monitoring.

Our proposal is to individually monitor the quality in UL and DL, as different actions

may be required to improve the quality in these two transmission directions. Quality is monitored within the certain coverage area of HeNB. The coverage area is defined based on $RSRP_{min}$, which is the minimum desirable $RSRP$ an UE should experience within the coverage area of the cell. The UEs with $RSRP$ below $RSRP_{min}$ are considered out of coverage area as shown in figure 6.6. This criterion avoids the measurement samples from UEs, that are significantly far off from the serving HeNB.

In DL, the RSRQ measurements of UEs within the coverage area are monitored. A target $RSRQ_{th}$ is set as a threshold, shown in figure 6.7, which is the minimum RSRQ an UE should report within the coverage area of the cell. If $X\%$ of the reported RSRQ measurements is below $RSRQ_{th}$, then a quality problem in DL is detected. In UL, the UL received SINR is monitored for the users within the coverage area. A UL SINR threshold UL $SINR_{th}$ is specified as shown in figure 6.7. If $X\%$ of uplink received SINR measurements is below $ULSINR_{th}$, then a quality problem in UL is detected. The $RSRQ_{th}$, UL $SINR_{th}$ and $X\%$ are configurable parameters.

6.2.5 Recovery Actions to Improve Primary Quality

Based on the above criteria, if the quality of primary is found to be low in UL and /or DL, a recovery action is triggered to restore it. Two potential actions are considered.

- Option #1 : Request neighboring HeNBs to reduce the interference on the primary component carrier.
- Option#2 : Reconfigure a new primary component carrier.

Option # 1:

This is based on the transmission of Interference Reduction Request (IRR) message, indicating a high interference condition on primary. Upon detection of lower quality, the HeNB tries to keep the same primary and sends an IRR message to the neighboring HeNBs via over-the-air-communication [70]. The IRR message includes information on whether the quality problem is in uplink or in downlink.

In order to further outline the principle of the IRR, Figure 6.8 shows an example with 5 HeNBs, where P and S indicate the component carriers they have selected for primary and secondary respectively. HeNB #1 is assumed to experience a quality problem and therefore sends an IRR message. As eNB #2 and #4 have selected the same component carrier for secondary, they have to react to the IRR and reduce the interference.

Action upon Receipt of IRR

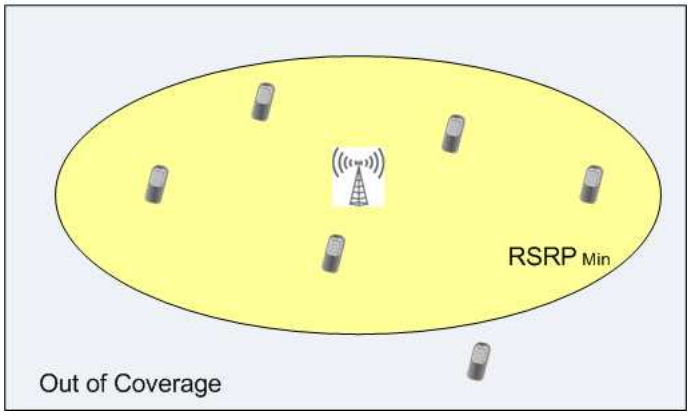

Figure 6.6: Coverage area of a HeNB based on the RSRP measurements. $RSRP_{min}$ defines the cell edge boundary.

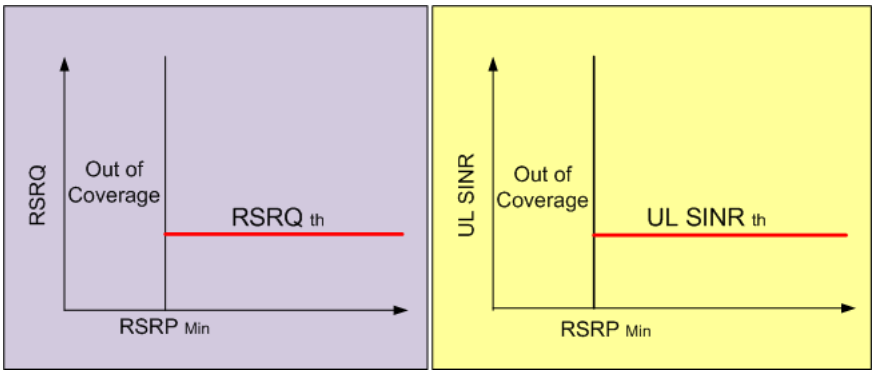

Figure 6.7: The criteria to determine the quality of the primary component carrier is based on $RSRQ_{th}$ in the downlink and $UL\ SINR_{th}$ in the uplink.

Actions for reducing the interference depend on whether the IRR message is for DL or UL. For DL, HeNBs #2 and #4 shall reduce their transmit power on component carrier #2. This is a simple method for reducing the interference in the downlink. Whether the step size of transmission power reduction should be fixed or it should be a reconfigurable parameter is a subject of further investigation.

If the IRR message is for uplink, there could be many candidate options for reducing the uplink interference [81]. The possible actions could include adjustment of UE transmit powers, scheduling high interference users less often, or potentially on different component carriers, etc. In most cases it is not straightforward to identify the best solution for uplink interference reduction. Which action to take is left to the HeNB implementation. It could be vendor specific similar to LTE Release'8, where also the specific actions an eNB takes upon receiving an Overload Indicator (OI) is vendor specific [80].

Sending IRR

We further propose that an alternative to an IRR broadcast would be to include more specific information in the message, such as which HeNB should reduce its interference.

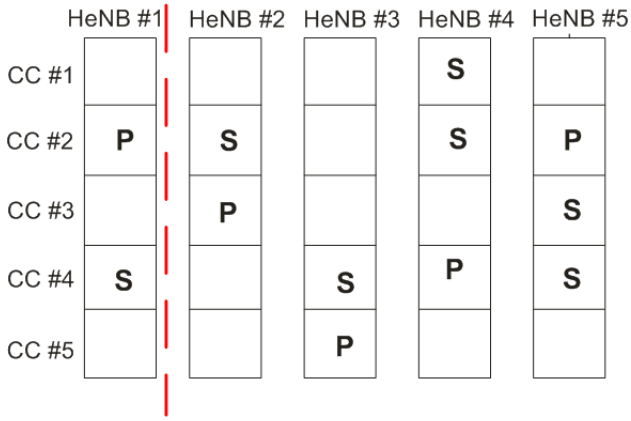

Figure 6.8: Simple example showing the component carriers selected by HeNBs. In this example HeNB #1 is assumed to experience low quality on its primary [80].

This would only be possible when the potentially strongest interferer is identified. Again, let us refer to the example in figure 6.8 and assume that HeNB #2 is relatively close to HeNB #1 (i.e. the eNB having primary quality problems), while HeNBs #4 and #5 are much further away from HeNB #1. For such a case, it would make sense to expand the content of the IRR message so that it specifically only requests HeNB #2 to reduce the interference on component carrier #2. However, the latter requires that HeNB #1 is able to identify which HeNBs are causing the quality problems on its PCC. Here the inter-HeNB path loss measurements combined with the information on the component carrier selection of surrounding HeNBs will be useful to identify the potential interferer. However, identifying the strongest potential interferer is not always straightforward. The background interference matrix (BIM) based approach could be useful to identify the potential interferer [82], [83].

Option # 2: Reconfiguration of Primary Component Carrier

In case the IRR approach fails to improve the quality, then option #2 will be used, where a new primary component carrier will be reconfigured. This could be illustrated using figure 6.8, where it is assumed that the option #1 fails to improve the situation. The HeNB #5 has selected the same component carrier as HeNB #1 for its primary. However, HeNB #5 cannot be asked to reduce its transmission power over the primary, because it should have full cell coverage. In such condition, the quality problem can only be solved through reconfiguration . Therefore, in a situation, where the quality problem is caused by two (or more) HeNBs having selected the same component carrier for primary could be resolved via option #2, where at least one of them selects another component carrier for primary.

We recommend that option #1 is first pursued, whenever possible, and only if it fails to improve the quality, option #2 should be taken up. The main reason for not taking option #2 as the first choice is that this option requires additional signaling to all the UEs in the cell as it nearly corresponds to reconfiguration of the cell. Hence, if the currently

selected component carrier for primary is released, and a new one is selected as primary, then all the UEs in the cell associated with the primary component carrier have to be informed via signaling. In the cases where option #2 is the only choice for improving the quality of primary component carrier, the scheme described for initial selection of primary used in state #1 (section 6.2.3) can be performed. A minimum time between consecutive reconfigurations is also required to be enforced as there is signaling overhead associated with change of component carrier.

6.3 Modeling Assumptions

The LTE-A system model described in chapter 2 (section 2.6) is used for performance evaluations. The indoor regular corporate and regular residential scenarios as depicted in figures 2.8 and 2.9 are employed. However, in addition to these two scenarios, extended residential scenario is also used. The regular and extended scenarios refer to the deployment with 4 and 16 HeNBs respectively. The extended residential scenario consists of 2×2 replica of the regular residential scenario with corridors in between. The extended residential scenario is shown in Figure 6.9. The simulations are performed at full traffic load. The adjusted Shannon throughput mapping following [84] is used, where, for a given SINR value within [$SINR_{min}$, $SINR_{max}$], the throughput is estimated by:

$$S = BW_{eff} \cdot \log_2 \left(1 + \frac{SINR}{SINR_{eff}}\right) \tag{6.1}$$

where S is the estimated spectral efficiency in bps/Hz, BW_{eff} accounts for the system bandwidth efficiency and SNR_{eff} accounts for the SNR implementation efficiency. For a Single Input Single Output (SISO) system, if SINR is less than $SINR_{min}$, then $S = 0$ and if SINR is larger than $SINR_{max}$, then $S = 5.4$. The typical values of the parameters in the above expression are given in table 6.1 [85].

Table 6.1: The Adjusted Shannon Parameters for Throughput Estimation

	BW_{eff}	$SINR_{eff}$	$SINR_{min}$	$SINR_{max}$
Downlink	0.56	2.0	-10	32
Uplink	0.52	2.34	-10	35

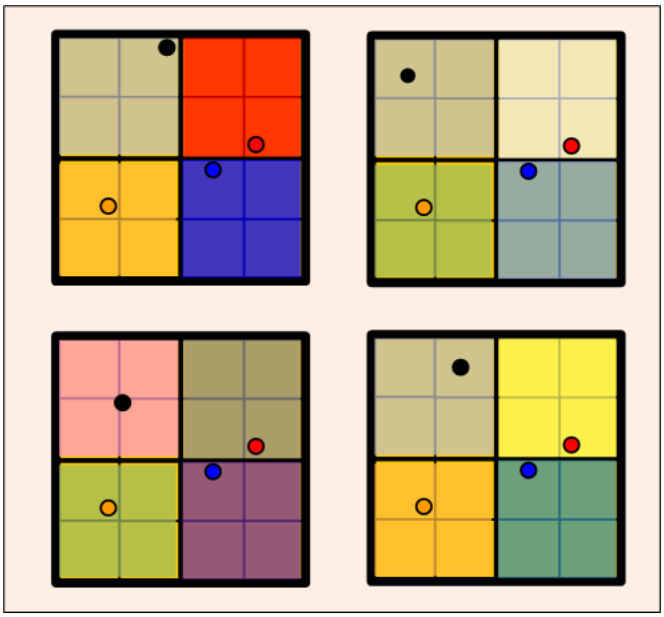

Figure 6.9: Extended residential scenario with 16 HeNBs. This is 2 x 2 times replica of the regular residential deployment with corridors in between the two regular deployments.

6.4 Performance Evaluation

The performance results are presented in two phases. In the first phase, HeNBs are assumed to switch on in a sequence, whereas in the second phase, HeNBs are assumed to switch on in a random order. The latter represents a more realistic situation. After switching on, each HeNB selects a PCC. No simultaneous selection is assumed. The simulation continues until all the HeNBs have acquired one and only one PCC. The results are collected from the last simulation step. The results do not include the effect of any recovery action, i.e. the HeNBs will not change their primary after initial selection.

The primary focus is to evaluate the sensitivity of the proposed algorithm in selection of PCC in comparison with the corresponding fixed frequency reuse schemes. The fixed frequency reuse schemes are planned and are expected to provide optimal frequency allocation over the network. The PCC selection by proposed algorithm should converge to the fixed frequency reuse schemes.

In order to evaluate the performance with a different number of component carriers, the assumed system bandwidth of 100 MHz is divided into 2, 4, 8 and 16 component carriers. The performance in each case is compared with the corresponding fixed frequency reuse schemes, i.e. with reuse factors 2, 4, 8 and 16. The comparison is performed in terms of average cell throughput and 5% outage user throughput, normalized against the results of fixed frequency reuse 1 (universal frequency reuse) scheme.

Sequential HeNB Switching

With sequential switching, 2 and 4 component carriers are considered for regular corporate, and 2, 4, 8 and 16 component carriers are considered for extended residential scenario. For regular corporate 5-10 UEs are simulated within each HeNB, whereas, for extended residential 2-4 UEs are simulated.
Figure 6.10 shows SINR distribution in DL and UL for regular corporate scenario. The SINR distribution of reuse 1 is also included in the figure. The SINR distribution of the PCC algorithm is essentially the same as its corresponding reuse schemes. Figure 6.11 compares the distribution of average cell throughput and average user throughput in DL, which is also essentially the same. Further, figures 6.12 and 6.13 compare the normalized average cell throughput and 5% outage user throughput in DL and UL respectively. The proposed PCC algorithm provides nearly the same performance compared to the corresponding fixed frequency reuse schemes. This implies that the selection of the component carriers by PCC at HeNBs resembles the optimally planned fixed frequency reuse schemes.
The normalized cell throughput and user outage throughput in DL of extended residential scenario is presented in figure 6.14. The PCC algorithm with more than 2 component carriers gives nearly the same performance as it corresponding reuse schemes. A lower performance is realized with 2 component carriers, especially in the user outage through-

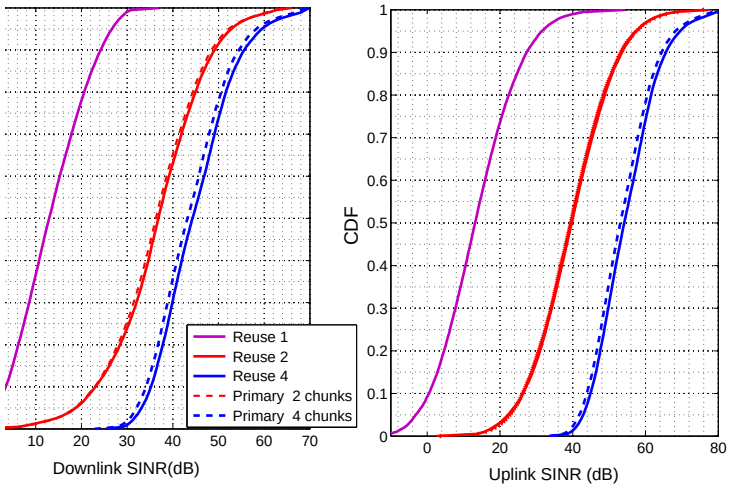

Figure 6.10: CDF of downlink and uplink SINR in regular corporate scenario.

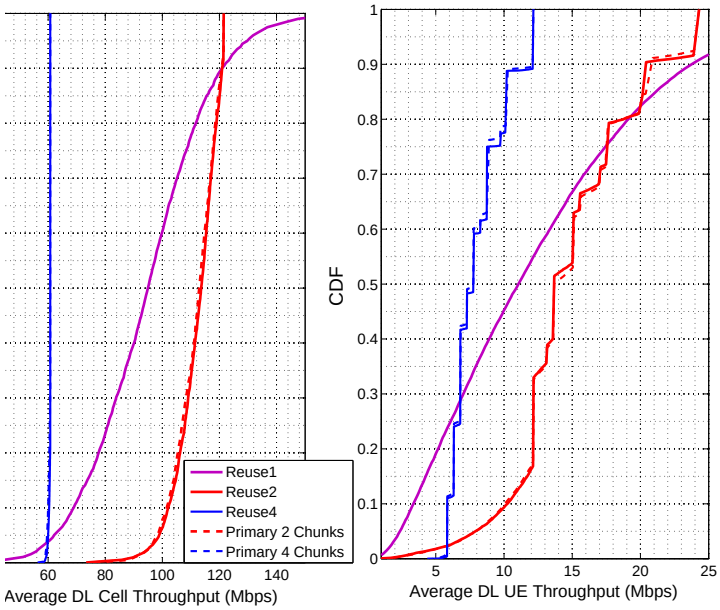

Figure 6.11: CDF showing comparison of cell and user throughput in regular corporate scenario.

put. This is due to the fact that algorithm always assumes that the worst interferer is the HeNB with the lowest HeNB to HeNB path loss. This may not always be true in case of local area uncoordinated deployment scenario with a large number of HeNBs. However, this is an attractive feature of the algorithm due to its simple implementation.

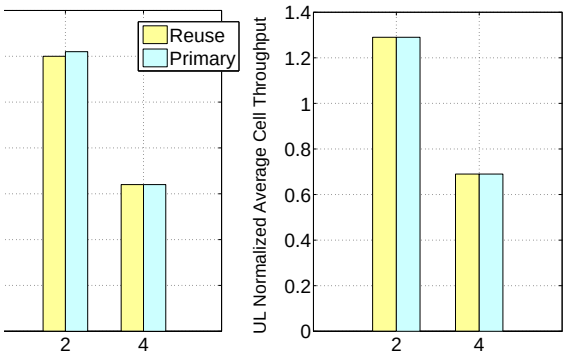

Figure 6.12: Comparison of average cell throughput in DL and uplink for regular corporate scenario. The results are normalized by the average cell throughput of frequency reuse 1 scheme.

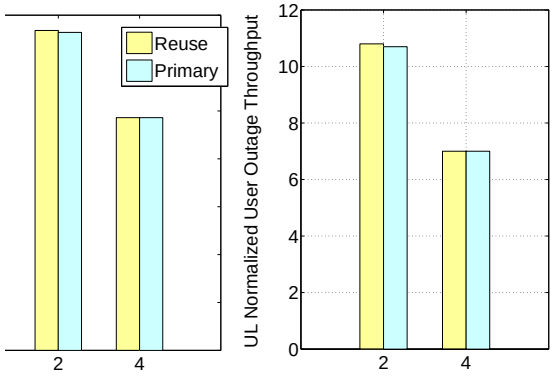

Figure 6.13: Comparison of 5 % outage user throughput performance in the DL and uplink of regular corporate scenario. The results are normalized by the average cell throughput of frequency reuse 1 scheme.

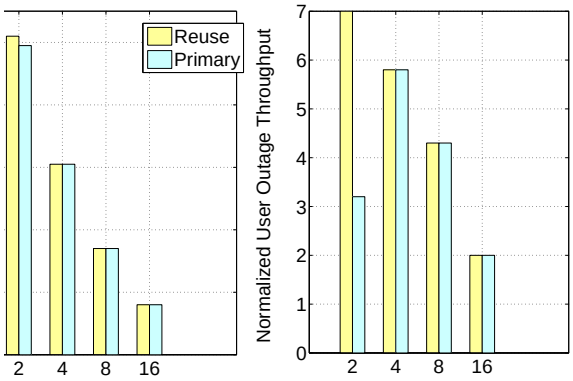

Figure 6.14: Comparison of normalized average cell throughput in the DL of extended residential scenario.

Random HeNB switching

For random switching 2, 4, 8 and 16 component carriers are considered for both regular corporate and extended residential. 4 UEs per HeNB are simulated for both the scenarios.

The SINR distributions in DL and UL for regular corporate are shown in Figure 6.15. Unlike sequential switching here the PCC algorithm with 2 component carriers shows a noticeable drop in SINR distribution. This happens because in random switching, with only 2 component carriers to choose from, the dead lock situation cannot be completely avoided. The dead lock situation is, when the HeNBs have to stay with the non optimal allocation of component carriers. The reconfiguration of the PCC becomes inevitable in this case. However, the SINR distributions with higher number of component carriers are in conformance with the previous results.

The distribution of DL cell throughput and user throughput is shown in figure 6.16. Except with 2 component carriers, the distribution for PCC algorithm is close to the corresponding reuse schemes. Figure 6.17 shows normalized DL average cell throughput and average user throughput. In terms of both, the cell throughput and user outage throughput, the PCC algorithm with 2 component carriers gives lower performance than its corresponding reuse scheme, i.e. reuse 2.

The similar trends are observed with extended residential scenario as well. The DL results for extended residential scenario are presented in Figures 6.18, 6.19 and 6.20. The results in UL (not included here) also shows the similar trends.

From the above results it could be stated that the selection of PCC by the proposed scheme resembles closely the optimally planned corresponding fixed frequency reuse schemes. However, when the number of component carriers is only 2, the desired performance is not achieved for most of the cases, except for regular corporate scenario with sequential switching.

Therefore, when only two component carriers are assumed, the reconfiguration may be required too often to avoid the deadlock situation. However, with a higher number of component carriers, the reconfiguration of PCC will not be required very often.

The PCC algorithm is an integral part of the overall component carrier selection algorithm, which includes secondary component carrier selection algorithm, monitoring and recovery action. The work has been further extended by a fellow researcher, and the results including SCC are presented in [82]. The result shows a cell throughput improvement by component carrier selection algorithm in uncoordinated local area indoor scenario, and therefore provides a viable mechanism for such deployment scenario. However, the results therein do not include monitoring and recovery action.

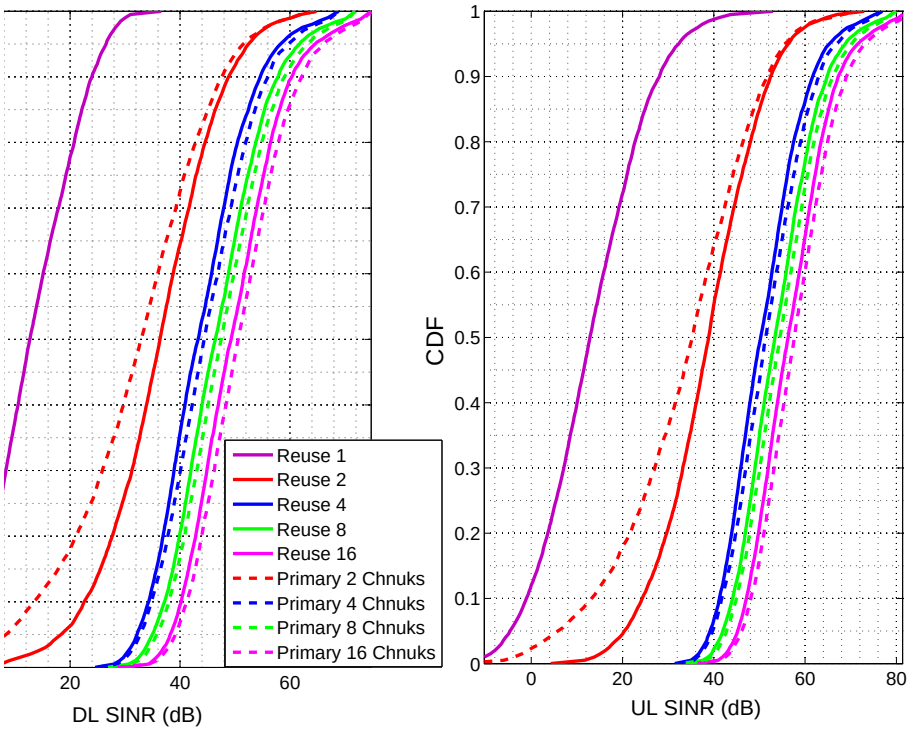

Figure 6.15: SINR distribution in DL and UL for regular office scenario in case of random HeNB switching.

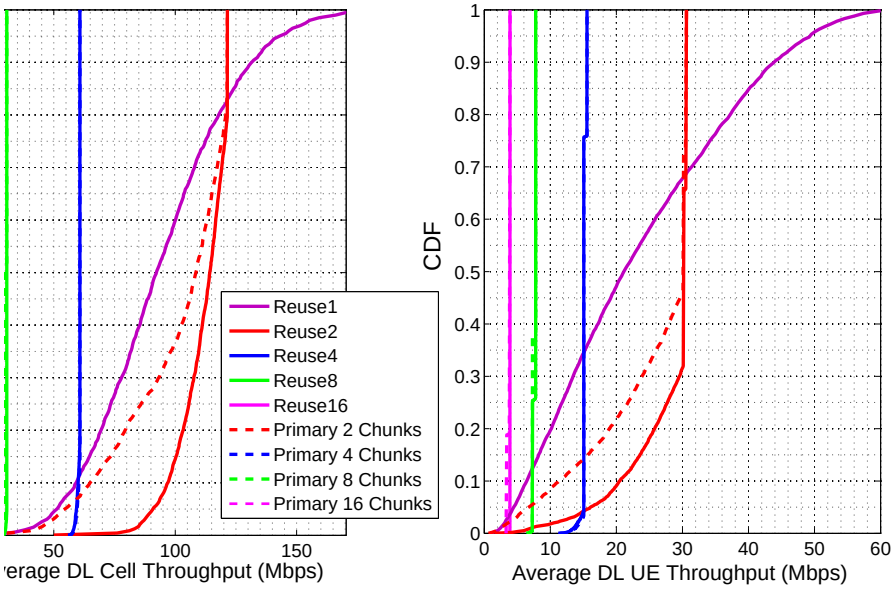

Figure 6.16: CDF of DL cell throughput and user throughput of regular office scenario with random HeNB switching.

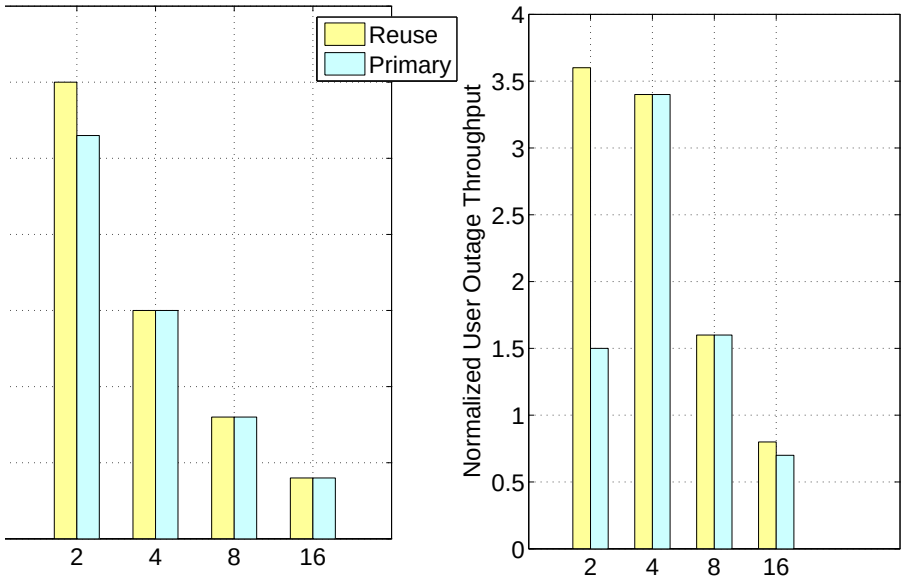

Figure 6.17: Comparison of normalized DL average cell throughput and normalized user throughput of regular office scenario with random HeNB switching.

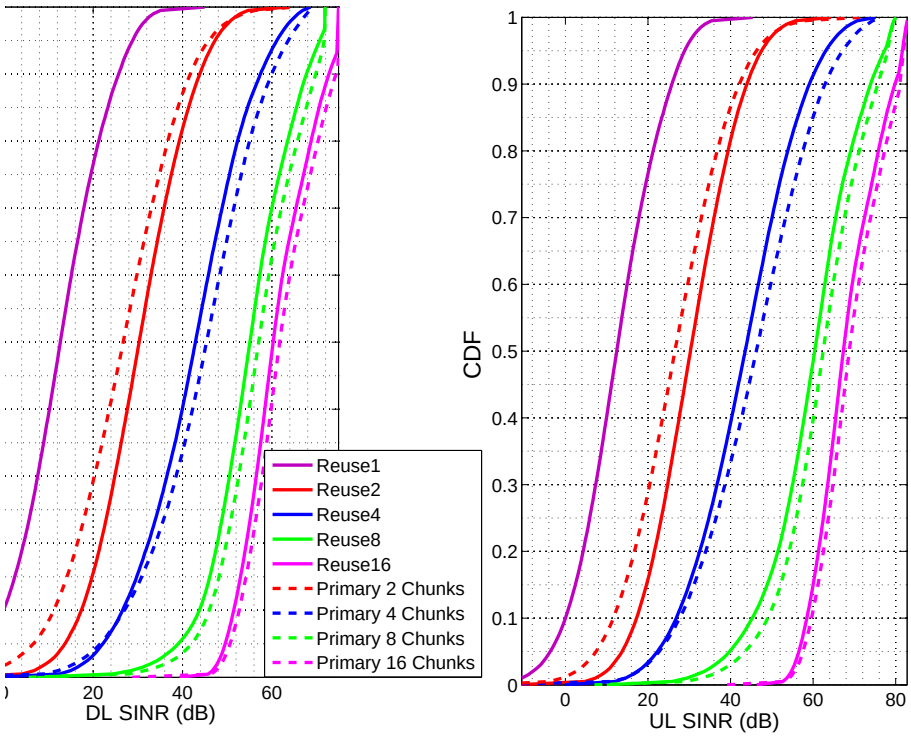

Figure 6.18: SINR distribution in DL and UL for extended residential scenario in case of random HeNB switching.

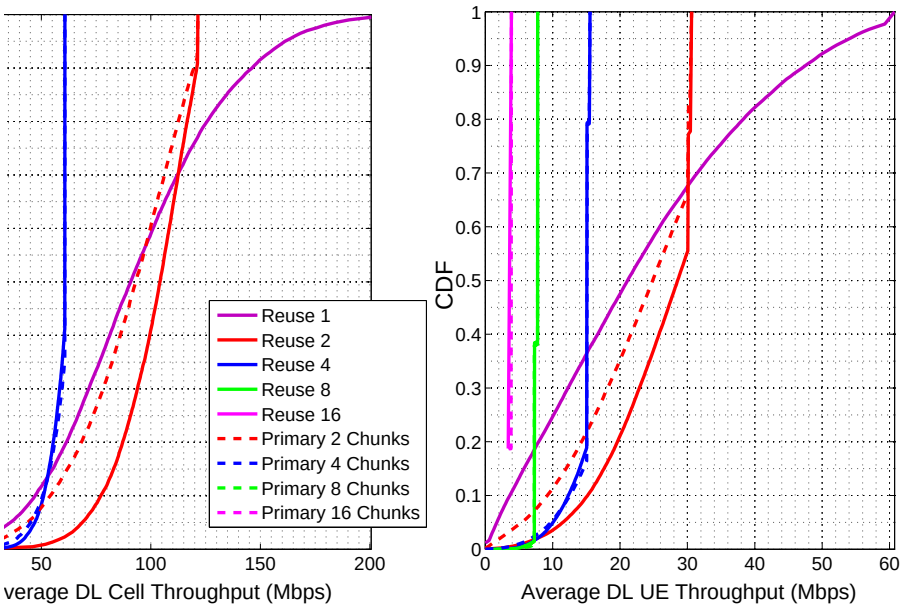

Figure 6.19: CDF of DL cell throughput and user throughput of extended residential scenario with random HeNB switching.

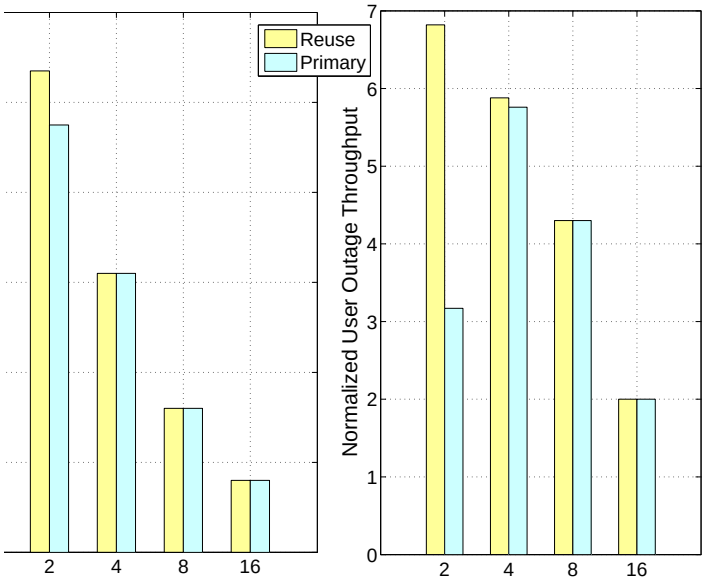

Figure 6.20: Comparison of normalized DL average cell throughput and user outage throughput of extended residential scenario.

6.5 Conclusions

In this chapter the carrier aggregation as a possible method to obtain LTE-A system bandwidth is discussed. The concept of primary and secondary component carriers is illustrated. A basic concept for the distributed autonomous component carrier selection is outlined. The concept is motivated by the fact that each HeNB does not always need the full LTE-Advanced system bandwidth; in many cases one only needs a sub-set of the available component carriers.

We proposed an algorithm for the initial selection of the primary component carrier. A mechanism is also proposed for monitoring and protection of the quality of primary component carrier. In case the quality of primary is found to be low, the HeNB can initiate the recovery action to restore the quality of primary component carrier. It is also proposed that the Interference Reduction Request (IRR) message based recovery action should be preferred as a first step over the reconfiguration of the primary component carriers.

The proposed concept for selection of primary component carrier is fully distributed and does not involve any centralized network components; the selection is rather performed locally and independently by each HeNB, where each HeNB always selects one, and only one, primary component carrier.

The simulation results presented in this chapter indicate that the presented concept helps to achieve an autonomous scalable and self-adjusting frequency reuse mechanism, which allows uncoordinated HeNB deployment without prior network planning.

Adaptation of the proposed concept for LTE-Advanced is simple since it entails minimal changes to the standard as it mostly relies on existing release 8 UE and HeNB measurements.

Chapter 7

Policy Assisted Light Cognitive Radio for FSU

7.1 Introduction

It is discussed in chapter 5 that currently HeNB is emerging as a potential solution for high data rate and high quality services in indoor local area deployment scenario. The FSU has been considered to allow coexistence of HeNBs in the given geographical area. FSU can be performed in single-operator as well as multi-operators' domain. Single operator FSU aims to facilitate high performance in uncoordinated and random deployments, whereas multi-operator FSU facilitates different operators to access the common spectrum pool in flexible manner, based on their individual traffic requirements. The FSU in multi operators' domain becomes necessary if the HeNBs are deployed by several operators in a given geographical area, sharing over the common spectrum pool.

7.1.1 Multi-Operator FSU

The multi-operator FSU is based on the concept that when one network operator is in demand of the extra spectrum, the other network operators might have the spectrum available in excess. In this situation the sharing of spectrum helps to exploit the unused spectrum, which leads to a higher degree of spectrum utilization. In order to facilitate FSU among the operators it is assumed that the operators access the spectrum in a flexible manner from a common pool of spectrum.

In a multi operator FSU scenario a certain number of different operators are considered to deploy HeNBs in the given geographical area and to have access to the same licensed frequency band using the same radio access technology. An operator is allowed to install HeNBs without prior coordination with the other operators having access to the same frequency band. Spectrum regulators decide how many operators have access to the given licensed spectrum bands in the given area. This implies that it is known a-priori by each

operator, how many other operators are operating in the same band.

When several network operators are deployed in the local area scenario and make use of the same radio spectrum, a major concern is the interference. In traditional macro cell and micro cell deployment scenario this has been handled by a proper network planning, including frequency re-use plans, base station location, transmit power levels, and antenna radiation characteristics. In contrast to these scenarios, in the case of local area deployments the installation of the HeNBs cannot be planned by operators. The HeNBs are user employable, resulting in a random deployment. It is also natural to envision the lack of coordination between operators providing LA services in the same geographical area. Therefore, in the LA deployment scenarios the radio interference problem becomes much more severe compared to the traditional cellular deployment cases, and new mitigation solutions need to be found. Another important aspect is high traffic load variability among different operators operating in the given geographical area over the same radio spectrum, requiring a mechanism to exploit the traffic load variations by utilizing spectrum in a flexible manner.

So far most of the deployment scenarios in either macro cells or micro cells consider coordinated deployment among operators. In this context, coordinated deployment means that the BS /access point installations are planned to have good coverage and low interference between adjacent cells, which typically implies radio network planning prior to installation of new BS/access point. However, in the considered scenario an uncoordinated HeNB deployment without prior radio network planning is envisioned. In this context, uncoordinated deployment refers to cases where HeNBs are more or less installed randomly to get coverage/capacity in one particular area, without considering the impact on/from potentially existing HeNBs radio performance in the immediate surroundings.

The FSU concept allows uncoordinated HeNB deployment without prior radio network planning exercises, therefore, the support for uncoordinated deployment is especially considered to be attractive for LA areas in case of multi operator deployment scenario. However, the uncoordinated deployment with multi operators represents new challenges for FSU. Moreover, the requirements of high spectral efficiency and fairness among operators demand a mechanism for FSU to enable overall radio resource utilization and sharing in a flexible manner.

7.1.2 State of the Art

Many studies have recently focused on inter-operator FSU [86], [87], [88], [89], [64]. In a wide area broadband network assuming all the operators using same radio access technology, an increase in overall spectrum efficiency is realized by spectrum sharing among the operators [86]. Taking into account the operational revenue and the QoS requirements, different criteria and optimization methods are outlined to improve the spectral efficiency by coordinated spectrum usage for flexible spectrum allocation in [64]. The performance of spectrum sharing for UMTS FDD DL for competing network operators is investigated in [88], wherein an algorithm is proposed using total transmitted energy thresholds in the

shared band, allowing multiple operators to coexist. The concept of FSU is outlined in the perspectives of private commons in [9]. The private commons enable multiple parties to access the spectrum in existing licensed band based on the discretion of license holders, where the ultimate ownership of the licensed spectrum is retained with them. The responsibility for setting rules and the enforcement of these rules lies entirely with the licensed holders. It seems that for licensed band the solution is easier to imagine, though may not be straightforward to implement [90], even though it is believed that in the long run the private-common will be the viable market option [9].

7.1.3 Aim of This Chapter

This chapter is focused on multi operator FSU, and therefore aims to provide a mechanism to enable FSU in LA indoor deployment with several operators, allowing them to coexist in the same geographical area with partially or completely preventing mutual interference on the shared spectrum while meeting individual traffic requirements. A random and uncoordinated deployment is considered. A very limited signaling exchange via over the air communication is assumed.

The proposed mechanism is based on the concept of policy assisted light Cognitive Radio (CR) enabled FSU. It follows the CR cycle and considers policy as an important element to assist FSU among the operators. The proposed concept is illustrated in the following section.

This chapter is organized as follows: in section 2 the proposed concept is described, whereas the proposed algorithm is described in section 3. Section 4 outlines the modeling assumptions and section 5 the performance results. Finally, section 6 outlines the conclusions.

7.2 Proposed Concept

7.2.1 Policy Assisted Light Cognitive Radio

We consider that each HeNB makes independent decision for spectrum allocation based on the interference conditions present over the spectrum with the support of Light Cognitive Radio and Policy, referred to as Policy-Assisted-Light-Cognitive-Radio(PA-LCR) for FSU.

Policy

It is considered that a policy based approach is needed to allow fair, efficient and flexible spectrum sharing among the operators from the common pool. In general, the term policy has been defined in several references. In [91] various Channel Access Mechanisms (CAMs) are discussed to handle the traffic generated in 802.11e WLAN, where a policy

is defined as a function that, given a set of different input parameters, selects a particular CAM. It is considered that the policy data base is built offline based on the results of network simulations [92]. The policy is also used to describe the constraints on using the spectrum resource[93]. Further, a more relevant concept of policy is outlined in [63], where it is stated that policies are required to control the dynamic spectrum usage and it is defined as a set of rules agreed among the operators, which is required to facilitate FSU. We follow this definition in our concept of policy. The main policy elements considered for the proposed concept is illustrated in section 7.3 in this chapter.

Light Cognitive Radio

In the face of random and uncoordinated network deployment by several operators, in order to achieve autonomous network configuration and operation, the HeNBs are required to sense the wireless environment and adopt the spectrum allocation accordingly keeping in view minimizing the mutual interference and improving the throughput performance. To this end the concept of cognitive radio seems to be useful. The cognitive radio is considered to have potential to become the key enabler to result in increased access to spectrum. It helps to rapidly configure the operating parameters to the changing requirements and conditions in order to automatically coordinate the usage of spectrum [90]. The cognitive radio is also defined as an intelligent wireless communication system that is aware of its surrounding environment, and uses the methodologies of understanding by building to learn from the environment and adapts its internal states to statistical variations in the incoming radio frequency stimuli [94]. Mitola's definition of cognitive radio is a radio or system that senses, and is aware of its operational environment, and can dynamically and autonomously adjust its radio operating parameters accordingly. In addition to this the cognitive radio also has capability to reconfigure based on Software Defined Radio (SDR) [95], where the SDR is considered as a radio system in which some or all of the physical layer functions are defined by software. Based on these concepts the cognitive radio cycle involves sensing, learning, decision making and adaptation.

However, we make use of the cognitive radio cycle, but we do not exploit the reconfigurability feature based on SDR, therefore we refer to our concept as light cognitive radio, because the cognitive radio is not used in its full sense. In our proposed concept the decision making process in the cognitive radio cycle is assisted by policy. Figure 7.1 describes the concept of policy assisted light cognitive radio used in this chapter.

7.2.2 Utility Function

The utility function is defined in 7.1. Each HeNB aims to maximize the utility function.

$$UF = \frac{T^{\alpha}}{B} \tag{7.1}$$

Where, T represents the achieved total sum throughput, which is defined as the aggregate of the users' throughput of a HeNB. B is the total bandwidth used by the HeNB and is computed from the number of users multiplied by the number of PRBs per user. 125 PRBs with 60 kHz inter carrier spacing is considered over the 100 MHz system bandwidth.

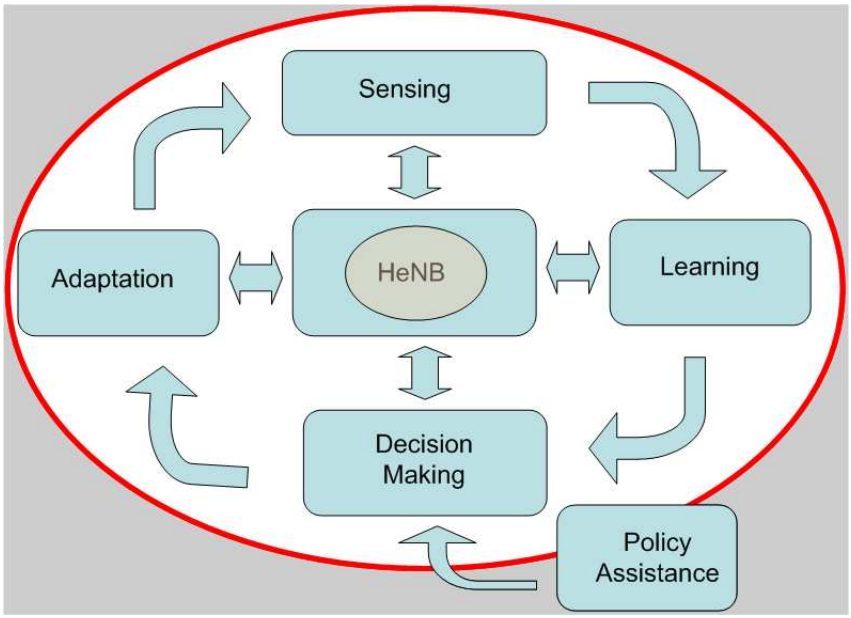

Figure 7.1: Policy Assisted Light Cognitive Radio Concept for FSU

The parameter α, which is used as an exponent over the throughput is assumed as a weighting factor, where different numerical values of α provide different amounts of weights to total sum throughput with respect to the spectrum utilization. The weighting factor is used in order to suitably select the utility function. When α = 1, the utility function is defined as spectral efficiency. It is worth mentioning that maximizing spectral efficiency leads to orthogonal allocation. The orthogonal allocation is not desirable in our concept, because it resembles fixed spectrum allocation scenario. On the other hand, maximizing throughput tends towards full frequency reuse resulting in increased interference and decreased spectral efficiency. Our objective is neither orthogonal allocation nor full spectrum reuse; instead we aim to allow overlapping of spectrum with acceptable degree of mutual interference in order to provide a mechanism for FSU. Therefore, α is used as an exponent in order to define the utility function, where different values of α result in different degrees of frequency reuse by allowing different amounts of spectrum allocation. The simulation results with α = 2 are presented in this chapter. A number of simulations with different values of α was performed in order to select a suitable value of α giving the highest throughput performance while maximizing the utility function.

7.3 Proposed Algorithm

Figure 7.2 presents the flow diagram of the proposed algorithm, and the description is given below. The algorithm is performed in the following steps.

Step1: Initialization Phase

The initialization phase starts as soon as a HeNB is switched on. In this phase the

HeNB randomly allocates PRBs to establish communication with its UEs and to meet the traffic requirements. In addition to this, the HeNB requires to establish its own position in the queue for updating spectrum allocation in the subsequent frames. This step is required because it is assumed that the HeNBs update their spectrum allocation in sequence, at their own turns. In order to establish its position in the sequence the new HeNB communicates with other potentially existing HeNBs using over-the-air-communication [70]. This process requires a limited amount of signaling exchange, because the setting of sequence is needed only when a HeNB leaves or enters the network. Once the sequence is set, it remains unchanged for the given set of active HeNBs.

The algorithm assumes, that HeNBs update their spectrum allocation in sequence on their own turns. This implies that when one HeNB updates, all other HeNBs follow their previous allocation. This assumption is made to ensure that while updating the spectrum allocation, the interference condition remains predictable for the HeNB. It also helps to avoid the yo-yo like situation which may happen if two or more HeNBs are allowed to update their spectrum allocation at the same time. If HeNBs are allowed to update at the same time, it is possible that they sense low interference over the same PRBs and decide to allocate, which will result in very high interference over those PRBs in the next frame. In the next frame those PRBs will not be allocated by any HeNB,resulting in lower interference in the subsequent frame. This process will be repeated, creating an yo-yo like unstable situation.

Therefore, during initialization phase two important tasks are accomplished: 1) establishing communication with UEs and 2) setting up sequence.

Step 2: Interference Sensing and PRB Sorting

Once the communication is established between UE(s) and HeNB during the initialization phase, it becomes possible for HeNB to sense interference over the spectrum. In this phase the HeNB senses interference over all the PRBs. A similar to UL Received Interference Power (RIP) measurement is assumed in the sensing phase. The UL RIP is defined as uplink received interference power, including thermal noise, measured at eNB within one PRB bandwidth [18]. The UL RIP has been standardized as a measurement that LTE physical layer should report to higher layer [79]. Once the interference, i.e. the UL RIP is measured over all the PRBs, the PRBs are sorted in an ascending order based on the amount of interference present over them. This implies that the sorted list starts with the best PRB.i.e. the PRBs with the lowest interference. When the PRBs are required to be selected, the selection starts with the best PRBs consecutively from the sorted list.

Step 3: Interference Threshold Based PRB Allocation

In this phase the HeNBs select PRBs from the sorted list based on interference threshold (I_{th}). The set of PRBs with interference level below I_{th} are considered as available PRBs ($N_{available}$)for allocation by a HeNB. The HeNB is allowed to allocate PRBs only from the $N_{available}$ set of PRBs. The I_{th} allows opportunistic allocation of PRBs with some degree of frequency domain overlap and ensures co-existence of mutually interfering HeNBs. The I_{th} corresponds to the minimum desirable level of QoS and also defines the coverage of the cell. The I_{th} is agreed among the operators as part of a policy, which

may be decided depending on the knowledge of the observed traffic conditions. During this phase the allocation of PRBs follows further policy constraints, described below.

- Only the required number of PRBs to meet the traffic requirement from the available PRBs will be selected with a constraint that the selected number of PRBs should not exceed N_{max}. where N_{max} is defined as the maximum number of PRBs that any HeNB is allowed to select and is defined as X % of total PRBs. The constraint on N_{max} aims to prevent one HeNB from allocating all the PRBs. The value of N_{max} is required to be carefully chosen in order to achieve the desired performance. The selection N_{max} depends on the knowledge of observed average interference conditions. A high value of N_{max} can be selected if the observed interference condition is very low otherwise, a low value is preferred.

- The proposed algorithm does not assume the QoS differentiation among the users. Therefore an equal number of PRBs to all the users will be allocated by a HeNB. Another policy constraint determines minimum ($N_{min/UE}$) and maximum ($N_{max/UE}$) number of PRBs per user. The $N_{min/UE}$ is used to ensure a certain minimum service quality to the users, whereas $N_{max/UE}$ is employed to impose restriction on the number of maximum PRBs one HeNB is allowed to allocate.

- If the number of available PRBs ($N_{available}$, number of PRBs below the interference threshold) is not enough to meet the $N_{min/UE}$ criteria, then some users will be dropped and the number of PRBs per user will be determined by the expression (7.2), subject to the $N_{min/UE}$, which is a policy constraint that determines the minimum number of PRBs to be allocated to each user.

$$\text{Number of PRBs per UE } = \frac{\text{Number of Available PRBs}}{\text{Number of UEs}} \tag{7.2}$$

- The policy also determines the initial number of PRBs to be allocated to each user denoted as $N_{initial}$. It is not necessary that the $N_{initial}$ should be equal to $N_{min/UE}$.

Step 4: Successive PRB Increment

In the subsequent frames the number of PRBs per user is increased in steps by providing a certain number of additional PRBs called N_{add}. Besides avoiding greedy allocation, it ensures that the HeNB with a higher number of users has the opportunity to allocate more PRBs in subsequent frames. In case due to lower number of $N_{available}$, if it is not possible to allocate N_{add} then the possibility for N_{add-1} will be examined. If this is not possible either, then the allocation will take place meeting $N_{min/UE}$ criteria. The process of successive increment in PRB per UE takes place for a definite number of frames called N_{frame}, after which this phase ends. During this phase the pay-off is computed using utility function for each allocation. The computed pay-offs are stored for future reference. This part of the algorithm constitutes the learning phase of the cognitive radio cycle, which assists the decision making process.

Step 5: Revision Process

The next phase of the algorithm is the revision process, where finally the decision making and adaptation is performed. In this phase the expected pay-off computed from the current PRB allocation is compared with the previously obtained pay-offs (taken from the learning phase). If the pay off due to the current allocation is higher than the maximum pay-off obtained so far, then HeNB adopts the current allocation, otherwise, one of the previous allocations with maximum payoff is adopted. This implies that at each turn a HeNB selects the best response based on the current information and the learning experience. A key element of this revision process is inertia, meaning that if there is no gain in pay-off the HeNB continues as before. During the revision process it is possible that a HeNB decides to allocate a lower number of PRBs compared to its previous turn. The basic notion behind this decision is that by using a lower number of PRBs one offers lower interference to others. If all the HeNBs follow the same principle, the total network interference will be reduced, which will result in a higher pay-off for all the HeNBs. Another important consideration is that the quality of PRB decreases (i.e. the level of interference increases) as the PRB index increases, therefore, in certain situations, using a lower number of PRBs may result in higher pay-off.

The N_{max}, $N_{min/UE}$, $N_{max/UE}$, $N_{initial}$, N_{add} and N_{frame} are the policy elements in the proposed concept. These have to agreed among the operators and followed by each HeNB in order to maintain fairness. For example, the considered values of these parameters chosen for two operators scenario in our study are in table 7.1.

Table 7.1: Considered parameter values of policy elements

N_{max}	$N_{min/UE}$	$N_{max/UE}$	$N_{initial}$	N_{add}	N_{frame}
80%	5	12	6	2	9

7.4 Modeling Assumptions

The LTE-A system model discussed in chapter 2 (section 2.6) is employed. The deployments with 2 and 4 operators are considered. The deployment with 4 operators is as shown in Figure 2.8, whereas, for 2 operators the $100m \times 50m$ is divided in two equal coverage areas. A simple model is assumed where each operator has one HeNB in the given geographical area. Ideal Shannon throughput mapping is used for throughput estimation. TDD with perfect synchronization and equal UL / DL ratio has been used. A frame of 10 ms duration is considered. The interference threshold is set at -70 dBm. Power control is not used. The exponent of the utility function, α = 2 is considered. Simulations are performed at full load. The main simulation assumptions and parameters employed are given in table 7.4.

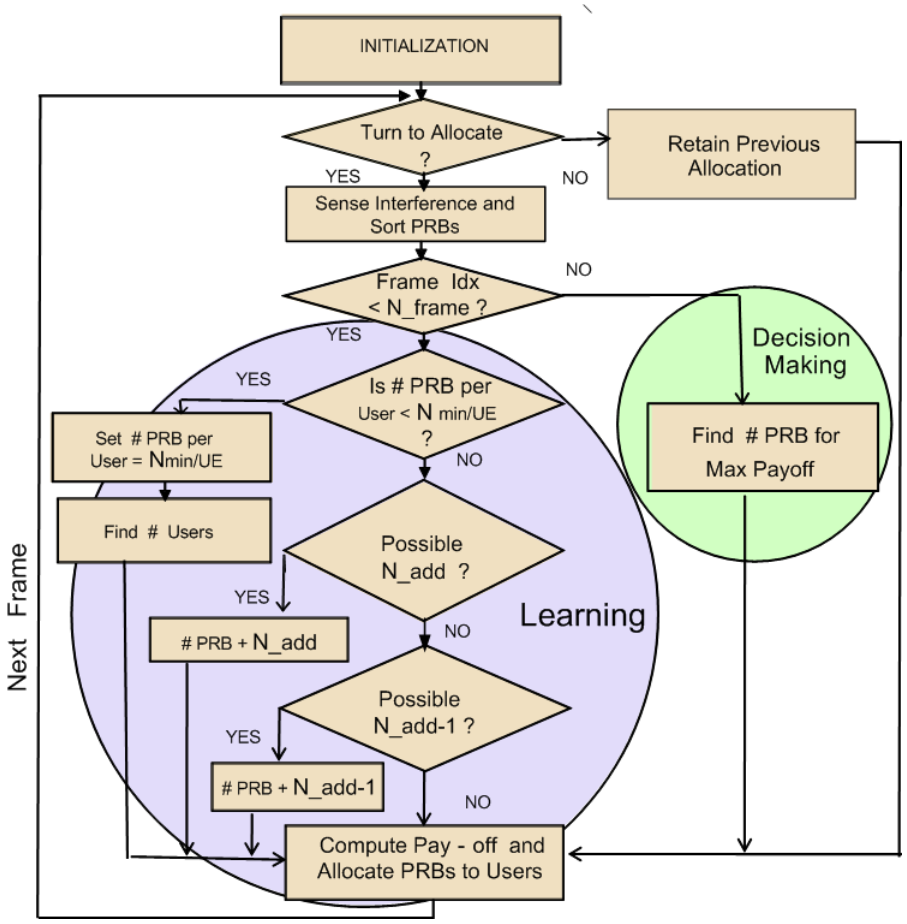

Figure 7.2: Flowchart of the proposed algorithm

7.5 Performance Evaluation

The proposed algorithm has been evaluated with 2 and 4 operators' deployment scenarios. The reference schemes chosen are universal frequency reuse (or frequency reuse 1) and Fixed Spectrum Allocation (FSA) schemes. In universal frequency reuse scheme each operator is allowed to use the whole bandwidth under consideration. A typical example is WLAN in local area deployment scenario. Under the FSA scheme the total assumed spectrum bandwidth is equally divided among the number of operators under consideration. This resembles the present spectrum allocation scenario, where each operator has a dedicated spectrum allocation. Average cell load, average cell throughput, and user outage throughput are taken as KPIs (described in chapter 3).

Figure 7.3 gives average experienced cell load in case of two as well as four operators' scenarios. The average experienced cell load of the proposed scheme is shown against the reference cases. The universal frequency reuse scheme obviously shows the 100 % average experienced cell load, since this scheme allows each operator to employ the full system bandwidth. Under FSA scheme the experienced average cell load are 50% and 25% for 2 and 4 operators respectively, which is also reflected in figure 7.3. However, the

Table 7.2: Main Parameters and Simulation Assumptions

Parameter	Settings
Deployment Scenario	Indoor Corporate
UE Mobility	Nomadic
Carrier Frequency	3.5 GHz
System Bandwidth	100 MHz
Number of PRBs	125
Access Scheme	DL : OFDMA; UL: SC-FDMA
Duplexing Scheme	TDD
Number of Operators	2 and 4
Number of HeNBs	One for each operator
Number of UEs per HeNB	Min. 5; Max. 10
HeNB Deployment Strategy	Random and Uncoordinated
HeNB Transmit Power	24 dBm
HeNB Antenna System	Omnidirectional, 0dBi gain, SISO
HeNB Receiver Noise Figure	9 dB
UL Transmit power	24 dBm
UL Antenna System	Omnidirectional, 0dBi gain, SISO
Serving Cell Selection	Geographical Location Based
Interference Threshold	-70 dBm

proposed algorithm assumes that the total spectrum bandwidth of 100 MHz is available as a common spectrum pool to be accessed by each operator based on their individual traffic requirements. Therefore the proposed scheme provides a mechanism for soft frequency reuse scheme and the experienced averaged cell load is not always fixed as in case of the reference schemes.

It can be observed in the figure that in the case with two operators the average cell load is in the order of 58% for the proposed scheme. This amount of average cell load is realized at -70 dBm interference threshold. The interference threshold plays an important role in determining the average cell load. A higher cell load will be realized with a higher amount of spectrum overlap and reverse is also true. If the interference threshold is set at a higher value, more spectrum will be allowed to overlap, resulting in a higher cell load. The lower interference threshold will impose restrictions on the spectrum overlap, and lower cell load will be experienced. The simulation results presented in this chapter are based on -70 dBm interference threshold. When a higher threshold is chosen, the more spectrum overlapping is realized, but this results in lower spectral efficiency due to presence of higher amount of interference. On the other hand a lower interference threshold does not support sufficient spectrum overlap and hence restricts the spectrum reuse.

An average cell load in the order of 58% for the scenario with two operators implies a 16 % ($2 \times 58 = 116$; $116 - 100 = 16$) improved spectrum utilization, realized by spectrum overlap. In case of a scenario with 4 operators the spectrum utilization is further

enhanced. The average cell load for each operator is in the order of 40%, which implies 60% ($4 \times 40 = 160$; $160 - 100 = 60$) improved spectrum utilization. These observations highlight the characteristic feature of the proposed algorithm in improving spectrum utilization compared to the FSA scheme.

Figure 7.4 presents the cdf of cell and user throughput for two operators. The FSA scheme shows a nearly uniform distribution, which is not true for proposed and universal frequency reuse schemes, because there is no in-band interference in the FSA scheme, where the spectrum is allocated among operators in orthogonal manner. However, the proposed and universal reuse schemes exhibit spectrum overlap causing in band interference, which results in high variance in the distribution curve. Further, when a comparison is made between the proposed scheme and the universal reuse scheme, it is clearly visible that the proposed scheme results in higher cell throughput performance.

Noticeably, this performance is achieved with only 58% spectrum use compared to universal reuse scheme (fig. 7.3). This results in improved spectrum efficiency. In case of universal reuse scheme the whole system bandwidth is used without interference considerations, whereas proposed scheme allocates spectrum to operators based on interference consideration. Further, when the proposed scheme is compared with FSA, it gives comparable average cell throughput, but uses 10 % extra spectrum resource (fig. 7.3). In FSA scheme the spectrum is orthogonally allocated to the operators therefore, there is no in band interference, resulting in higher SINR over the spectrum and hence there is higher throughput and spectral efficiency.

In terms of user outage throughput, the proposed scheme gives improved performance over the universal frequency reuse scheme. The higher spectrum overlap in universal reuse scheme results in poor SINR conditions at the cell edge, and hence lower user outage throughput performance is realized. When the proposed scheme is compared with FSA, its performance is comparatively lower. The orthogonal spectrum allocation in FSA helps to keep the cell edge conditions favorable, resulting in higher user outage throughput.

From the above discussion it becomes obvious that when two operators are considered over a 100 MHz system bandwidth, the FSA gives better performance compared to the proposed scheme. However, the proposed scheme is preferable over the universal frequency reuse scheme since it provides higher cell throughput and the user outage throughput performance using significantly lower spectrum resource.

Figure 7.5 presents the cdf of cell and user throughput performance. It is observed that the proposed scheme presents an overall higher cell throughput and user throughput distribution compared to the FSA and universal frequency reuse schemes. The FSA gives the lowest cell throughput performance, because it has significantly lower amount of the spectrum allocation, i.e. only one fourth of the total considered system bandwidth. The proposed scheme gives an average cell throughput higher than both the reference schemes, because it makes more amount of spectrum available to each operator from the common pool compared to the FSA scheme. Also, it improves performance compared to universal reuse scheme due to its interference aware spectrum allocation. When compared in terms of user outage throughput the performance of the proposed scheme is significantly higher

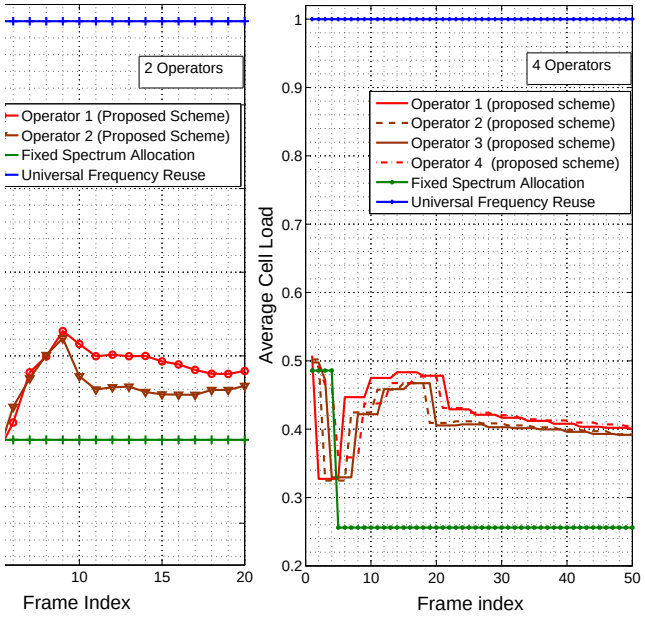

Figure 7.3: Average Cell Loads for 2 and 4 operators deployments.

than the universal reuse scheme but comparable with the FSA scheme. Therefore based on the discussion for the 4 operators' scenario, it can be concluded that the proposed scheme provides a better solution over FSA as well as universal reuse schemes.

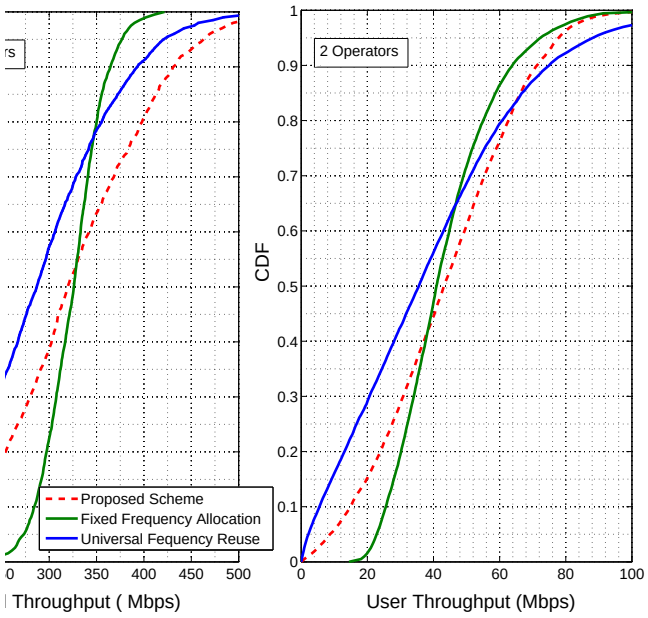

Figure 7.4: CDF of Cell Throughput and User Throughput for 2 operators deployment

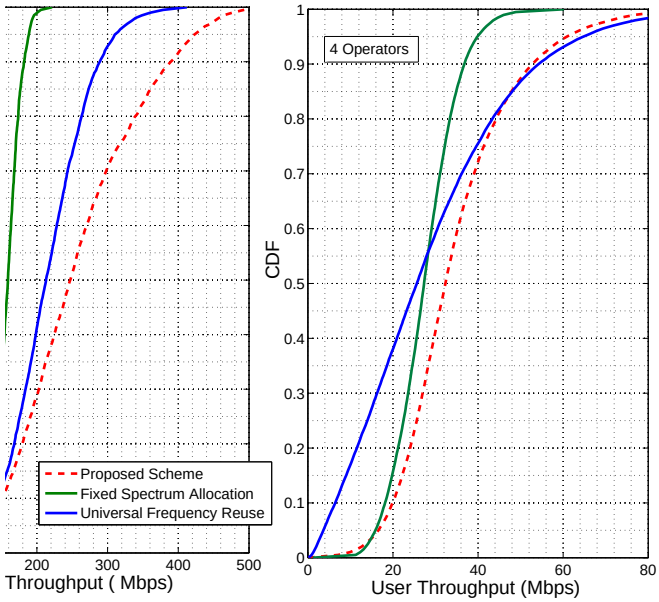

Figure 7.5: CDF of Cell Throughput and User Throughput for 4 operators deployment

7.6 Conclusions

In this chapter an algorithm for multi-operator FSU has been presented. In multi-operator scenario, the key concern is a fair, flexible and efficient spectrum allocation among the operators. The proposed algorithm is based on the concept of light cognitive radio and policy, where policy has been defined as a set of rules agreed among the operators for fair and flexible spectrum allocation. Various policy elements applicable for the proposed schemes are also outlined in this chapter.

The performance of the proposed scheme is compared with the universal frequency reuse and fixed spectrum allocation schemes with 2 and 4 operators deployments scenarios. It has been found that with 2 as well as 4 operators' deployment, the proposed scheme gives higher cell throughput and user outage throughput compared to universal frequency reuse scheme. Therefore this scheme should be preferred over the universal frequency reuse scheme.

When compared with fixed spectrum allocation scheme, with 2 operates's deployment, the proposed scheme provides a comparable cell throughput but a lower user outage throughput. Therefore, with 2 operators' deployment the proposed scheme does not bring any improvement in the assumed scenario. However, when 4 operators' deployment is considered, the proposed scheme provides significantly higher cell throughput as well as slightly higher user outage throughput. Therefore, with 4 operators' deployment the proposed scheme should be preferred.

Based on the results with 2 and 4 operators deployment, it becomes obvious that as the number of operators becomes higher the proposed scheme provides more efficient solution compared to fixed spectrum allocation scheme. Moreover the proposed scheme provides a self-configurable and scalable solution because each HeNB senses the dynamic wireless environment and takes the decision for spectrum allocation accordingly and independently.

Chapter 8

Overall Conclusions and Recommendations

The overall objective of this PhD study has been to investigate the potential techniques to enhance efficiency of the spectrum usage for the next generation mobile communication systems. The LTE and LTE-A systems were considered as example cases. In the first phase the study was focused on LTE, where Higher Order Sectorization (HOS) and Inter-Cell Interference Avoidance (ICIA) were considered. In the second phase the study was focused on LTE-A in local area indoor deployment scenario, where mechanisms for Flexible Spectrum Usages (FSU) were investigated. The techniques for improving the efficiency of spectrum usage mainly relied on the concept of aggressive spatial reuse of the given spectrum.

8.1 Higher Order Sectorization for LTE DL

The first topic investigated in the thesis was HOS. The main idea behind HOS has been to increase the usage of spectrum per unit area. In this respect, 6 sectors per site deployment has been considered against typically assumed 3 sectors per site deployment. When the performance is compared, it is found that the geometry factor for 6 sector deployment is approximately 0.5 dB to 1 dB lower compared to 3 sector deployment. This is due to increased inter sector antenna overlapping in 6 sector case because of increased number of sectors. Therefore, the average sector throughput for 6 sector is 6 % lower. However, average site throughput is 88% higher compared to 3 sectors, realizing a significantly enhanced system capacity gain. This increases spectrum utilization by increasing capacity per unit area.

Further, a mixed network topology has been proposed. A mixed network topology consists of a combination of 3 and 6 sectors site deployment. Two different mixed topologies, namely $mode1$ and $mode2$, are proposed, where $mode1$ consists of 6 sectors in the centre site and 3 sectors in the remaining 18 sites, and $mode2$ consists of centre site and

the sites in the first ring with 6 sectors surrounded by the remaining 12 sites with 3 sectors. The main idea behind this proposal was to investigate the performance of mixed deployment compared to 3 or 6 sectors homogeneous deployments. The $mode1$ is found to provide the highest overall geometry factor distribution. At cell edge the geometry of the $mode1$ is about 0.5 dB higher compared to the 3 sectors homogeneous deployment, presenting the lowest interference scenario, whereas 6 sector homogeneous deployment gives the lowest geometry factor distribution. High average site throughput gains with mixed topology are realized, which are 110 % and 96% higher for $mode1$ and $mode2$ respectively, over 3 sectors deployment.

These results were obtained by keeping the number of users per site the same in both 6 and 3 sector deployments. These relative gains in the mixed network and 6 sector site homogeneous deployments are at the cost of slightly increased hand-offs between the sectors, due to the increased number of sectors as well as slightly higher cost of installation due to extra cabling and antenna requirements.

One of the important observations was that the relative site capacity gain from upgrading existing 3 sector sites with 6 sector sites is comparatively larger for the single site upgrade ($mode1$), as compared to upgrading a cluster of sites ($mode2$). The $mode1$ could provide a viable option to meet high traffic demands in a localized area such as hot spots. Therefore, this is recommended to be used in order to provide high capacity in hot spot area. Moreover, a migration to 6 sector deployment is recommended to increase the system capacity and coverage.

8.2 Inter-Cell Interference Avoidance under Fractional Load

Further, the mechanisms were investigated to control Inter-Cell Interference (ICI) under fractional load conditions for LTE DL. Under fractional load it can be possible to employ a set of non-overlapping PRBs in the adjacent cells, which reduces the ICI. In fact under fractional load the CQI aware frequency domain packet scheduling can effectively minimize ICI. However, the performance of such packet scheduler is very sensitive to inaccuracy and delay in CQI reporting. The inaccuracy and delay in CQI reporting result in fast on-off transitions of PRBs and high BLER.

Therefore, several autonomous inter-cell interference avoidance schemes are proposed to allocate non-overlapping sets of PRBs in the adjacent cells as far as possible and also to provide time correlation to the allocated set of PRBs to avoid on-off transitions. Among all the proposed schemes, it was found that the Quality Estimation Based PRB selection Scheme (QES) gives the best performance. However, the simplest scheme, which randomly selects PRBs and then provides time correlation to the selected set of PRBs, also helps to improve effective SINR gain significantly. When QES with 50% fractional load is compared with full load under best effort traffic, it is found to improve the effective SINR by 6.5 dB over full load, which is more than 4 times higher. Moreover, even though

the full load employs twice the bandwidth, it offers only 29% increase in the sector (cell) throughput. Therefore, QES achieves a significantly higher throughput per PRB compared to full load.

Further, QES was compared to full load under Constant Bit Rate (CBR) traffic with Channel Blind traffic load Estimation (CBE) and ThroughPut based traffic load Estimation (TPE) methods. With CBE, most of the users result in throughput below the guaranteed bit rate and also experience delay much higher than the full load. This happens because CBE does not account for channel variations and spatial distribution of the users in the cell. However, TPE takes into account the channel variations and spatial distributions of the users in the cell, hence, estimates the traffic load more accurately. This significantly improves the performance over CBE, and the realized user throughput and delay become close to full load case. However, an important observation is that this performance is achieved at very low fractional load factor, as low as 0.17 only. Therefore a significantly higher throughput per PRB, in the order of 5 times compared to full load, is realized.

From the performance evaluation it is found that the proposed schemes significantly improve the effective SINR condition leading to improved efficiency of the spectrum utilization. Moreover, the schemes are autonomous, requiring no signaling exchange for ICIA. It is recommended to integrate the proposed scheme with the packet scheduler functionality.

8.3 Flexible Spectrum Usage in Local Area Deployment

In the second phase, the issues related to the local area indoor deployment of HeNBs for LTE-A were addressed. Considering the expected large scale, random and uncoordinated deployments of HeNBs, the main challenges considered are controlling mutual interference and allowing coexistence of HeNBs in the given area. The Flexible Spectrum Usage (FSU) is considered a key enabler, and therefore to realize the FSU the Spectrum Load Balancing (SLB) and Resource Chunk Selection (RCS) algorithms are proposed. The SLB is SINR threshold-based, whereas RCS is a comparative interference threshold-based algorithm. Both algorithms work on the principle of self-assessment of surrounding radio environment and ensure coexistence of HeNBs by partially or completely preventing mutual interference on the shared spectrum. The algorithms support self-configurable, decentralized and scalable deployment of HeNBs. The SLB provides granularity for spectrum allocation at the PRB level, whereas RCS has a granularity of a chunk, where one chunk is considered to have half of the system bandwidth in the considered case. A very limited signaling exchange via over-the-air-communications is assumed to perform FSU. The proposed algorithms support flexible spectrum usage, self-configuration, flexible and scalable deployment. Therefore, the algorithms are suitable for implementation in the uncoordinated and random deployment in local area solution envisioned for IMT-A systems.

8.4 Autonomous Component Carrier Selection

Since LTE-A will be an evolution of LTE, it is desirable to have backward compatibility. It is considered that the desired bandwidth for LTE-A can be achieved by carrier aggregation. Several component carriers are assumed for LTE-A. Further, it is assumed that each HeNB will not require all of the component carriers at all times, hence a concept of primary and secondary component carrier has been proposed. The primary component carrier is assumed to be used for initial connections of the terminals in the cell, and later on a cell may additionally select secondary component carrier(s) depending on offered traffic in the cell and on mutual interference coupling.

An algorithm for the selection of the primary component carrier has been proposed, which is fully distributed and does not involve any centralized network component; the selection is rather performed locally and independently by each HeNB. The simulation results presented in this chapter provide an indication that the presented concept helps to achieve an autonomous scalable and self-adjusting frequency re-use mechanism, which allows uncoordinated HeNB deployment without prior network planning. Further, mechanisms are also proposed for monitoring and recovery of the quality of primary component carrier. It is recommended that Interference Reduction Request (IRR) message based recovery action should be preferred as a first step over the reconfiguration of the primary component carriers.
Adaptation of the proposed concept for LTE-Advanced is simple since it entails minimal changes to the standard as it mostly relies on existing Release'8 UE and HeNB measurements.

8.5 Policy Assisted Light Cognitive Radio Enabled FSU

Further, the multi-operators domain FSU was considered, where it was assumed that several operators may deploy HeNBs in the given geographical area and share the spectrum from a common pool. The multi-operator uncoordinated deployment scenario presents new challenges, such as fair, efficient and flexible spectrum usage among operators. Therefore the need for policy and the concept of light cognitive radio is envisaged. The scheme proposed is referred to as policy assisted light cognitive radio enabled FSU, where the decision making process during the cognitive radio cycle is assisted by policy.

The proposed scheme is compared with universal frequency reuse and Fixed Spectrum Allocation (FSA) schemes with 2 and 4 operators' deployments scenarios. For both the deployment scenarios, the proposed scheme gives higher cell throughput and user outage throughput over the universal reuse scheme. However, when compared with FSA, in the scenario with two operators, the proposed scheme is found to give comparable cell throughput, but lower user outage throughput. Instead, with 4 operators' scenario the proposed scheme outperforms FSA in both average cell throughput and user outage throughput.

The proposed scheme provides a self-configurable solution, because each HeNB senses the dynamic wireless environment and takes the decision for spectrum allocation independently. The implementation of the proposed scheme requires only a small amount of signaling exchange. The proposed scheme provides a viable solution for multi-operators FSU and is therefore recommended for the LTE-A local area indoor deployment with multi operators.

8.6 Topics for Future Research

With respect to higher order sectorization, the performance of 6 sector deployment was only evaluated in Downlink. As a next step the performance can be evaluated in uplink as well. Further, the impact of antenna tilting in vertical domain can be investigated along with the 6 sector deployment, in order to evaluate the impact on the system capacity and coverage. The study on Inter-Cell Interference Avoidance under fractional load was conducted with 3 sector deployment, the study can be further carried out in the 6 sector deployment scenario.

In the performance results of the SLB algorithm, a homogeneous traffic load for all HeNBs was assumed with full buffer. A dynamically varying cell load was not considered. The SLB is expected to perform more efficiently under such conditions. It will be useful to investigate the performance of SLB algorithm under such conditions. The SLB algorithm presently assumes the selection of PRBs to be limited within the scheduled PRBs only, which limits the diversity gain and range of the PRBs for selection. This assumption was used to avoid the complexity in SINR estimation over full range of PRBs and also to limit the power consumption of the user equipment. Further, development of the SLB algorithm with full range of PRBs selection will be a useful step. The performance of the SLB and RCS algorithms are evaluated only in the regular corporate scenario. A deeper insight can be gained if the performance is evaluated in residential as well as extended deployment scenarios. Presently RCS works on the uplink RIP measurement only; a DL measurement based approach will be more accurate for DL spectrum allocation.

In Autonomous component carrier selection algorithm the implementation of the quality monitoring and recovery action is not yet implemented, it is considered for the future work. With regard to policy assisted light cognitive radio enabled FSU, only a simple case with one HeNB per operator has been evaluated. Performance with higher number of HeNBs per operator will be useful to gain further insight on the proposed concept.

Appendix A

Link Level Performance and Propagation Conditions

Figure A.1 represents the Actual Value Interface (AVI) used in the simulator for the case of 2 PRBs. As expected, BLock Error Rate (BLER) decreases as the SINR increases for all the considered MCSs. A higher MCS requires a larger SINR in order to keep the BLER constant. Figure A.2 represents the required SINR to keep a 30% BLER target as function of the bandwidth. the slight dependency on the bandwidth is due to the following factors:

- The code block size (resulting in higher coding gain as the bandwidth increases).
- The frequency diversity (which improves as the bandwidth increases)
- The accuracy of the channel estimation (which worsens as the bandwidth increases)

The channel profile used is ITU Typical Urban 20 path (TU20). The time domain response of the channel is represented by Power Delay Profile (PDP) given in figure A.3 and whose values are listed in table A.1. the PDP depicts the relative power and the time delay of the different reflections.

The time and frequency dispersive properties of the multipath channel are characterized by : maximum delay spread (τ_{max}), mean excess delay (τ_{mean}), root mean square (r.m.s.) delay spread (τ_{rms}) and coherence bandwidth (B_c).

- The τ_{max} represents the maximum time interval during which reflections of significant energy are received.
- The τ_{mean} is defined as :

$$\tau_{mean} = \sum_{i=1}^{N} \tau_i \cdot |h(t, \tau_i)|^2 \tag{A.1}$$

  where,N is the number of taps.

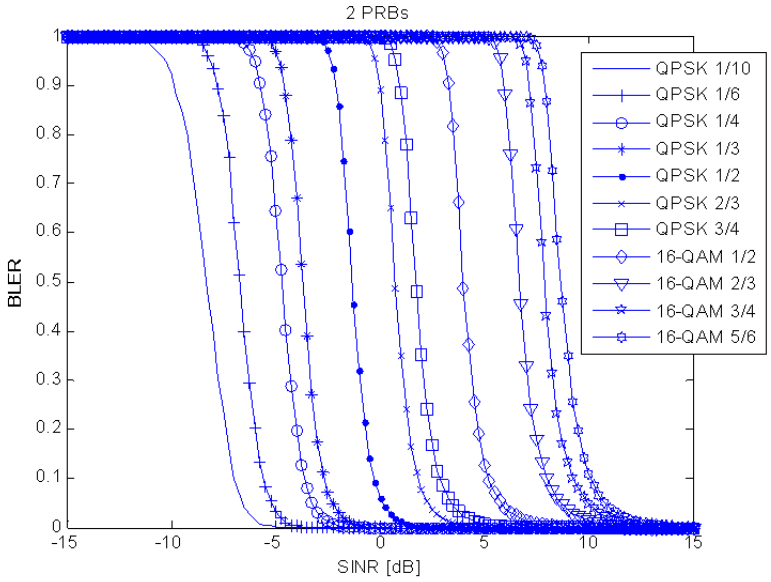

Figure A.1: Actual value Interfaces (AVIs) for 2 PRBs

- The τ_{rms} is defined as :

$$\tau_{rms} = \sqrt{\sum_{i=1}^{N}(\tau_i - \tau_{mean})^2 |h(t,\tau_i)|^2} = \sqrt{\tau_{mean}^2 - (\tau_{mean})^2} \tag{A.2}$$

  where, τ_{mean}^2 is the second moment and the $\tau_{mean})^2$ is the mean squared.

- The B_c is defined as :

$$B_c \approx \frac{1}{\tau_{max}} \tag{A.3}$$

Table A.2 shows the values used for time and frequency dispersive properties.

SINR calculation

The SINR together with the AVI represent the interface with the link level results. In downlink the SINR to be used in input to the AVI is computed using the Exponential Effective SINR mapping (EESM) model which exploits as estimation of the SINR per subcarrier obtained in a previous transmission and is given as [22] :

$$SINR_{eff} = -\beta \cdot \ln\left(\frac{1}{N}\sum_{i=1}^{N} e^{\frac{SINR_i}{\beta}}\right) \tag{A.4}$$

where, $SINR_i$ denotes the SINR of the i^{th} subcarrier and β is a parameter, which is obtained from link level simulations and is adjusted for each MCS separately. N denotes the number of active OFDM sub carriers.

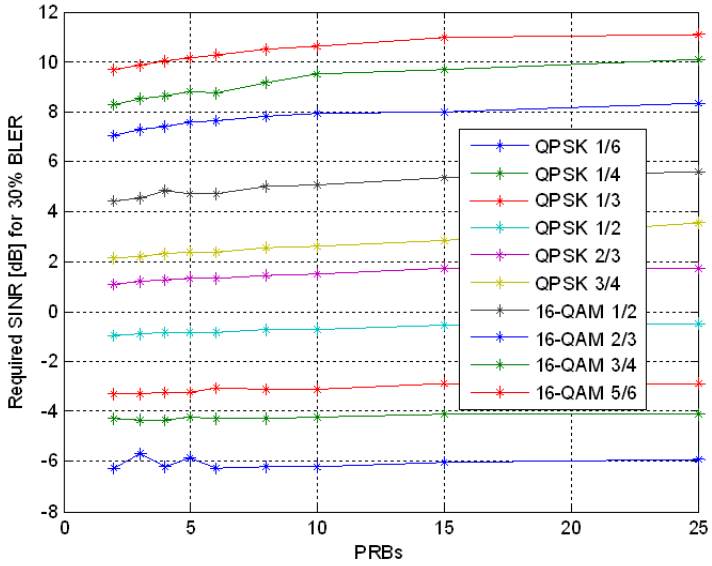

Figure A.2: Required SINR to have 30% BLER depending on number of PRBs for different MCSs.

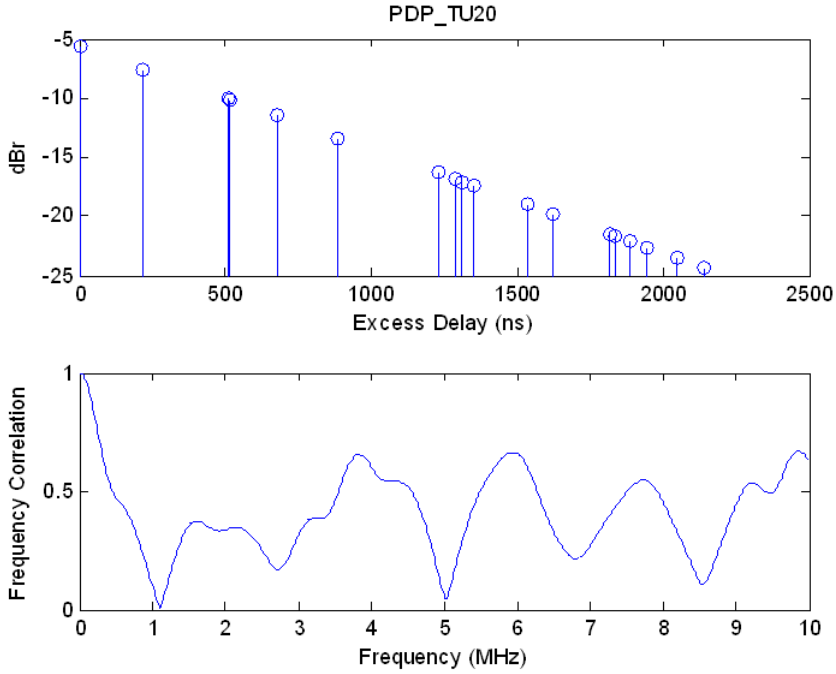

Figure A.3: Power delay profile and frequency correlation for TU20 channel model

Table A.1: Typical Urban 20 channel power delay profile

Tap Number	Delay (ns)	Power (dBr)
1	0	-5.7000
2	217	-7.6000
3	512	-10.1000
4	514	-10.2000
5	517	-10.2000
6	674	-11.5000
7	882	-13.4000
8	1230	-16.3000
9	1287	-16.9000
10	1311	-17.1000
11	1349	-17.4000
12	1533	-19.0000
13	1535	-19.0000
14	1622	-19.8000
15	1818	-21.5000
16	1836	-21.6000
17	1884	-22.1000
18	1943	-22.6000
19	2048	-23.5000
20	2140	-24.3000

Table A.2: Time and frequency dispersive properties of TU20 channel model

Properties	Values
τ_{max}	2.14 μs
τ_{min}	0.5 μs
τ_{rms}	0.5 μs
B_c	350 kHz

Bibliography

[1] D. McQueen, "The Momentum Behind LTE Adoption," *IEEE Communiations Magazine*, vol. 47, no. 02, pp. 44–45, February 2009.

[2] K. Etemad, "Overview of Mobile WiMAX Technology and Evolution," *IEEE Communiations Magazine*, vol. 46, no. 10, pp. 31–40, October 2008.

[3] E. Dahlman, S. Parkvall, J. Skold, and P. Beming, Eds., *3G Evolution : HSPA and LTE for Mobile Broadband*. Academic Press, 2007.

[4] H. Holma, T. Kolding, K. Pedersen, and J. Wigard, *HSDPA/HSUPA for UMTS – High Speed Radio Access for Mobile Communications*. ISBN 0-470-01884-4: John Wiley & Sons Ltd, 2006, ch. Radio Resource Management, pp. 95–122.

[5] D.Astely, E. Dalhman, A. Furuskar, Y. Jading, M. Lindstorm, and S. parkvall, "LTE: The Evolution of mobile Broadband," *IEEE Communications Magazine*, vol. 47, no. 04, pp. 44–51, April 2009.

[6] 3GPP Technical Report 36.913, version 8.0.0, *Requirement for Further Advancements for E-UTRA (LTE-Advance) (Release 8)*, 2008.

[7] ITU-R, "Framework and Overall Objectives of the Future Deployment of IMT-2000 and Systems beyond IMT-2000," *Recommendations ITU-R M-16452*, 2003.

[8] R. Irmer, H. Mayer, A. Weber, V. Braun, M. Schmidt, M. Ohm, N. Ahr, A. Zoch, P. Marsch, and G. Fettweis, "Multisite Field Trial for LTE and Advanced Concepts," *IEEE Communiations Magazine*, vol. 47, no. 02, pp. 92–98, February 2009.

[9] M. M. Buddhikot, "Understanding Dynamic Spectrum Access : Models Taxonomy and Challenges," in *Proceedings of the IEEE Symposium on Dynamic Spectrum Access (DySPAN)*, Dublin, Ireland, April 2007.

[10] V. Chandrasekhar and J. Andrews, "Femtocell Networks: A Survey," *IEEE Communiations Magazine*, vol. 46, no. 9, pp. 59–67, September 2008.

[11] 3GPP Technical Report 25.814, version 7.1.0, *Physical Layer Aspect for Evolved Universal Terrestrial Radio Access (UTRA)*, September 2006.

[12] 3GPP Technical Specification 36.201, version 0.2.0, *LTE Physical Layer - General Description*, November 2006.

[13] WiMAX Forum, "Mobile WiMAX - Part I: A Technical Overview and Performance Evaluation'," *White Paper*, August 2006.

[14] ETSI, "Digital Video Broadcasting (DVB): Framing Structure, Channel Coding and Modulation for Digital Terrestrial Television," *ETSI, ETS EN 300 744 v 1.1.2*, ??

[15] R. Prasad, *OFDM for Wireless Communications Systems*. Artech House Publishers, 2003.

[16] H. Yang, "A Road to Future Broadband Wireless Access: MIMO-OFDM-Based Air Interface," *IEEE Communiations Magazine*, vol. 43, no. 1, pp. 53–60, January 2005.

[17] 3GPP Technical Report 25.892, version 6.0.0, *feasibility study for OFDM for UTRAN Enhancement*, June 2004.

[18] 3GPP Technical Specification 36.211, version 8.3.0, *Evolved Universal Terrestrial Radio Access (E-UTRA); Physical Channels and Modulation*, May 2008.

[19] H. G. Myung, J. Lim, and D. J. Goodman, "Single Carrier FDMA for Uplink Wireless Transmission," *IEEE Vehicular Technology Magazine*, p. ??, September 2006.

[20] A. Pokhariyal, T. E. Kolding, and P. E. Mogensen, "Performance of Downlink Frequency Domain Packet Scheduling for the UTRAN Long Term Evolution," in *Proceedings of IEEE Personal Indoor and Mobile Radio Communications Conference (PIMRC)*, Helsinki, Finland, September 2006, pp. 1–5.

[21] K. I. Pedersen, G. Monghal, I. Z. Kovacs, T. E. Kolding, A. Pokhariyal, F. Frederiksen, and P. E. Mogensen, "Frequency Domain Scheduling for OFDMA with Limited and Noisy Channel Feedback," in *Proceedings of IEEE Vehicular Technology Confreence (VTC)*, Baltimore, USA, October 2007.

[22] K. Brueninghaus, D. Astley, T. Salzer, S. Visuri, A. Alexiou, S. Karger, and G.-A. Seraji, "Link Performance Models for System Level Simulations of Broadband Radio Access Systems," in *Proceedings of the IEEE Personal Indoor and Mobile Radio Communications Conference (PIMRC)*, vol. 4, Berlin, Germany, September 2005, pp. 2306–2311.

[23] A. Pokhariyal, K. I. Pedersen, G. Monghal, I. Z. Kovacs, C. Rosa, T. E. Kolding, and P. E. Mogensen, "HARQ Aware Frequency Domain Packet Scheduler with Different Degrees of Fairness for the UTRAN Long Term Evolution," in *Proceedings of the IEEE Vehicular Technology Conference (VTC)*, Dublin, Ireland, April 2007, pp. 2761–2765.

[24] 3GPP Technical Report 36.913, version 4.0.0, *Requirement for Further Advancements for E-UTRA (LTE-Advance) (Release 8)*, 2008.

[25] Nokia Siemens Network, Nokia, "LTE-Advanced Simulation Methodology and Assumptions," *3GPP TSG-RAN1, R1-083102*, August 2008.

[26] Internal Document Nokia Siemens Networks, Aalborg, "Rel'9 / LTE-A FSU Scenarios and Light Simulation Tool," June 2008.

[27] TR 101 112 (UMTS 30.03 V3.2.0), *ETSI Technical Report, Selection procedures for the choice of radio transmission technologies of the UMTS* , 2004.

[28] IST-4-027756 WINNER II, D1.1.2, *WINNER II Channel Models part I*, September 2007.

[29] "http://www.ist-winner.org."

[30] M. Schacht, A. Dekorsy, and P. Jung, "System Capacity from UMTS Smart Antenna Concepts," in *Proceedings of the IEEE Vehicular Technology Conference (VTC)*, vol. 5, Florida, USA, October 2003, pp. 3126–3130.

[31] B. Hagerman, D. Imbeni, J. Barta, A. Pollard, R. Wohlmuth, and P. Cosimini, "WCDMA 6 Sector Deployment-Case study of a real installed UMTS-FDD Network," in *Proceedings of the IEEE Vehicular Technology Conference (VTC)*, vol. 2, Melbourne, Australia, May 2006, pp. 703–707.

[32] W. C. Jakes, Ed., *Microwave Mobile Communications*. ISBN 0-7803-1069-1: IEEE Press, New Jersey, 1994.

[33] B.Christer, V. Johansson, and S. Stefansson, "Optimizing Antenna Parameters for Sectorized WCDMA Networks," in *Proceedings of the IEEE Vehicular Technology Conference (VTC)*, vol. 4, Rhodes, Greece, September 2000, pp. 1524–1531.

[34] T.I.Song, D.J.Kim, and C.H.Cheon, "Optimization of Sectorized Antenna Beam Pattern for CDMA 2000 Systems," in *Proceedings of the IEE Conference Publication Number 489 on 3G Mobile Communications Technologies*, May 2002, pp. 428–432.

[35] G. K. Chan, "Effects of Sectorization on the Spectrum Efficiency of Cellular Radio Systems," *IEEE Transactions on vehicular Technology*, vol. 41, no. 3, pp. 217–225, August 1992.

[36] A. Waker, J.L.steffens, K.Sipila, and K.Heiska, "The Impact of Base Station Sectorization on WCDMA Radio Network Performance," in *Proceedings of the IEEE Vehicular Technology Conference (VTC)*, Houston, USA, April 1999, pp. 2611–2615.

[37] X. Yang, S. G. Niri, and R. Tafazolli, "Sectorization Gain in CDMA Cellular Systems," in *3G Mobile Communication Technologies,Conf. Publ. No. 471*, 2000, pp. 70–75.

[38] C.-C. Lee and R. Steele, "Effects of Soft and softer Handoffs on CDMA System Capacity," *IEEE Transactions on vehicular Technology*, vol. 47, no. 3, pp. 830–841, August 1998.

[39] F. Athley, "On Base Station Beamwidth for Sectorized WCDMA Systems," in *Proceedings of the IEEE Vehicular Technology Conference (VTC)*, Montreal, Canada, September 2006, pp. 1–5.

[40] W.-J. Wang, I.-T. Lu, and S.-C. Liu, "Soft Handoff Performance of 3-sector and 6-sector Multicell CDMA Systems," in *Proceedings of the IEEE Vehicular Technology Conference (VTC)*, vol. 4, Rhodes, Greece, May 2001, pp. 2338–2342.

[41] 3GPP Technical Specification 36.300, version 8.3.0, *Evolved Universal Terrestrial Radio Access (E-UTRA) and Evolved Universal Terrestrial Radio Access (E-UTRAN); Overall Description; Stage 2*, January 2008.

[42] 3GPP Technical Report 25.996, version 6.1.0, *Spatial Channel Model for MIMO Simulations*, September 2003.

[43] K. Brueninghaus, D. Astley, T. Salzer, S. Visuri, A. Alexiou, S. Karger, and G.-A. Seraji, "Link Performance Models for System Level Simulations of Broadband Radio Access Systems," in *Proceedings of the IEEE Personal Indoor and Mobile Radio Communications Conference (PIMRC)*, vol. 4, Berlin, Germany, September 2005, pp. 2306–2311.

[44] A. Pokhariyal, "Downlink Frequency-Domain Adaptation and Scheduling – A Case Study Based on the UTRA Long Term Evolution," Ph.D. dissertation, Radio Access Technology Section, Institute of Electronic Systems, Aalborg University, Aalborg, Denmark, August 2007.

[45] K. I. Pedersen, P. Mogensen, and B. Fleury, "Spatial Channel Characteristics in Outdoor Environments and Their Impact on BS Antenna System Performance," in *Proceedings of the IEEE Vehicular Technology Conference (VTC)*, Ottawa, Canada, May 1998, pp. 719–723.

[46] Ericsson, "Reactive and Pro-active use of Uplink Overload Indication in LTE," *3GPP TSG-RAN1, R1-074379*, October 2007.

[47] 3GPP Technical Specifications 36.423, version 8.3.0, *Evolved Universal Terrestrial Radio Access Network(E-UTRAN); X2 application protocol, (Release 8)*, May 2008.

[48] A. Simonsson, "Frequency Reuse and Intercell Interference Co-Ordination In E-UTRA," in *Proceedings of the IEEE Vehicular Technology Conference (VTC)*, Dublin, Ireland, April 2007, pp. 3091–3095.

[49] Nokia, Nokia Siemens Networks, "Downlink Interference Coordination," *3GPP TSG-RAN1, R1-072974*, June 2007.

[50] Ericsson, "On Inter-cell Interference Coordination Schemes without/with Traffic Load indication," *3GPP TSG-RAN1, R1-073039*, June 2007.

[51] Alcatel-Lucent, "Semi-Static Interference Coordination Method," *3GPP TSG-RAN1, R1-081873*, May 2008.

[52] Siemens, "Interference Mitigation by Partial Frequency Reuse," *3GPP TSG-RAN1, R1-060135*, January 2006.

[53] Ericsson, "Options for Inter-cell Interference Coordination (ICIC)," *3GPP TSG-RAN3, R3-061199*, September 2006.

[54] Nokia, Nokia Siemens Networks, "Low load scenarios with CQI-based interference coordination," *3GPP TSG-RAN1, R1-073679*, August 2007.

[55] A. Pokhariyal, G. Monghal, K. I. Pedersen, P. E. Mogensen, I. Z. Kovacs, C. Rosa, and T. E. Kolding, "Frequency Domain Packet Scheduling Under Fractional Load for the UTRAN LTE Downlink," in *Proceedings of the IEEE Vehicular Technology Conference (VTC)*, Dublin, Ireland, April 2007, pp. 699–703.

[56] S. Kumar, G. Monghal, J. Nin, I. Ordas, K. I. Pedersen, and P. E. Mogensen, "Autonomous Inter Cell Interference Avoidance under Fractional Load for Downlink Long Term Evolution," in *Proceedings of the 69th IEEE Vehicular Technology Conference (VTC)*, Barcelona, Spain, April 2009, pp. ??–??

[57] T. E. Kolding, F. Frederiksen, and A. Pokhariyal, "Low-Bandwidth Channel Quality Indication for OFDMA Frequency Domain Packet Scheduling," in *Proceedings of International Symposium on Wireless Communication Systems (ISWCS)*, Valencia, Spain, September 2006.

[58] J. N. Guerrero and I. O. Villamandos, "Autonomous Physical Resource Block Selection in Fractional Load Scenario for 3GPP Long Term Evolution Downlink," Master's thesis, Aalborg University, Aalborg, Denmark, 2007.

[59] G. Monghal, S. Kumar, K. I. Pedersen, and P. E. Mogensen, "Integrated Fractional Load and Packet Scheduling for OFDMA Systems," in *Proceedings of the IEEE International Conference on Communications(ICC)*, Dresden, Germany, June 2009, pp. ??–??

[60] A. Pokhariyal, K. I. Pedersen, G. Monghal, I. Z. Kovacs, C. Rosa, T. E. Kolding, and P. E. Mogensen, "HARQ Aware Frequency Domain Packet Scheduler with Different Degrees of Fairness for the UTRAN Long Term Evolution," in *Proceedings of the IEEE Vehicular Technology Conference (VTC)*, Dublin, Ireland, April 2007, pp. 2761–2765.

[61] 3GPP RAN, "Workshop on IMT-Advanced, Shenzhen, China,," *available at ftp://ftp.3gpp.org/workshop/*, April 2008.

[62] 3GPP Technical Report 25.820, version 8.2.0, *3G Home NodeB Study Item Technical Report(Release 8)*, September 2008.

[63] L. B. et al, "Policy Based Reasoning for Spectrum Sharing in Cognitive Radio Networks," in *IEEE International Symposium on Spread Spectrum Techniques and Applications (ISSSTA)*, vol. 3, Sydney, Australia, September 2005, pp. 355–358.

[64] Y. Bai and L. Chen, "Flexible Spectrum Allocation Methods for Wireless Network Providers," in *IEEE International Symposium on Personal, Indoor and Mobile Radio Communications (PIMRC)*, Helsinki, Finland, September 2006, pp. 1–5.

[65] J. P. Kermoal, S. Pfletschinger, k. Hooli, S. Thilakawardana, J. Lara, and Y. Zhu, "Spectrum Sharing for WINNER Radio Access Networks," in *IEEE International Conference on Cognitive Radio Oreiented Wireless Networks and Communications*, Greece, june 2006, pp. 1–5.

[66] S. Mangold, L. Berlemann, and S. Nandagopalan, "Spectrum Sharing with Value Orientation for Cognitive Radio," *European Transactions on Telecommunications*, pp. 383–394, 2006.

[67] Wireless World Initiative New Radio+, "WINNER II Spectrum Sharing Studies," *IST-4-027756 WINNER D5.10.3 v1.0, website; http://www.ist-winner.org*, November 2006.

[68] L. Berlemann and B. Walke, "Spectrum Load Smoothing for Optimized Spectrum Utilization-Rationale and Algorithm," in *Proceedings of the IEEE Wireless Communications and Networking Conference(WCNC)*, vol. 3, New Orleans, USA, March 2005, pp. 1952–1956.

[69] L. Berlemann, S. Mangold, G. R. Hiertz, and B. H. Walke, "Spectrum Load Smoothing : distributed quality od service Support for Cognitive Radios in Open Spectrum," *European Transactions on Telecommunications*, pp. 395–406, 2006.

[70] Nokia Siemens Network, Nokia, "Inter eNB Over the Air Communication (OTAC)for LTE-Advanced," *3GPP TSG-RAN1, R1-090236*, January 2009.

[71] A. A. et. al., "Duplexing, Resource Allocation and Inter-cell Coordination : Design Recommendations for Next Generation Wireless Systems," *Wireless Communications and Mobile computing in Wiley InterScience*, vol. 5, pp. 77–93, January 2005.

[72] S. Parkvall, E. Dahlman, A. Furuskar, Y. Jading, M. Olsson, S. Wanstedt, and K. Zangi, "LTE-Advanced Evolving LTE towards IMT-Advanced," in *Proceedings of the IEEE Vehicular Technology Conference (VTC)*, Calgary, Canada, September 2008, pp. 1–5.

[73] Huawei, "Consideration on Carrier Aggreagation for Home eNB," *3GPP TSG-RAN 1, R1-090817*, Feb 2009.

[74] Alcatel Shanghai Bell, Alcatel-Lucent, "Support of Wider Bandwidth for Home eNodeB in LTE-Advanced," *3GPP TSG-RAN1, R1-084125*, November 2008.

[75] Ericsson, "Carrier Aggregation in LTE-Advanced," *3GPP TSG-RAN1, R1-082468*, June 2008.

[76] Qualcomm Europe, "Notion of Anchor Carrier in LTE-A," *3GPP TSG-RAN1, R1-080356*, January 2009.

[77] Nokia Siemens Network, Nokia, "Autonomous Component Carrier selction for LTE-Advanced," *3GPP TSG-RAN1, R1-083103*, August 2008.

[78] Internal Document Nokia Siemens Networks, Aalborg, "Autonomous Component Carrier Selction Concept," December 2008.

[79] 3GPP Technical Specification 36.214, version 8.2.0, *Evolved Universal Terrestrial Radio Access (E-UTRA); Physical Layer - Measurements (Release 8)*, May 2008.

[80] Nokia Siemens Network, Nokia, "Primary Component Carrier selction, Monitoring and Recovery Action," *3GPP TSG-RAN1, R1-090735*, February 2009.

[81] Nokia Siemens Network, Nokia., "On Definition and Usage of the Uplink Overload Indicator," *3GPP TSG-RAN1, R1-080332*, January 2009.

[82] L. G. U. Garcia, K. I. Pedersen, and P. E. Mogensen, "Autonomous Component Carrier Selection for Local Area Uncoordinated Deployment of LTE-Advanced."

[83] Nokia Siemens Network, Nokia, "Use of Background Interference Matrix for Autonomous Component Carrier selction for LTE-Advanced," *3GPP TSG-RAN1, R1-090235*, January 2009.

[84] P. E. Mogensen, W. Na, I. Z. Kovacs, F. Frederiksen, A. Pokhariyal, K. I. Pedersen, T. Kolding, K. Hugl, and M. Kuusela, "LTE Capacity Compared to the Shanon Bound," in *Proceedings of the 65^{th} IEEE Vehicular Technology Conference (VTC)*, Dublin, Ireland, April 2007, pp. 1234–1238.

[85] Y. Wang, S. Kumar, L. Garcia, K. I. Pedersen, I. Z. Kovács, S. Frattasi, N. Marchetti, P. E. Mogensen, and T. B. Sørensen, "Fixed Frequency Reuse for LTE-Advanced Systems in Different Scenarios," in *Proceedings of the 69^{th} IEEE Vehicular Technology Conference (VTC)*.

[86] G. Middleton, K. Hooli, A. Tolli, and J. Lilleberg, "Inter Operator Spectrum Sharing in a Broadband Cellular Network," in *Proceedings of the IEEE International Symposium on Spread Spectrum Techniques and Applications*, Brazil, August 2008, pp. 376–380.

[87] M. Bennis and J. Lilleberg, "Inter Operator Resource Sharing for 3G Systems and Beyond," in *Proceedings of the IEEE International Symposium on Spread Spectrum Techniques and Applications*, Brazil, August 2006, pp. 401–405.

[88] J. L. M. D. M.K. Pereirasamy and C. Hartmann, "An Approach for Inter Operator Spectrum Sharing for 3G Systems and Beyond," in *Proceedings of IEEE Personal Indoor and Mobile Radio Communications Conference(PIMRC*, vol. 3, Barcelona, Spain, September 2004, pp. 1952–1956.

[89] M. Pereirasamy, J. Luo, M. Dillinger, and C. Hartmann, "Dynamic Inter Operator Spectrum Sharing for UMTS FDD with Displaced Cellular Network," in *Proceedings of the IEEE Wireless Communications and Networking Conference(WCNC)*, New Orleans, USA, March 2005, pp. 1720–1725.

[90] A. Attar and A. H. Aghvami, "A framework for Unified Spectrum Management in heterogeneous Wireless Networks," *IEEE Communications Magazine*, vol. 45, pp. 44–51, September 2007.

[91] D. Gozalvez, J. Monserrat, and D. Calabuig, "Policy Based Channel Access Mechanism Selection for QoS Provision in IEEE 802.11e," *IEEE Vehicular Technology magazine*, September 2007.

[92] S. Horrich, S.B.Jamaa, and P. Houze, "Policy Based RRM for Network Terminal Decision Sharing," *IEEE Vehicular Technology magazine*, September 2007.

[93] D. Elenius, G. Denker, M. O. Stehr, R. senanayake, C. Talcott, and D. Wilkins, "CoRaL policy language and reasoning techniques for spectrum policies," *IEEE computer society*, 2007.

[94] S. Haykin, "Cognitive Radio: Brain-Empowered Wireless Communication," *IEEE JSAC*, February 2005.

[95] J. M. III and G. Q. Marguire, "Cognitive Radio: Making Software Radio More Personal," *IEEE Persona Communications Mag.*, vol. 6, no. 4, pp. 13–18, August 1999.